ANALYTICAL STUDY ON PERIODICALLY INTERRUPTED ELECTRIC CIRCUITS AND ITS APPLICATIONS TO CONTROL SYSTEMS

ANALYTICAL STUDY ON PERIODICALLY INTERRUPTED ELECTRIC CIRCUITS AND ITS APPLICATIONS TO CONTROL SYSTEMS

KŌICHI MIZUKAMI

Department of Electric Engineering II
Kyoto Japan

PREFACE

The material presented in this text is a set of the results of investigations studied by the author at the graduate school of Kyoto University for five years from 1958 to 1963.

His effort has been made to contribute especially to the mathematical theories of the Periodically Interrupted Electric Circuits and to the techniques for applying these theories to the study of various engineering problems.

During the past decade there has been considerable interest on the part of engineers and physicists in the problems dealing with electric networks and control systems. As the consequences of the mathematical techniques in those fields, for instance, the fundamentals of linear and non-linear system analysis, the probability theory, the topological theory, the optimization and adaptive methods, etc., the more generalized synthesis and analysis of systems have been extensively progressed.

The fundamental theories of the Periodically Interrupted Electric Circuits constructed by Professor S. Hayashi of Kyoto University are well-known and usefull methods in the fields of networks, control processes and various engineering problems, and these fundamentals have been devoted obviously to clarify the properties of the various systems in those fields.

My research works were carried out under the guidance and support of Professor S. Hayashi during my graduate course, and I now write this text under his supervision, the contents of which consist of my published papers in the Memoirs of the Faculty of Engineering, Vols. XXV and XXVI, Kyoto University, with the association of Professor S. Hayashi.

I am thankful to him not only for his continuous guidance but for his support in my works and in making this text. I wish also to express my sincere appreciation for the valuable suggestions and discussions given me by a large number of staffs of the Department of Electrical Engineering II, the Department of Electrical Engineering and the Department of Electronics. Thanks are due to staff members of the center of the Digital Computer (KDC-1) of Kyoto University, for their helps to my works.

Kōichi MIZUKAMI

Department of Electrical Engineering II,
Kyoto University, Japan,
September, 1964.

CONTENTS

INTRODUCTION

This text is devoted to the study on periodically interrupted electric circuits and its applications to control systems.

In general the periodically interrupted electric circuits are classified into the first, second and third genera, whose general descriptions[1] are given as follows.

The periodically interrupted electric circuit of the first genus is so defined that the durations of opening and closing of the circuit can be controlled only by external causes quite independent of the phenomena themselves.

Chopper amplifiers, chopper-modulated circuits and sampled-data feedback control systems belong to the first genus, and these are investigated in detail in this text.

The periodically interrupted electric circuit of the second genus is so defined that only the electromotive forces and the current sources in the circuit vary periodically and impulsively, while the arrangement of the impedances and the admittances remains unchanged, or, in other words, the connections of the circuit elements are not interchanged.

The periodically interrupted electric circuit of the third genus is so defined that the durations of opening and closing of the interrupter are affected by the phenomena themselves. The harmonic producer circuits are worked out in detail in the text by the method of the third genus.

The text consists of six chapters. The subjects of investigation are limited to the field of electric circuits and sampled-data control systems. The method of analysis presented in the text may also be applicable to other physical systems. Now we summarize the contents and the obtained results of each chapter.

Chapter I is concerned with "A Study of the Transfer Function of Chopper Amplifier." We first consider on the general analysis of the ciruit containing a periodically operated switch such as a chopper. This analytical method is established in complex domain based on some modification of the theories of the Periodically Interrupted Electric Circuits. In this establishment, the solution for the difference equation plays an important role, and also the usefulness of the complex Fourier series is demonstrated for the steady-state analysis of the chopper amplifier.

(1) S. Hayashi, Periodically Interrupted Electric Circuits, published by Denki-Shoin, Inc., 1961.

The transfer functions of the two types of the chopper amplifier, that is, the transformer coupled chopper amplifier and the resistance-capacitance coupled one, are derived for a sinusoidal input signal. The frequency characteristics result in the form of the first order attenuation characteristic for the two types of the chopper amplifier.

Chapter II deals with "The Steady-State and Transient Characteristics of the Chopper-Modulated Circuit Having Four Circuit Modes". In Chapter I we discussed the chopper-modulated circuit having common two circuit modes. Here we generally extend the foregoing analytical method for a periodically interrupted electric circuit having m circuit modes and driven by a complex sine wave input. Basing on this method, only a type of most practical interest, that is, the transformer coupled chopper-modulated circuit which is frequently used with conventional chopper amplifiers, is treated.

The transient and the steady-state responses to sine wave and step inputs are easily obtained, and these numerical results are illustrated to make clear the transmission characteristics of the chopper-modulated circuit. The difference of the characteristics between the "break before make" and "make before break" types of the chopper-modulated circuit under consideration is clarified to some extent.

Chapter III describes an approach to the "Statistical Analysis of Chopper Modulated Circuits" excited by random inputs.

In general the output response of the networks containing time variable elements such as a periodically operated switch becomes a nonstationary random function. First we introduce, in general, the statistical method of the analysis of variable networks for input signals of random function. On the basis of this technique the transmission characteristics of the chopper-modulated circuits of two types, that is, the transformer coupled chopper-modulated circuit and the resistance-capacitance coupled one, are clarified by examing the properties of the output correlation function and power spectrum.

Chapter IV introduces a mathematical method for the "Analysis of the Harmonic Producer Circuits" with a ferromagnetic saturable core coil, taking the effect of magnetic hysteresis into consideration. This method is based on the theories of the Periodically Interrupted Electric Circuits of the Third Genus, and the application of a digital computer to these theories especially plays an important role to obtain the steady-state performance of the harmonic producer as accurately as possible. From the results obtained, we can find that the effect of the hysteresis of the coil makes the peak pulse voltage decrease, and that the width of the pulse voltage increases in proportion to the increase of the measure of the hysteresis.

Chapter V is devoted to "An Analysis of Non-Linear Sampled-Data Feedback Control System". Higher order systems containing a saturating element or a backlash element are investigated by the analytical method based on the theories of the Periodically Interrupted Electric Circuits of the First Genus, and also by making use of the digital computer simulation of these method and the non-linear element under discussion.

The method presented here can be applied to any higher order systems with any non-linear element.

Some illustrative examples are treated to show the performance of the system dynamics on the basis of the analytical method presented here. The examples under consideration show that in the case of a step input as well as initial conditions existing, slight variations of initial values result in different modes of periodic oscillations, while in the case of a sinusoidal input, a slight modification of non-linear characterietics results in forced oscillations in one case and in sub-harmonic oscillations in another.

Chapter VI develops a method for "Analysis of Sampled-Data Feedback Control Systems with Finite Pulse Width".

The analytical method presented in this chapter make it possible to obtain the transient and ths steady-state response of such systems containing a sampler with any pulse width. Also the stability criterion is readily developed, and its application to systems under consideration makes clear the effects of the sampler with finite pulse width on the performance of sampled-data feedback control systems.

It is evident from the numerical results of the examples that the effects of the sampler with finite pulse width is of considerable importance for the performance of the system, and that even if the controlled object is originally unstable, its system can be made stable by making use of a sampler with finite pulse width.

The analytical results in this investigation are examined by the simulation of the control system in question by means of analog computer, and the simulated results indicate a close coincidence with the analytical ones.

CHAPTER I

A STUDY OF THE TRANSFER FUNCTION OF CHOPPER AMPLIFIERS

A Study of the Transfer Function of Chopper Amplifiers

Synopsis.

The chopper amplifier is frequently used in several types of *d.c* and *a.c* amplifiers as well as in *d.c* servomechanisms employing *a.c* control elements.

In this paper the transfer function of the chopper amplifier is derived for a sinusoidal input signal. The chopper amplifier has a chopper, or, a contact modulator at the input element of an *a.c* coupled amplifier to provide a means of converting *d.c* and low frequency signals to signals which lie within the pass band of the amplifier. Therefore, we first consider on the general analysis of the circuits containing a periodically operated switch such as a chopper. This analytical method is based on the theories of the Periodically Interrupted Electric Circuits and the complex Fourier series. The demodulation of the amplified signal is obtained by employing a synchronizing rectifier circuit, or a 2-phase induction motor at the output of the amplifier.

In these systems we can easily derive the transfer function of some types of chopper amplifiers and of which the steady-state performance can be clearly stated in detail.

1. Introduction

Choppers or contact modulators play an important role in many circuit designs where modulation (or demodulation) at a fixed frequency is required.

Their advantages for this service include extremely high ratio of open-circuit to closed-circuit resistance, almost negligible internal noise and drift, and excellent stability and reproducibility.

These properties make the chopper particularly suitable for use in several types of d.c and a.c amplifiers as well as in d.c servomechanism employing a.c control elements.

As the input element of an a.c coupled amplifier, the chopper modulator, which is driven at a fairly low audio rate such as a 60 c/s, converts d.c and low-frequency signals to signals which could be applied to the conventional amplifier. After one or more stages of voltage amplification, the signal may be demodulated in a second converter such as a synchronizing rectifier circuit to produce a high level output having essentially the input wave form.

There are various applications of the chopper amplifier stated above, for example, the amplification of very small direct voltages with a minimum of drift such as a d.c microvoltmeter, the operational amplifier in the analog computer, and the elements of the carrier-type servomechanism in which the demodulation is usually obtained by making use of a 2-phase induction motor.

In recent years, several results[1~4] have served to clarify the performance of the chopper amplifiers. Especially the analysis of the circuits[5] containing a periodically operated switch such as the chopper-modulated circuits has been progressed as well as the study on the time division multiplex system and on the theory of the time varying parameter circuit.

However, these procedures may be not sufficient to show the over-all characteristics, the steady-state and transient characteristics of the chopper amplifier.

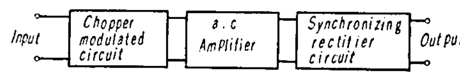

Fig. 1. Chopper amplifier.

The present paper introduces an approach[6] for the analysis of the chopper amplifier shown in Fig. 1. For the purposes of this analysis, first the chopper-modulated circuits, which are the fundamental circuits in the configurations of the chopper amplifier, are discussed more generally on the basis of the theories of the Periodically Interrupted Electric Circuits[7] and next in order to show the steady-state behaviour, the transfer function of the chopper amplifier is derived for a sinusoidal input signal through some approximations of neglecting the higher harmonics at the output of the synchronizing rectifier circuit in the chopper amplifier.

2. Analysis of the Chopper-Modulated Circuit

As was mentioned above, the chopper-modulated circuit plays an important role of the modulation which converts input signals to signals which lin within the pass band of the amplifier.

Now let us consider the general form of the chopper-modulated circuit containing one chopper and the passive network with l storage elements of L, C shown in Fig. 2, where the chopper operates ideally taking two modes (close and open) as illustrated in Fig. 3.

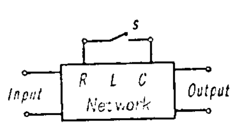

Fig. 2. Chopper-modulated circuit.

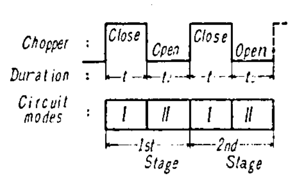

Fig. 3. Chopper operation and circuit modes.

Hence the input signal is supposed to be the voltage signal of the form as a function of the frequency ω.

$$E(t) = e^{j\omega t} \tag{1}$$

which is connected with a loop containing the j-th element of the l storage elements of L, C when the chopper is close (the 1st circuit mode), while which is connected with a loop containing the j'-th element of that when the chopper is open (the 2nd circuit mod). Then the differential equations can be set up in the matrix form, for the 1st circuit mode

$$\begin{pmatrix} z_{111} & z_{112} & \cdots & z_{112} \\ z_{121} & \ddots & & \vdots \\ \vdots & & \ddots & \vdots \\ z_{1l1} & \cdots & \cdots & z_{1ll} \end{pmatrix} \begin{pmatrix} y_1(t) \\ y_2(t) \\ \vdots \\ y_j(t) \\ \vdots \\ y_l(t) \end{pmatrix} = \begin{pmatrix} 0 \\ 0 \\ \vdots \\ e^{j\omega t} \\ \vdots \\ 0 \end{pmatrix} \tag{2}$$

and for the 2nd circuit mode

$$\begin{pmatrix} z_{211} & z_{212} & \cdots & z_{21l} \\ z_{221} & \ddots & & \vdots \\ \vdots & & \ddots & \vdots \\ z_{2l1} & \cdots & \cdots & z_{2ll} \end{pmatrix} \begin{pmatrix} y_1(t) \\ y_2(t) \\ \vdots \\ y_{j'}(t) \\ \vdots \\ y_l(t) \end{pmatrix} = \begin{pmatrix} 0 \\ 0 \\ \vdots \\ e^{j\omega t} \\ \vdots \\ 0 \end{pmatrix} \tag{3}$$

where $y_1(t), \cdots, y_l(t)$ represent the unknown currents or voltages such that if the element is a inductance L, $y(t)$'s is a current flowing through the inductance L, and if the element is a capacitance C, $y(t)$'s is a voltage at terminals of the capacitance C. The origin of time is placed at time when each circuit mode begins. z_1's and z_2's are given by

$$\begin{aligned} z_{rij} &= L\frac{d}{dt}+R \\ &= C\frac{d}{dt}+Q \qquad (r=1,2,\quad i,j=1,2,\cdots,l) \end{aligned} \tag{4}$$

or

$$\begin{aligned} z_{rij} &= 0 \\ &= \pm 1. \end{aligned}$$

By use of the Laplace transformation*, Eqs. (2) and (3) become respectively

* $F(p)=p\int_0^\infty f(t)\,e^{-pt}\,dt.$

$$\begin{pmatrix} Y_1(p) \\ Y_2(p) \\ \vdots \\ \vdots \\ Y_l(p) \end{pmatrix} = \begin{pmatrix} Z_{111}(p) & Z_{112}(p) & \cdots & Z_{11l}(p) \\ Z_{121}(p) & \ddots & & \vdots \\ \vdots & & \ddots & \vdots \\ Z_{1l1}(p) & \cdots & \cdots & Z_{1ll}(p) \end{pmatrix}^{-1} \begin{pmatrix} 0 \\ 0 \\ \vdots \\ \dfrac{p}{p-j\omega} \\ \vdots \\ 0 \end{pmatrix} + p \begin{pmatrix} Z_{111}(p) & Z_{112}(p) & \cdots & Z_{11l}(p) \\ Z_{121}(p) & \ddots & & \vdots \\ \vdots & & \ddots & \vdots \\ Z_{1l1}(p) & \cdots & \cdots & Z_{1ll}(p) \end{pmatrix}^{-1}$$

$$\cdot \begin{pmatrix} z^0_{111} & z^0_{112} & \cdots & z^0_{11l} \\ z^0_{121} & \ddots & & \vdots \\ \vdots & & \ddots & \vdots \\ z^0_{1l1} & \cdots & \cdots & z^0_{1ll} \end{pmatrix} \begin{pmatrix} y_1^{-0} \\ y_2^{-0} \\ \vdots \\ \vdots \\ y_l^{-0} \end{pmatrix} \tag{5}$$

and

$$\begin{pmatrix} Y_1(p) \\ Y_2(p) \\ \vdots \\ \vdots \\ Y_l(p) \end{pmatrix} = \begin{pmatrix} Z_{211}(p) & Z_{212}(p) & \cdots & Z_{21l}(p) \\ Z_{21l}(p) & \ddots & & \vdots \\ \vdots & & \ddots & \vdots \\ Z_{221}(p) & \cdots & \cdots & Z_{2ll}(p) \end{pmatrix}^{-1} \begin{pmatrix} 0 \\ 0 \\ \vdots \\ \dfrac{p}{p-j\omega} \\ \vdots \\ 0 \end{pmatrix} + p \begin{pmatrix} Z_{211}(p) & Z_{212}(p) & \cdots & Z_{21l}(p) \\ Z_{221}(p) & \ddots & & \vdots \\ \vdots & & \ddots & \vdots \\ Z_{2l1}(p) & \cdots & \cdots & Z_{2ll}(p) \end{pmatrix}^{-1}$$

$$\cdot \begin{pmatrix} z^0_{211} & z^0_{212} & \cdots & z^0_{21l} \\ z^0_{221} & \ddots & & \vdots \\ \vdots & & \ddots & \vdots \\ z^0_{1l1} & \cdots & \cdots & z^0_{2ll} \end{pmatrix} \begin{pmatrix} y_1^{-0} \\ y_2^{-0} \\ \vdots \\ \vdots \\ y_l^{-0} \end{pmatrix} \tag{6}$$

where z^0_{rij} are constants composed of L, C and 0, and y^{-0}'s are initial values of $y(t)$'s in each circuit mode at time $t=0$.

Now for the sake of abbreviation, Eqs. (5) and (6) can be written, respectively,

$$[Y(p)] = [\psi_1(p)] + [X_1(p)][y^{-0}] \tag{7}$$

and

$$[Y(p)] = [\psi_2(p)] + [X_2(p)][y^{-0}]. \tag{8}$$

By use of the inverse Laplace transformation**, Eqs. (7) and (8) are transformed into the time function, respectively, as, for the 1st circuit mode (chopper s : close)

$$[y(t)] = [\varphi_1(t)] + [x_1(t)][y^{-0}] \tag{9}$$

and for the 2nd circuit mode (chopper s : open)

$$[y(t)] = [\varphi_2(t)] + [x_2(t)][y^{-0}]. \tag{10}$$

In these equations the origin of time is at time when each circuit mode

---

** $f(t) = \dfrac{1}{2\pi i} \lim_{\beta\to\infty} \displaystyle\int_{r-i\beta}^{r+i\beta} \frac{F(p)}{p} e^{pt}\, dp.$

begins, here for generality, we change it to the point that the 1st circuit mode in the 1st stage begins, and we suppose the input voltage $E(t)$ to be

$$E(t) = Ee^{j(\omega t+\theta)}. \tag{11}$$

By the change of the orign of time, the input $E(t)$ is rewritten as

$$\left.\begin{aligned} E(t) &= Ee^{j(\omega nT+\theta)}\cdot e^{j\omega(t-nT)} \\ \text{and} \qquad & \\ E(t) &= Ee^{j(\omega\overline{nT+t_1}+\theta)}\cdot e^{j\omega(t-nT-t_1)} \end{aligned}\right\} \tag{12}$$

which can be supposed to be applied at $t=nT$ and at $t=nT+t_1$, respectively,

where $T=t_1+t_2=2\pi/\omega_c$: one period of the chopper s,
t_1 : duration of the chopper s closed,
t_2 : duration of the chopper s opened,
$n=0, 1, 2, \cdots\cdots\cdots, .$

Therefore the solutions of Eqs. (9) and (10) may be rewritten as follows to the input $E(t)$ of the form shown in Eq. (11) during the n-th stage, respectively,

$$[y(t)] = Ee^{j(\omega nT+\theta)}[\varphi_1(t-nT)]+[x_1(t-nT)][y(nT)] \qquad nT\leq t\leq nT+t_1 \tag{13}$$

and

$$[y(t)] = Ee^{j(\omega\overline{nT+t_1}+\theta)}[\varphi_2(t-nT-t_1)]+[x_2(t-nT-t_1)][y(nT+t_1)] \qquad nT+t_1\leq t\leq nT+T. \tag{14}$$

To determine the unknown matrices $[y(nT)]$ and $[y(nT+t_1)]$, setting $t=nT+t_1$ in Eq. (13), we have

$$[y(nT+t_1)] = Ee^{j(\omega nT+\theta)}[\varphi_1(t_1)]+[x_1(t_1)][y(nT)]. \tag{15}$$

Substituting this value into Eq. (14) and setting $t=nT+T$, we have

$$[y(nT+T)] = Ee^{j(\omega nT+\theta)}[H]+[B][y(nT)] \tag{16}$$

where

$$\left.\begin{aligned} [H] &= e^{j\omega t_1}[\varphi_2(t_2)]+[x_2(t_2)][\varphi_1(t_1)] \\ [B] &= [x_2(t_2)][x_1(t_1)]. \end{aligned}\right\} \tag{17}$$

Hence we find that Eq. (16) is the difference equation having the difference T with respect to nT. The solution $[y(nT)]$ of this equation is easily obtained according to the general method for the difference equation, described in Appendix 1, then we have

$$[y(nT)] = [B]^n[I]+Ee^{j(\omega nT+\theta)}\{e^{j\omega T}[U]-[B]\}^{-1}[H] \tag{18}$$

where $[U]$ is a unit matrix and the initial value matrix $[I]$ is given by

$$[I] = [y(0)]-Ee^{j\theta}\{e^{j\omega T}[U]-[B]\}^{-1}[H]. \tag{19}$$

The matrix $[B]^n$ is calculable by use of the Sylvester expansion theorem (see Appendix 2) as follows.

$$[B]^n = \sum_{r=1}^{l} a_r^u \frac{\prod_{\substack{s=1,\cdots,l \\ r\neq s}} \{a_s[U]-[B]\}}{\prod_{\substack{s=1,\cdots,l \\ r\neq s}} (a_s-a_r)} \tag{20}$$

where $a_1, \cdots, a_l$ are the distinct latent roots of $[B]$.

From Eqs. (16) and (18), we can determine the unknown matrices, therefore the voltage and current of the R.L.C network in any circuit modes of any stages are calculated by Eqs. (13) and (14) step by step, starting with arbitrary initial conditions.

The stability of this system could be treated by examining the latent roots of $[B]$ as follows[7].

Now assume that the maximum absolute value of the latent roots $a_1, \cdots, a_l$ is a_i, then if $|a_i| \geq 1$, the circuit is unstable and if $|a_i| < 1$, the circuit is stable.

Next consider the case of the steady-state phenomena for a sufficiently great value of n when the circuit is stable.

From Eq. (20), we have

$$\lim_{n\to\infty} [B]^n = 0\,. \tag{21}$$

In this case Eq. (18) becomes

$$[y(nT)] = Ee^{j(\omega nT+\theta)}\{e^{j\omega T}[U]-[B]\}^{-1}[H] \tag{22}$$

and substituting Eqs. (15) and (22) into Eqs. (13) and (14) yield finally

$$[y(t)] = Ee^{j(\omega nT+\theta)}([\varphi_1(t-nT)]+[x_1(t-nT)]\{e^{j\omega T}[U]-[B]\}^{-1}[H]) \qquad nT \leq t \leq nT+t_1 \tag{23}$$

and

$$[y(t)] = Ee^{j(\omega nT+\theta)}(e^{j\omega T_1}[\varphi_2(t-nT-t_1)]+[x_2(t-nT-t_1)]\{[\varphi_1(t_1)]+[x_1(t_1)] \cdot\{e^{j\omega T}[U]-[B]\}^{-1}[H]\}) \qquad nT+t_1 \leq t \leq (n+1)T\,. \tag{24}$$

Hence in order to obtain the components of the different frequency in the solutions, the steady-state solution may be expressed in the matrix Fourier series expansion

$$[y(t)] = Ee^{j(\omega t+\theta)} \sum_{n=-\infty}^{\infty} [K_m]e^{jm\omega_c t} \tag{25}$$

where $[K_m]$ is the $1\times l$ column matrix having the elements $K_{m1}, K_{m2}, \cdots, K_{ml}$ defined as follows and the harmonics of the input signal frequency do not appear in the solutions which are linealy related to the input.

Setting

$$\frac{[y(t)]}{Ee^{j(\omega t+\theta)}} = [g(t)] = \sum_{m=-\infty}^{\infty} [K_m] \tag{26}$$

we have

$$[K_m] = \frac{1}{T}\int_{nT}^{(n+1)T} [g(t)]e^{-jm\omega_c t}dt. \tag{27}$$

From Eqs. (23) and (24), the matrix $[K_m]$ is rewritten in the form

$$[K_m] = \frac{1}{T}\left\{\int_0^{t_1}([\varphi_1(t)]+[x_1(t)][D])e^{-j(\omega+m\omega_c)t}dt+\kappa\int_0^{t_2}(e^{j\omega t_1}[\varphi_2(t)] + [x_2(t)][P])e^{-j(\omega+m\omega_c)t}dt\right\} \tag{28}$$

where

$$\left.\begin{aligned}[D] &= \{e^{j\omega T}[U]-[B]\}^{-1}[H] \\ [P] &= [\varphi_1(t_1)]+[x_1(t_1)]\{e^{j\omega T}[U]-[B]\}^{-1}[H] \\ \kappa &= e^{-j(\omega+m\omega_c)t_1}\end{aligned}\right\}$$

Substituting Eq. (28) into Eq. (25), we can obtain in general the steady-state solution without any approximations which is complex but of which numerical evaluation may be readily done by such as a digital computer.

3. Transfer Function of the Chopper Amplifier

Consider the general system of the chopper amplifier shown in Fig. 1.

In this system, the synchronizing rectifier circuit is assumed to be the 2-phase induction motor which converts a.c voltages to torques, and with no loss of generality the a.c amplifier is assumed to have no attenuation and phase shift. It is right to consider that high-order harmonic components of the chopper frequency may be remarkably attenuated in this system, therefore it is sufficient to consider only those components in the output of the system having the same frequency as the fundamental frequency $\omega+\omega_c$ and $\omega-\omega_c$ of the input signal, that is, in Eq. (25) we take only $m=\pm 1$ and other components may be negligibly small at the system output.

Accordingly, in one case, the output voltage of the a.c amplifier is expressed in the form

$$y_i(t) = Ee^{j(\omega t+\theta)}\{K_{1i}e^{j\omega_c t}+K_{-1i}e^{-j\omega_c t}\} \qquad (i=1, 2, \cdots, l) \tag{30}$$

where K_{1i} and K_{-1i} is derived from Eq. (27).

Considering the condition of the synchronizing rectifier circuit, the complete system output becomes

$$v(t) = \frac{1}{2}Ee^{j(\omega t+\theta)}\{K_{1i}e^{-j\phi}+K_{-1i}e^{j\phi}\}, \tag{31}$$

multiplying the 1st term and 2nd term of (30) by $\frac{1}{2}e^{-j(\omega_c t+\phi)}$ and $\frac{1}{2}e^{j(\omega_c t+\phi)}$, respectively, where ϕ is the phase angle shifted in phase with respect to the input modulater which have to be determined to maximize the value $v(t)$.

The transfer function is the relationship between the input and output voltages in the system, then we have

$$|G(\omega)|e^{j\phi'} = \frac{v(t)}{Ee^{j(\omega t+\theta)}} = 0.5\ (K_{1i}e^{-j\phi}+K_{2i}e^{j\phi}). \tag{32}$$

In the remainder of this paper we will show the characteristics of two types of the chopper amplifier by the use of above procedures.

4. The Transformer Coupled Chopper Amplifier

The type considered in this section is widely used in many applications, of which the chopper-modulated circuit consists of the transformer type shown in Fig. 4. The equivalent circuit of this type is derived as Fig. 5.

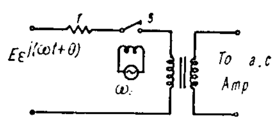

Fig. 4. Chopper-modulated circuit of transformer type.

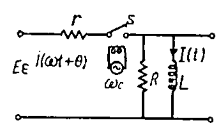

Fig. 5. Equivalent circuit of Fig. 4.

From Eqs. (2) and (3), the following differential equations can be set up, when the chopper is closed

$$L\left(\frac{r}{R}+1\right)\frac{d}{dt}y(t)+ry(t) = e^{j\omega t} \tag{33}$$

and when the chopper is open

$$L\frac{d}{dt}y(t)+Ry(t) = 0 \tag{34}$$

where $y(t)\equiv I(t)$.

Similarly, from Eqs. (22) and (23), the steady-state solution results in

$$y(t) = Ee^{j(\omega nT+\theta)}\{\varphi_1(t-nT)+x_1(t-nT)(e^{j\omega T}-B)^{-1}H\} \qquad nT\leq t\leq nT+t_1 \tag{35}$$

$$y(t) = Ee^{j(\omega nT+\theta)}x_2(t-nT-t_1)\{\varphi_1(t_1)+x_1(t_1)(e^{j\omega T}-B)^{-1}H\} \tag{36}$$

$$nT+t_1\leq t\leq (n+1)T$$

where

$$\left.\begin{array}{l}\varphi_1(t) = \dfrac{\alpha}{r}\cdot\dfrac{1}{\alpha+j\omega}(e^{j\omega t}-e^{-\alpha t}),\quad x_1(t) = e^{-\alpha t},\quad x_2(t) = e^{-\beta t}\\ B = x_2(t_2)x_1(t_1),\quad H = x_2(t_2)\varphi_1(t_1),\quad \alpha = Rr/r(r+R),\quad \beta = R/L,\end{array}\right\} \tag{37}$$

Then the output voltage $L\frac{d}{dt}y(t)$ is easily found from Eqs. (35) and (36).

According to the same process as before, we find

$$K_m = \frac{L}{T}\left\{\int_0^{t_1}(\varphi_1'(t)+x_1'(t))De^{-j(\omega+m\omega_c)t}dt + \kappa\int_0^{t_2}x_2'(t)Pe^{-j(\omega+m\omega_c)t}dt\right\} \tag{38}$$

wher $\kappa=e^{-j(\omega+m\omega_c)t_1}$, $D=(e^{i\omega T}-B)^{-1}H$, $P=\varphi_1(t_1)+x_1(t_1)D$ and accent notations mean differentiation.

For simplicity, setting the duty-ratio to be 0.5, that is,

$$t_1 = t_2 = 0.5$$

we have

$$\left.\begin{aligned} K_1 &= \frac{L}{T}\cdot\frac{\alpha}{r(\alpha+j\omega)}\left\{\frac{2\omega}{\omega_c}+\frac{\alpha}{\alpha+j(\omega+\omega_c)}+\frac{\beta}{\beta+j(\omega+\omega_c)}+0(o)\right\} \\ K_{-1} &= \frac{L}{T}\cdot\frac{\alpha}{r(\alpha+j\omega)}\left\{-\frac{2\omega}{\omega_c}+\frac{\alpha}{\alpha+j(\omega+\omega_c)}+\frac{\beta}{\beta+j(\omega-\omega_c)}+0(o)\right\} \end{aligned}\right\} \tag{39}$$

where the term $0(o)$ is almost negligible comparing with other terms.

Since the frequency ω of the input signal is less than the chopper frequency ω_c and in general α, $\beta \ll \omega_c$ is satisfied, therefore taking into account these conditions we can finally obtain the transfer function as follows by substituting Eq. (39) into Eq. (32), where some negligible terms are removed,

$$\dot{G}(\omega) = |G(\omega)|e^{i\phi'} = k\frac{1}{1+j\dfrac{\omega}{\alpha}} \tag{40}$$

where

$$k = \frac{R(L\omega+r+R)}{2\pi r(r+R)}\sin(-\phi). \tag{41}$$

In this case the maximam gain of $\dot{G}(\omega)$ is given when $\phi=-\pi/2$ and the amplitude and phase characteristics as a function of the ratio ω/α or ω/ω_c are shown in Fig. 6.

Throughout these procedures, the duty-ratio t_2/t_1 was assumed to be 0.5, now we consider the relation between the duty-ratio and output voltage. This relation is readily found by checking the coefficient K_1 or K_{-1} for some duty-ratio. The re-

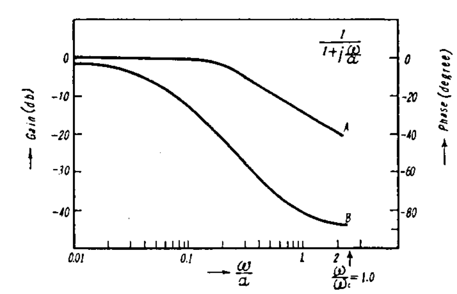

Fig. 6. Transfer function of the transformer coupled chopper amplifier
(A : amplitude characteristic)
(B : phase characteristic)

lative result is shown in Fig. 7 which shows that the optimam duty-ratio becomes 0.5 as expected

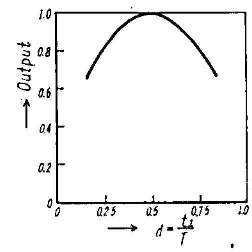

Fig. 7. Relation between the duty-ratio and output amplitude.

5. The Resistance-Capacitane Coupled Chopper Amplifier

The resistance-capacitance type shown in Fig. 8 has a high impedance characteristic in contrast with the transformer type having a low impedance one.

Similar to the previous section, the derivation of the transfer function is given in the following without careful discussions. The fundamental differential equation is represented in the form as follows, for the chopper s closed

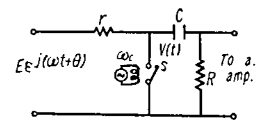

Fig. 8. R.C Chopper-modulated circuit.

$$C(r+R)\frac{d}{dt}y(t)+y(t)=e^{j\omega t} \tag{42}$$

and for the chopper s opened

$$RC\frac{d}{dt}y(t)+y(t)=0 \tag{43}$$

where $y(t)\equiv V(t)$.

Similarly, the steady-state solution is

$$y(t)=Ee^{j(\omega nT++\theta)}\{\varphi_1(t-nT)+x_1(t-nT)(e^{j\omega T}-B)^{-1}H\} \qquad nT\leq t\leq nT+t_1 \tag{44}$$

$$y(t)=Ee^{j(\omega nT+\theta)}\cdot x_2(t-nT-t_1)\{\varphi_1(t_1)+x_1(t_1)(e^{j\omega T}-B)^{-1}H\} \tag{45}$$

$$nT+t_1\leq t\leq(n+1)T$$

where

$$\left.\begin{aligned}&\varphi_1(t)=\frac{\alpha}{\alpha+j\omega}(e^{j\omega t}-e^{-\alpha t}),\quad x_1(t)=e^{-\alpha t},\quad x_2(t)=e^{-\beta t},\\&B=x_2(t_2)x_1(t_1),\quad H=x_2(t_2)\varphi_1(t_1),\quad \alpha=1/CR,\quad \beta=1/C(R+r).\end{aligned}\right\} \tag{46}$$

The input voltage $RC\frac{d}{dt}y(t)$ to the a.c complifier is readily obtained from Eqs. (44) and (45), and obviously because of the same form as that in the previous case except for several constants, we can straightforwardly write the transfer function in the form, setting the duty-ratio to be 0.5,

$$\dot{G}(\omega)=|G(\omega)|e^{j\phi'}=k\frac{1}{1+j\dfrac{\omega}{\alpha}} \tag{47}$$

where

$$k = \frac{2R+r}{2\pi(R+r)} \sin(-\phi).$$

Setting ϕ to be $-\pi/2$, the gain of $\dot{G}(\omega)$ becomes the maximum value too and the frequency characteristic in this case is quite evident to be the same one as shown in Fig. 6, but the value k and α are different.

6. Conclusion

The purpose of this paper is to explain briefly the transfer function of chopper amplifiers. First, we have discussed in general the chopper-modulated circuit by the modified theories of the Periodically Interrupted Electric Circuits. This modified analytical method has been established for the complex domain, therefore it is more general and will be applied in various fields.

In this establishment, the solution for the difference equation has played an important role and the usefulness of the complex Fourier series has been demonstrated for the steady-state analysis of the system.

The transient behaviour of the circuit also could be worked out in detail, although here it has not been examined.

Based on the modified theories presented in this paper, and provided that somewhat negligible terms could be removed, the transfer function has been determined for the two types of the chopper amplifier.

The frequency characteristics have resulted in the same function in the two configurations which were expressed in the form of the 1st order attenuation characteristic.

It is hoped that the results given in the 3rd section will not in any sense represent the limit of the application of this analysis, but it will be widely available in other fields, and that the transfer function presented in this paper may serve as a guide to the circuit designer to obtain good system performance.

Acknowledgments

The authors are very grateful to Prof. A. Kishima as well as to staff members of the Department of Electrical Engineering, II for this discussions and valuable comments in this work.

Appendix 1

Solutions of the difference equation

The linear difference equation is written in general in the form

$$\sum_{i=0}^{n} P_{xi} y_{x+i} = K_x \tag{A.1}$$

where P_{xi} and K_x represent constants or functions of x.

The general solution of this equation becomes

$$y_x = \sum_{i=1}^{n} \eta_i(x) \int \Delta c_i(x) \Delta x + c_1\eta_1(x) + c_2\eta_2(x) + \cdots + c_n\eta_n(x) \tag{A.2}$$

where the 1st term on the right side is one particular solution of the non-homogeneous equation of (A. 1) by Lagrange's method and the term $c_1\eta_1(x)+\cdots+c_n\eta_n(x)$ is the general solution of the homogeneous equation of (A. 1):

$$\sum_{i=0}^{n} P_{xi} y_{x+i} = 0 . \tag{A.3}$$

In the special case where K_x is b^x and P_{xi} is constants a_i, the perticular solution $\eta_0(x)$ of the nonhomogeneous equation can be readily derived as follows

$$\eta_0(x) = \gamma b^x / \varphi(b) \tag{A.4}$$

where $\varphi(b)$ is defined by the fact that if setting $y_x = \lambda^x$ in the following homogeneous equation

$$\sum_{i=0}^{n} a_i y_{x+i} = 0 , \tag{A.5}$$

we have

$$\varphi(\lambda) \equiv a_0 + a_1\lambda + a_2\lambda^2 + \cdots + a_n\lambda^n = 0 \tag{A.6}$$

and when we put $\lambda = b$ in (A. 6), $\varphi(b)$ is determined.

For our case treated in section 3, it is clear that, by the above method

$$\left.\begin{aligned} \varphi(\lambda) &= \lambda^T[U]-[B] \\ \lambda &= [B]^{1/T} \\ b &= e^{j\omega} \\ \gamma &= Ee^{j\theta}[H] \end{aligned}\right\} \tag{A.7}$$

and the particular solution becomes

$$\eta_0(nT) = Ee^{j(\omega nT+\theta)} \{e^{j\omega T}[U]-[B]\}^{-1}[H] \tag{A.8}$$

and the general solution of the homogeneous equation becomes

$$c_1\eta_1(nT) = [B]^n[I] , \tag{A.9}$$

therefore the solution $[y(nT)]$ can be written in the form as Eq. (18).

Appendix 2

Sylvester expansion theorem

This theorem states that, if α_r is an s_r-ple latent root of a square matrix

$[A]$ of order m, and provided that the corresponding characteristic matrix has full degeneracy for that root, and

$$s_1+s_2+\cdots+s_i = m$$

then

$$F([A]) = \sum_{r=1}^{i} F(a_r)[K(a_r)] \tag{A.10}$$

where

$$[K(a_r)] = \prod_{k \neq r}^{k=1,2,\cdots,i} \frac{(a_k[U]-[A])}{(a_k-a_r)} \tag{A.11}$$

For our case treated in section 3, the function of matrix is

$$F([A]) = [A]^n.$$

therefore the Sylvester expansion theorem for this is written as Eq. (20).

References

1) F. H. Krantz, O. M. Salati and R. S. Berkowitz : Trans. AIEE, vol. 75, No. 2, pp. 23~28, March (1957).
2) Y. Tooma and K. Awaya : Jour. Inst. Elect. Eng. of Japan, vol. 78, No. 837, pp. 683~694, June (1958).
3) T. Numakura, Z. Abe and T. Kinugawa : Jour. Inst. Elect. Eng. of Japan, vol. 79, No. 846, pp. 187~193, Feb. (1959).
4) Y. Takahashi : Jour. Inst. Elect. Eng. of Japan, vol. 79, No. 846, pp. 291~298, March (1959).
5) A. Fettweis : Trans. IRE on Circuit Theory, vol. CT-6, pp. 252~260, Sept. (1959).
6) S. Hayashi and K. Mizukami : Convention Records at annual meeting of Inst. Elect. Eng. of Japan, No. 3, July (1960).
7) S. Hayashi : Periodically Interrupted Electric Circuits, Denki-Shoin, (1961).

CHAPTER II

THE STEADY-STATE AND TRANSIENT CHARACTERISTICS OF THE CHOPPER-MODULATED CIRCUIT HAVING FOUR CIRCUIT MODES

The Steady-State and Transient Characteristics of the Chopper-Modulated Circuit Having Four Circuit Modes

Synopsis

The problem considered in this paper is one, in general, of making clear the characteristic of chopper-modulated circuits from the theoretical point of view.

The chopper-modulated circuit under consideration is assumed to have four circuit modes. In a previous investigation, we have already discussed a chopper-modulated circuit having common two circuit modes, and also have developed the valuable analytical method for a periodically interrupted electric circuit having two circuit modes excited by a complex sinusoidal input.

Here we shall generally extend the foregoing analytical method for a periodically interrupted electric circuit having m circuit modes driven by a complex sine wave input and basing on this method, we shall discuss a chopper-modulated circuit having four circuit modes. Only a type of practical interest is treated, that is, the transformer coupled chopper-modulated circuit which is frequently used with conventional chopper amplifiers, and other types which are not considered here. The method considered in this paper is an available technique explained to make clear the steady-state and transient performance of these types.

1. Introduction

In conventional chopper amplifiers, the chopper-modulated circuit commonly contains a mechanical contact modulator, or a chopper as an element of its circuit. This circuit has an important mean of converting an extremely low d-c voltage or a very low frequency alternating voltage with small amplitude into an alternating voltage being able to be amplified by a stable audio-frequency amplifier.

The usage of the modulating device of such a chopper-modulated circuit generating an alternating voltage has several advantages, that is, a very low internal impedance of the circuit, almost negligible internal noises, and no producing drift through the chopper amplifier.

The chopper may be supposed to take only two operations of "make" and "break" synchronously according to a driving force of the chopper, which is one of the types of the chopper-modulated circuits.

However, other types of operation of the chopper in practice may be considered, that is, the chopper "makes before break" and "breaks before make" synchronously at an extrmely low voltage given as an input to the chopper amplifier. Here we shall discuss in detail the latter type of operation of the chopper. This type is seen to have four circuit modes per one cycle of a driving force to the chopper as shown later in this paper.

The circuit of such a chopper-modulated circuit converting d-c or a-c voltages into an alternating voltage may be considered as a periodically interrupted electric circuit of the first genus[1]. This circuit having two circuit modes driven by a complex sinusoidal input has been already discussed, we have developed the analytical method of such a circuit and, by the use of this method, we have clarified the performance of one type of the chopper-modulated circuit[2].

First, the remainder of this paper is devoted to the development of the foregoing method, which is expanded to be applicable to the circuits having m different modes[3].

Next, the analysis of the chopper-modulated circuit having four circuit modes is worked out in detail to illustrate the application of this expanded theory, and to make clear the circuit characteristics[4][5].

2. Analytical Method of a Periodically Interrupted Electric Circuit having *m* Circuit Modes

The general form of this interrupted circuit contains one chopper and several passive elements of networks with l storage elements $L.C$ as shown in Fig. 1. It may be supposed in general that this circuit may have the different operations of the chopper in each circuit modes, and also have the variable $L.C.R$ passive elements in different circit modes. That is, it may be considered one of the networks containing variable elements.

Now let us suppose that the interrupted circuit under discussion has m

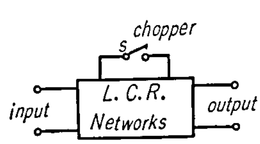

Fig. 1. Periodically interrupted electric circuit.

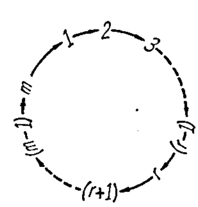

Fig. 2. Cyclic diagram illustrating the modes of a periodically interrupted electric circuit per one stage.

different circuit modes $1, 2, \cdots, r, (r+1), \cdots, (m-1), m, 1, 2, \cdots$ altermately as illustrated in Fig. 2.

Hence the input signal is assumed to be the voltage signal of the form as a function of the frequency ω

$$E(t) = \varepsilon^{j\omega t} \tag{2.1}$$

which is connected with a loop containing the r-th element of the l storage elements L, C when the operation of the interrupted circuit exists in the r-th circuit mode, while which is connected with a loop containing the k-th element of the l strorage elements L, C when the operation of the circuit exists in the $(r+1)$-th circuit mode, and so on.

Furthermore, assume that the interval t_r of the r-th circuit mode is independent of the number of the stage, where $r=1, 2, \cdots, m$.

Then the differential equations can be written in the matrix notation for the r-th circuit mode

$$\begin{pmatrix} z_{r11} & z_{r12} & \cdots\cdots & z_{r1l} \\ z_{r21} & \ddots & & \vdots \\ \vdots & & \ddots & \vdots \\ z_{rl1} & \cdots\cdots & & z_{rll} \end{pmatrix} \begin{pmatrix} y_1(t) \\ y_2(t) \\ \vdots \\ y_r(t) \\ \vdots \\ y_l(t) \end{pmatrix} = \begin{pmatrix} 0 \\ 0 \\ \vdots \\ \varepsilon^{j\omega t} \\ \vdots \\ 0 \end{pmatrix} \tag{2.2}$$

where $y_1(t), \cdots, y_l(t)$ represent the unknown currents or voltages, which are denoted in such a way that if the elemet is a inductance L, $y(t)$'s is a current flowing through the inductance L, and if the element is a capacitacce C, $y(t)$'s is a voltage at terminals of the capacitance C, and z's are given by

$$\begin{aligned} z_{rij} &= Ld/dt+R \\ &= Cd/dt+G, \end{aligned}$$

or

$$\begin{aligned} z_{rij} &= 0 \\ &= \pm 1 \quad (r = 1, 2, \cdots, m. \quad i, j = 1, 2, \cdots, l). \end{aligned}$$

For simplicity, Eq. (2.2) is expressed of the abbreviate form

$$[z_r(D)][y(t)] = [w_r(t)] \tag{2.3}$$

where $D=d/dt$, $r=1,2, \cdots, m$ and the origin of the time is chosen at the initial instant of the r-th circuit mode.

By the use of the Laplace transformation*, Eq. (2.3)

* $F(p)=p\int_0^\infty f(t)\varepsilon^{-pt}dt$

$$[Z_r(p)][Y(p)]=[W_r(p)]+p[z_r^0][y^{-0}], \tag{2.4}$$

then

$$[Y(p)] = [Z_r(p)]^{-1}[W(p)]+p[Z_r(p)]^{-1}[z_r^0][y^{-0}] \tag{2.5}$$

where the elements of the matrix $[y^{-0}]$ generally denote the initial values of the first kind corresponding to the elements of the matrix $[y(t)]$, which are identically equal to the final values of the element of the current- and voltage-matrices $[y(t)]$ in the preceding $(r-1)$-th circuit mode, and $[z_r^0]$ denote the initial matrix corresponding to the matrix $[z_r(D)]$, but in this paper, for simplicity of the analysis with no loss of generality, we shall treat the special case of that the matrix $[z_r]$ is uniform at $t=0$, or in other words, provided that $[z_r^{-0}]=[z_r^{+0}]\equiv[z_r^0]$, therefore the initial values of elements of the matrix $[y^{-0}]$ are uniform at $t=0$.

The operational solutions of Eq. (2.5) are transformed into the time function by the use of the inverse Laplace transformation*, then we have

$$[y(t)] = [\varphi_r(t)]+[x_r(t)][y^{-0}] \tag{2.6}$$

where

$$\left.\begin{aligned}[\varphi_r(t)] &= \mathfrak{H}[Z_r(p)]^{-1}[W_r(p)] \\ [x_r(t)] &= \mathfrak{H}p[Z_r(p)]^{-1}[z_r^0].\end{aligned}\right\} \tag{2.7}$$

In this equation, the origin of time is at the initial instant of the r-th circuit mode. Here for generality, we choose the origin of the time at a time when the 1st circuit mode on the 1st stage starts, and we suppose the input voltage $E(t)$ to be

$$E(t) = E\varepsilon^{j(\omega t+\theta)}. \tag{2.8}$$

By changing the origin of time, the input $E(t)$ is rewritten of the form

$$E(t) = E\exp\{j(\omega(nT+\sum_{i=1}^{r-1}t_i)+\theta)\}\cdot\exp\{j\omega(t-nT-\sum_{i=1}^{r-1}t_i)\} \tag{2.9}$$

which is seen to be applied at time $t=nT+\sum_{i=1}^{r-1}t_i$, that is, the input in the r-th circuit mode on the n-th stage, where $T=\sum_{r=1}^{m}t_r$ is one period of the operations of the chopper or a duration of one stage of the interrupted circuit, and $n=0, 1, 2, \cdots$.

Therefore, Eq. (2.6) may be rewritten as follows, for the input $E(t)$ of the form shown in Eq. (2.9) during the r-th circuit mode on the n-th stage.

$$\begin{aligned}[y(t)] = {} & E\exp\{j(\omega(nT+\sum_{i=1}^{r-1}t_i)+\theta)\}[\varphi_r(t-nT-\sum_{i=1}^{r-1}t_i)] \\ & +[x_r(t-nT-\sum_{i=1}^{r-1}t_i)][y(nT+\sum_{i=1}^{r-1}t_i)]. \quad nT+\sum_{i=1}^{r-1}t_i\leq t\leq nT+\sum_{i=1}^{r}t_i\end{aligned} \tag{2.10}$$

---

* $f(t)=\mathfrak{H}F(p)=\dfrac{1}{2\pi i}\lim_{\beta\to\infty}\int_{r-i\beta}^{r+i\beta}\dfrac{F(p)}{p}\varepsilon^{pt}\,dp.$

The initial value matrix $[y(nT+\sum_{i=1}^{r-1} t_i)]$ on the right-hand side of Eq. (2.10) is represented by the following recurrence formula as reduced from Eq. (2.10)

$$[y(nT+\sum_{i=1}^{r-1} t_i)] = E\exp\{j(\omega(nT+\sum_{i=1}^{r-2} t_i)+\theta)\}[\varphi_{r-1}(t_{r-1})] + [x_{r-1}(t_{r-1})][y(nT+\sum_{i=1}^{r-2} t_i)]. \tag{2.11}$$

For abbreviation, using a symbol τ_{r-1}^n such as $\tau_{r-1}^n = nT+\sum_{i=1}^{r-1} t_i$, then we have

$$\begin{aligned}[y(\tau_{r-1}^n)] &= E\exp\{j(\omega\tau_{r-2}^n+\theta)\}[\varphi_{r-1}(t_{r-1})]+[x_{r-1}(t_{r-1})][y(\tau_{r-2}^n)] \\ &= E\exp\{j(\omega\tau_{r-2}^n+\theta)\}[\varphi_{r-1}(t_{r-1})]+E\exp\{j(\omega\tau_{r-3}^n+\theta)\}[x_{r-1}(t_{r-1})][\varphi_{r-2}(t_{r-2})] \\ &\quad +E\exp\{j(\omega\tau_{r-4}^n+\theta)\}[x_{r-1}(t_{r-1})][x_{r-2}(t_{r-2})][\varphi_{r-3}(t_{r-3})]+\cdots \\ &\quad +E\exp\{j(\omega\tau_0^n+\theta)\}[x_{r-1}(t_{r-1})][x_{r-2}(t_{r-2})]\cdots[x_2(t_2)][\varphi_1(t_1)] \\ &\quad +[x_{r-1}(t_{r-1})][x_{r-2}(t_{r-2})]\cdots[x_1(t_1)][y(\tau_0^n)]. \end{aligned} \tag{2.12}$$

This recurrence formula means that the initial value matrix $[y(nT+\sum_{i=1}^{r-1} t_i)] \equiv [y(\tau_{r-1}^n)]$ in the r-th circuit mode on the n-th stage is given by the initial value matrix $[y(nT)] \equiv [y(\tau_0^n)]$ which could be generally determined by the given initial value matrix $[y(0)]$ in the 1st circuit mode on the 1st stage as shown later.

Now substituting Eq. (2.12) into Eq. (2.10), we have

$$\begin{aligned}[y(t)] &= E\exp\{j(\omega\tau_{r-1}^n+\theta)\}[\varphi_r(t-\tau_{r-1}^n)] \\ &\quad +E\exp\{j(\omega nT+\theta)\}[x_r(t-\tau_{r-1}^n)]\sum_{u=1}^{r-1}\{\exp(j\omega\sum_{s=1}^{r-u-1} t_s)(\prod_{s=1}^{u-1}[x_{r-s}(t_{r-s})])[\varphi_{r-u}(t_{r-u})]\} \\ &\quad +[x_r(t-\tau_{r-1}^n)](\prod_{s=1}^{r-1}[x_{r-s}(t_{r-s})])[y(nT)]. \qquad \tau_{r-1}^n \le t \le \tau_r^n \end{aligned} \tag{2.13}$$

Setting $t=nT+T$ and $r=m$ in Eq. (2.13), we obtain the important relation of the form

$$[y(nT+T)] = E\exp\{j(\omega nT+\theta)\}[H]+[B][y(nT)] \tag{2.14}$$

where

$$\left.\begin{aligned}[H] &= \sum_{u=0}^{m-1}\{\exp(j\omega\sum_{s=1}^{m-u-1} t_s)(\prod_{s=0}^{u-1}[x_{m-s}(t_{m-s})])[\varphi_{m-u}(t_{m-u})]\} \\ [B] &= \prod_{s=0}^{m-1}[x_{m-s}(t_{m-s})]. \end{aligned}\right\} \tag{2.15}$$

Since it is evident that Eq. (2.14) is the difference equation having the difference T with respect to nT, the solution $[y(nT)]$ of this equation is easily determined by the general method solving the difference equation which was described in detail in Appendix 1 of References (2).

The result becomes

$$[y(nT)] = [B]^n[I]+E\exp\{j(\omega nT+\theta)\}\{\exp(j\omega T)[U]-[B]\}^{-1}[H] \tag{2.16}$$

where $[U]$ is a unit matrix and the initial value matrix $[I]$ is given by

$$[I] = [y(0)]-E\exp(j\theta)\{\exp(j\omega T)[U]-[B]\}^{-1}[H]. \tag{2.17}$$

The matrix $[B]^n$ is calculable by the use of the Sylvester expansion theorem (see Appendix 2 in References (2)) of the form

$$[B]^n = \sum_{r=1}^{l} a_r^n \frac{\prod\limits_{\substack{s=1,2,\cdots,l \\ r\neq s}} \{a_s[U]-[B]\}}{\prod\limits_{\substack{s=1,2,\cdots,l \\ r\neq s}} (a_s-a_r)} \tag{2.18}$$

where $a_1, \cdots, a_l$ are the distinct latent roots of $[B]$.

Substituting Eq. (2.16) into Eq. (2.13), the solution $[y(t)]$ can be determined, that is, the current and voltage of the interrupted circuit in any circuit mode on any stage are obtained in general with given initial values.

Now, clearly as was mentioned in References (2), the periodically interrupted circuit in question is stable, provided that the matrix $[B]$ has distinct latent roots and the absolute value of every root is less than unity.

If we consider only the case of the steady-state phenomena for sufficiently great value of n when the circuit is stable, then we have, from Eq. (2.18)

$$\lim_{n\to\infty} [B]^n = 0 \tag{2.19}$$

Therefore the intial value matrix $[y(nT)]$ becomes more simple forms as

$$[y(nT)] = E\exp\{j(\omega nT+\theta)\}\{\exp(j\omega T)[U]-[B]\}^{-1}[H] \tag{2.20}$$

and substituting Eq. (2.20) into Eq. (2.13) results in the steady-state solution.

3. Steady-State Characteristics of the Chopper-Modulated Circuit

Now let us consider a transformer coupled chopper-modulated circuit shown in Fig. 3, having four circuit modes which is a type of "break before make" as illustrated in Fig. 4.

Here we replace this modulated circuit by an equivalent circuit shown in Fig. 5, whose circuit constants are reduced to those on the primary side of an input transformer, and the chopper on s_1 and on s_2 are equivalent to the

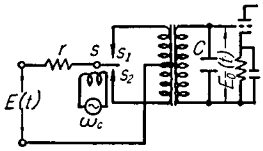

Fig. 3. Transformer coupled chopper-modulated circuit.

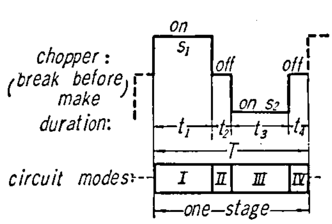

Fig. 4. Chopper operation and circuit modes.

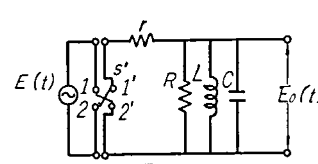

Fig. 5. Equivalent circuit corresponding to Fig. 3 (s on s_1 : 1–1′ & 2–2′, s on s_2 : 1–2′ & 1′–2).

switch s' on 1-1′ & 2-2′ and on 1-2′ & 2-1′ in Fig. 5 respectively.

By the application of the method in above section to the problem in this case, we can easily obtain the steady-state solution as follows.

The elements of the matrices in Eq. (2.13) in this case are given by

$$[y(t)] = \begin{bmatrix} y_1(t) \\ y_2(t) \end{bmatrix} \tag{3.1}$$

where $y_1(t)$ is the current flowing through the inductance L and $y_2(t)=E_0(t)$ is the terminal voltage of the capacitance C.

$$[\varphi_1(t)] = -[\varphi_3(t)] = \begin{bmatrix} \varphi_{11}(t) \\ \varphi_{12}(t) \end{bmatrix} \tag{3.2}$$

and

$$[\varphi_2(t)] = [\varphi_4(t)] = 0 \tag{3.3}$$

where

$$\varphi_{11}(t) = \mathfrak{H}p/\{\Delta_1(p-j\omega)\}, \quad \varphi_{12}(t) = \mathfrak{H}Lp^2/\{\Delta_1(p-j\omega)\}\,.$$

$$[x_1(t)] = [x_3(t)] = \begin{bmatrix} x_{111}(t), & x_{112}(t) \\ x_{121}(t), & x_{122}(t) \end{bmatrix} \tag{3.4}$$

where

$$x_{111}(t) = \mathfrak{H}\{LCrp^2+L(1+r/R)p\}/\Delta_1, \quad x_{112}(t) = \mathfrak{H}(LCp)/\Delta_1,$$
$$x_{121}(t) = \mathfrak{H}-(rLp)/\Delta_1, \quad x_{122}(t) = \mathfrak{H}(LCrp^2)/\Delta_1\,.$$

$$[x_2(t)] = [x_4(t)] = \begin{bmatrix} x_{211}(t), & x_{212}(t) \\ x_{221}(t), & x_{222}(t) \end{bmatrix} \tag{3.5}$$

where

$$x_{211}(t) = \mathfrak{H}\{LCp^2+(L/R)p\}/\Delta_2, \quad x_{212}(t) = \mathfrak{H}Cp/\Delta_2, \quad x_{221}(t) = \mathfrak{H}-Lp/\Delta_2,$$
$$x_{222}(t) = \mathfrak{H}LCp^2/\Delta_2$$

and

$$\Delta_1 = LCrp^2+L(1+r/R)p+r, \quad \Delta_2=LCp^2+(L/R)p+1\,.$$

By introducing the steady-state solutions in each circuit mode from Eq. (2.13), the solutions are expressed of the form, when n is sufficiently great value

1) for the 1st circuit mode

$$[y(t)] = E\exp\{j(\omega nT+\theta)\}[\varphi_1(t-nT)]+[x_1(t-nT)][y(nT)]$$
$$nT \leq t \leq nT+t_1 \tag{3.6}$$

2) for the 2nd circuit mode

$$[y(t)] = E\exp\{j(\omega nT+\theta)\}[x_2(t-nT-t_1)][\varphi_1(t_1)]+[x_2(t-nT-t_1)][x_1(t_1)][y(nT)]$$
$$nT+t_1 \leq t \leq nT+t_1+t_2 \tag{3.7}$$

3) for the 3rd circuit mode

$$[y(t)] = E\exp\{j(\omega(nT+t_1+t_2)+\theta)\}[\varphi_3(t-nT-t_1-t_2)]$$
$$+E\exp\{j(\omega nT+\theta)\}[x_3(t-nT-t_1-t_2)][x_2(t_2)][\varphi_1(t_1)]$$
$$+[x_3(t-nT-t_1-t_2)][x_2(t_2)][x_1(t_1)][y(nT)]$$
$$nT+t_1+t_2 \leq t \leq nT+t_1+t_2+t_3 \qquad (3.8)$$

4) for the 4th circuit mode

$$[y(t)] = E\exp\{j(\omega(nT+t_1+t_2)+\theta)\}[x_4(t-nT-t_1-t_2-t_3)][\varphi_3(t)]$$
$$+E\exp\{j(\omega nT+\theta)\}[x_4(t-nT-t_1-t_2-t_3)][x_3(t_3)][x_2(t_2)][\varphi_1(t_1)]$$
$$+[x_4(t-nT-t_1-t_2-t_3)][x_3(t_3)][x_2(t_2)][x_1(t_1)][y(nT)]$$
$$nT+t_1+t_2+t_3 \leq t \leq nT+T \qquad (3.9)$$

where

$$[y(nT)] = E\exp\{j(\omega nT+\theta)\}\{\exp(j\omega T)[U]-[B]\}^{-1}[H]. \qquad (3.10)$$

Substituting Eqs. (3.1), (3.2), (3.3), (3.4) and (3.5) into Eqs. (3.6), (3.7) (3.8) and (3.9), we can determine the steady-state solutions in this case.

Now to illustrate the present technique, some numerical results are presented as follows, by making use of the Digital Computer (KDC-1).

The circuit constants are assumed to be

$$r = 5\times10^2\,\Omega, \quad R = 10^3\,\Omega, \quad C=(5/\pi)\times10^{-6}\,F, \quad L = 1/20\pi\,H$$

and the chopper is driven synchronously at ω_c=1000 cycle per second and, that is, $t_1=t_3=4\times10^{-4}$ sec, $t_2=t_4=1\times10^{-4}$ sec and $T=10^{-3}$ sec, and $n=10^{\alpha}$ is a sufficient great value, where α is integer.

Moreover the input signal to the chopper-modulated circuit under discussion is supposed to be $\sin\omega t$, putting $E=1$ and $\theta=0$

$$E(t) = E\varepsilon^{j(\omega t+\theta)} = \mathcal{I}m(e^{j\omega t}).$$

First we examine the stability of the circuit in question whether it is stable or not, by checking the matrix $[B]$ of the form

$$[B] = \begin{bmatrix} 3.981870\times10^{-1}, & 2.000955\times10^{-5} \\ 6.219725, & 4.895580\times10^{-1} \end{bmatrix} \qquad (3.11)$$

Solving the following characteristic function of the matrix $[B]$

$$\delta\{\lambda[U]-[B]\} = 0, \qquad (3.12)$$

the latent roots λ of the matrix $[B]$ are

$$\lambda_1 = 4.881754\times10^{-1}$$

and
$$\lambda_2 = 3.995696\times10^{-1},$$

whose volues are less than unity, then the circuit is stable.

From Eqs. (3.6), (3.7), (3.8) and (3.9), the wave forms of the modulated output $E_0(t)$ are obtained as illustrated in Figs. 6, 7, 8 and 9 with the sine wave

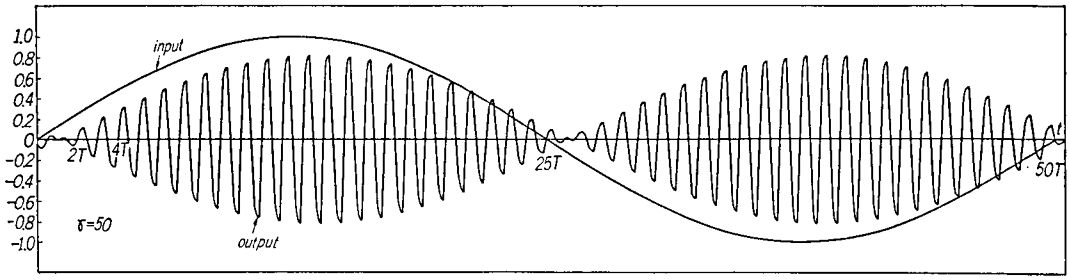

Fig. 6. Wave form of the modulated output voltage in steady-state where $\gamma=\omega_c/\omega=50$.

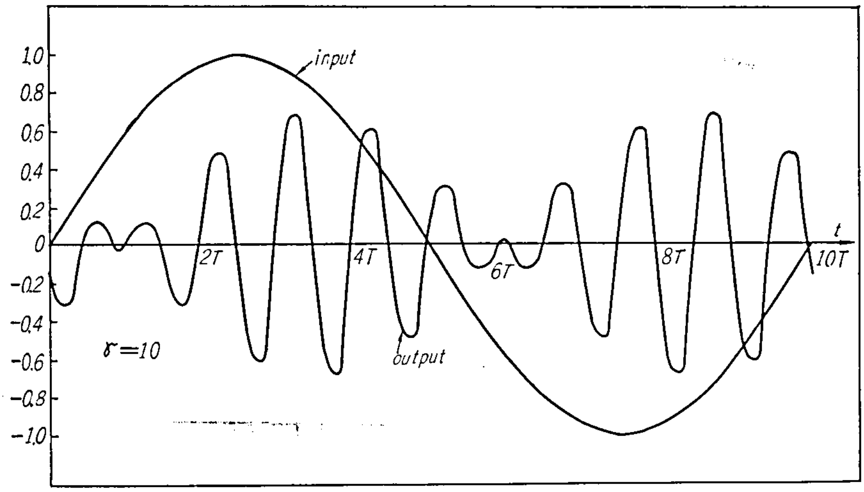

Fig. 7. Wave form of the modulated output voltuge in steady-state where $\gamma=10$.

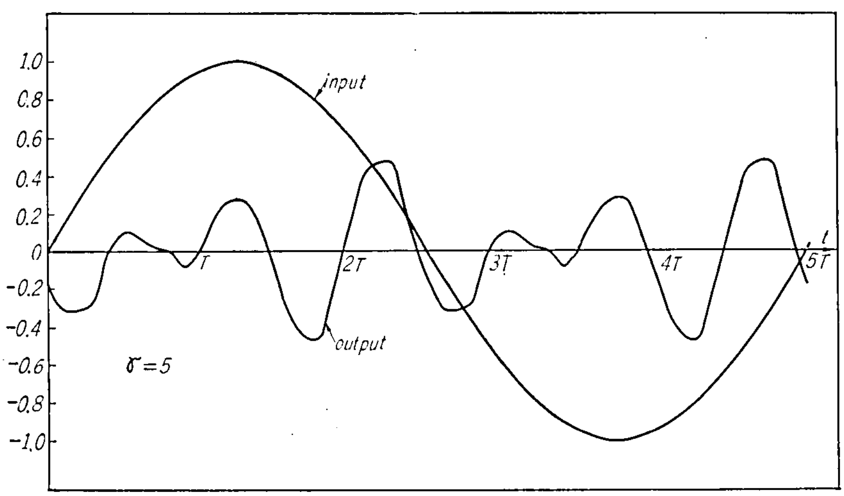

Fig. 8. Wave form of the modulated output voltage in steady-state where $\gamma=5$.

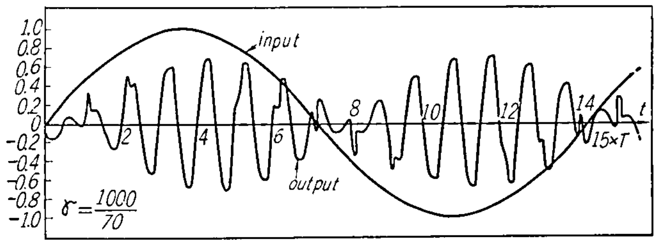

Fig. 9. Wave form of the modulated output voltage in steady-state where $\gamma=1000/70$ is irrational.

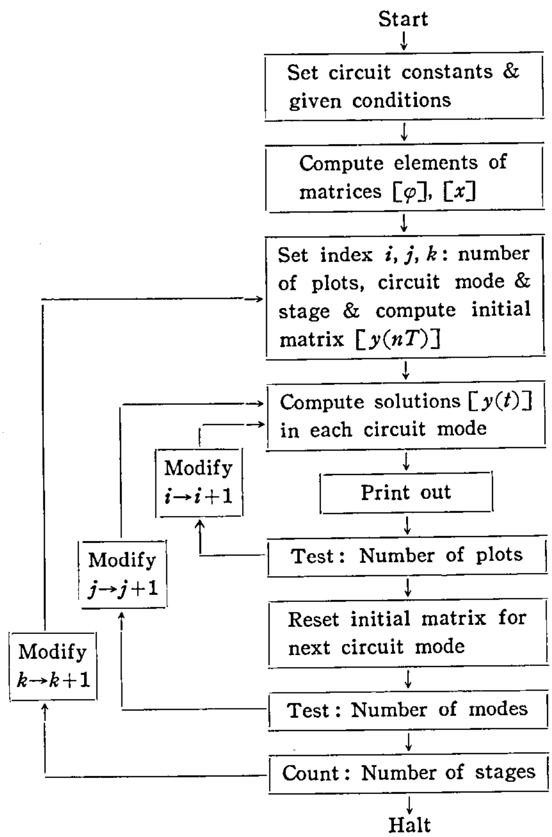

Fig. 10. Digital computer flowchart for calculating the modulated output voltage in steady-state.

input, whose calculations have been done in such a way as shown in Fig. 10.

By virtue of Figs. 6 and 7, the wave forms are considered sufficiently good results when $\gamma=\omega_c/\omega$ is a large value to some extent, but, when γ is small, the wave form is slightly distorted and its magnitude is highly decreased too, as shown in Fig. 8.

When γ is irrational, the wave form is remarkably distorted as indicated in Fig. 9, whose phenomena seems physically to exist in the circuit considering the experimental point of view.

From many numerical calculations of the wave forms of the modulated outputs, Fig. 11 illustrates the frequency response of the transformer coupled chopper-modulated circuit, that is, the amplitue and phase characteristics as a function of the ratio ω/ω_c.

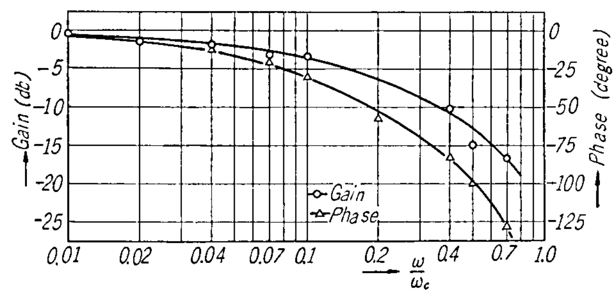

Fig. 11. Frequency response of the transformer coupled chopper-modulated circuit.

4. Transient Characseristics of the Chopper-Modulated Circuit

In this section we first consider the transient response of the same circuit of the type of the "break before make" treated in the 3rd section to a sinusoidal input. Next the transient response to a step input is discussed for two types of the "break before make" and "make before break" of the transformer coulped chopper-modulated circuit.

4.1. The Transient Response to the Sinusoidal Input

Setting the constants to be the same one as one in above section and other conditions are the same one too, the results can be obtained by using Eq. (2.13) where we take first $n=0$ and next $n=1$ and so on according to step by step calculations, and assume $[y(0)]=0$.

By means of the Digital Computer (KDC–1), the transient response of the transformer coupled chopper-modulated circuit of the type of the "break before make" is illustrated in Figs. 12 and 13 for the sine wave input with a frequency of 40 c/s and with a frequency of 100 c/s respectively, when the frequency of the chopper is 1000 c/s.

Accordingly it is concluded that in such a case where the frequency of input signal is 40 c/s or 100 c/s with respect to the chopper frequency 1000 c/s, the transient phenomena may be almost diminished in one cycle of the frequency of the input signal.

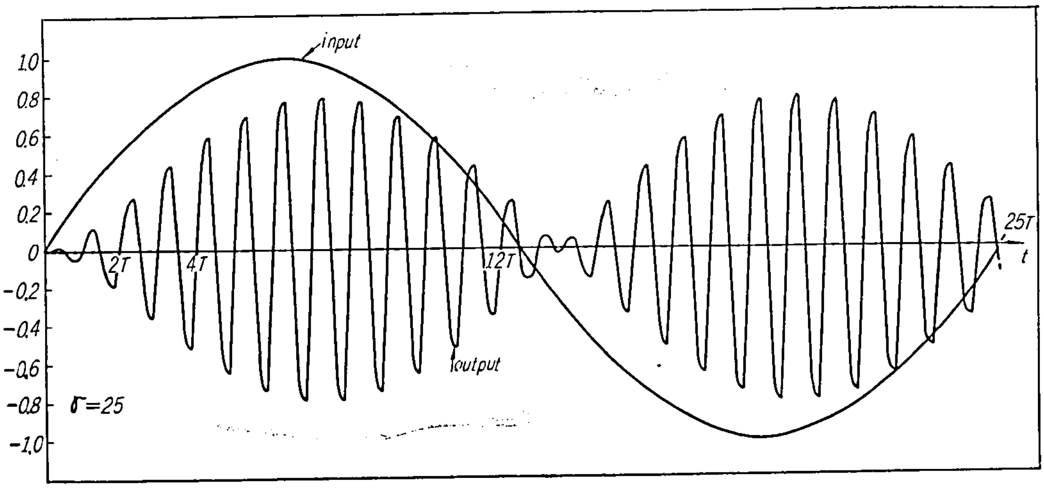

Fig. 12. Transient response of the modulated output voltage to the sinusoidal input where $\gamma=25$.

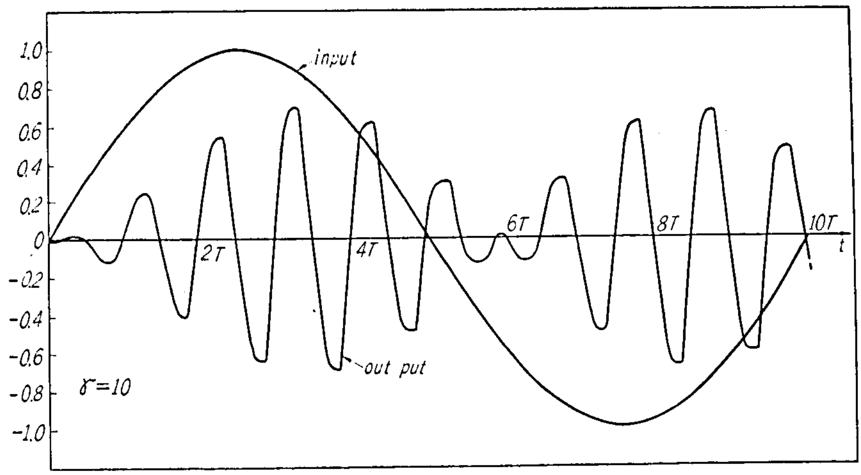

Fig. 13. Transient response of the modulated output voltage to the sinusoidal input where $\gamma=10$.

4.2. The Transient Response to the Step Input

For comparison, we consider the performances of the "break before make" and "make before break" types of the circuit shown in Fig. 3.

In the case of the latter, the chopper s operates of the form as shown in Fig. 14, therefore, for simplicity of the analysis, we may take the equivalent circuit shown in Fig. 15 corresponding to Fig. 3, in which the operation of the of the chopper s is replaced by the switch s' and s'' synchronously operating of the form as illustrated in Fig. 16 and an added resistance R' in Fig 15 is very small such as a contact one of the switch.

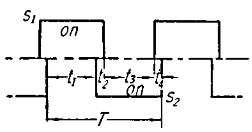

Fig. 14. Chopper operation of the "make before break" type.

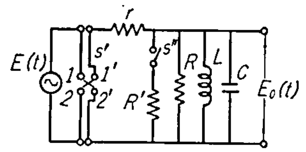

Fig. 15. Equivalent circuit when the chopper operates of the form as shown in Fig. 14.

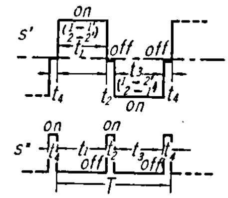

Fig. 16. Operations of the switch s' and s'' corresponding to the chopper s.

The operations of the switch s' and s'' are considered in such a way that when the chopper s is on s_1, the switch s' is off and s'' is on during t_4 and t_2, and during t_1 the switch s' is on (1–1′) & (2–2′) and s' is off, and that when the chopper s is on s_2, the swich s' is off and s'' is on during t_2 and t_4, and during t_3 the switch s' is on (1–2′) & (2–1′) and s'' is off.

The solutions in two cases under consideration become of the simple forms described in no complex domain, since the input signal is a unit step one.

Putting $n=0$, $\theta=0$ and $[y(0)]=0$ in Eqs. (3.6), (3.7), (3.8) and (3.9), the transient solutions to a unit step input are written of the forms, only on the 1st stage

1) for the 1st circuit mode

$$[y(t)] = [\varphi_1(t)] \qquad 0 \leq t \leq t_1 \tag{4.1}$$

2) for the 2nd circuit mode

$$[y(t)] = [\varphi_2(t-t_1)] + [x_2(t-t_1)][\varphi_1(t_1)] \qquad t_1 \leq t \leq t_2 \tag{4.2}$$

3) for the 3rd circuit mode

$$[y(t)] = [\varphi_3(t-t_1-t_2)] + [x_3(t-t_1-t_2)][\varphi_2(t_2)] + [x_3(t-t_1-t_2)][x_2(t_2)][\varphi_1(t_1)] \qquad t_2 \leq t \leq t_3 \tag{4.3}$$

4) for the 4th circuit mode

$$\begin{aligned}[y(t)] = {} & [\varphi_4(t-t_1-t_2-t_3)] + [x_4(t-t_1-t_2-t_3)][\varphi_3(t_3)] \\ & + [x_4(t-t_1-t_2-t_3)][x_3(t_3)][\varphi_2(t_2)] \\ & + [x_4(t-t_1-t_2-t_3)][x_3(t_3)][x_2(t_2)][\varphi_1(t_1)] \qquad t_3 \leq t \leq t_4\end{aligned} \tag{4.4}$$

where the elements of the matrices are given by Eqs. (3.1), (3.2), (3.3), (3.4) and (3.5), but in the case of the "make before break" type, the resistance R in Eqs. (3.2), (3.4) and (3.5) must be replaced by $R_0=RR'/(R+R')$.

The transient solutions in any circuit mode on other stage are determined by step by step calculations basing on Eqs. (4.1), (4.2), (4.3) and (4.4).

The transient response to the unit step input is plotted as indicated in

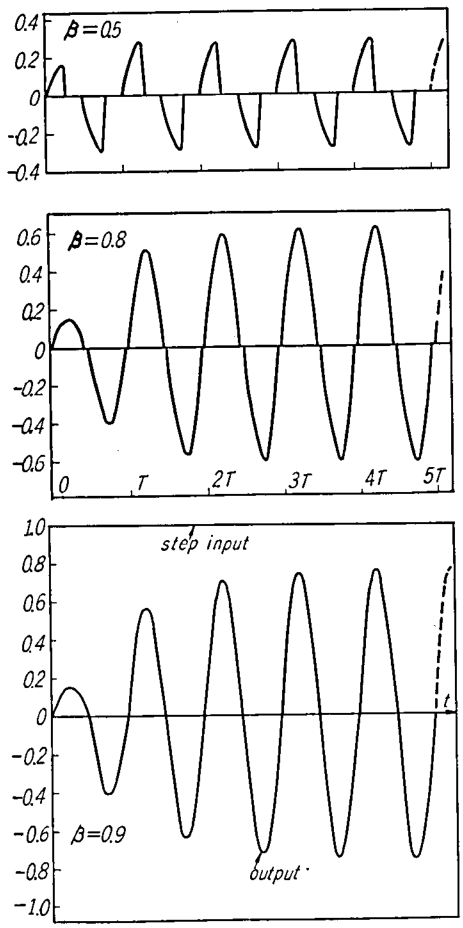

Fig. 17. Transient response to the unit step in the "make before break" type of the chopper where $\beta=0.5$, 0.8 and 0.9 respectively.

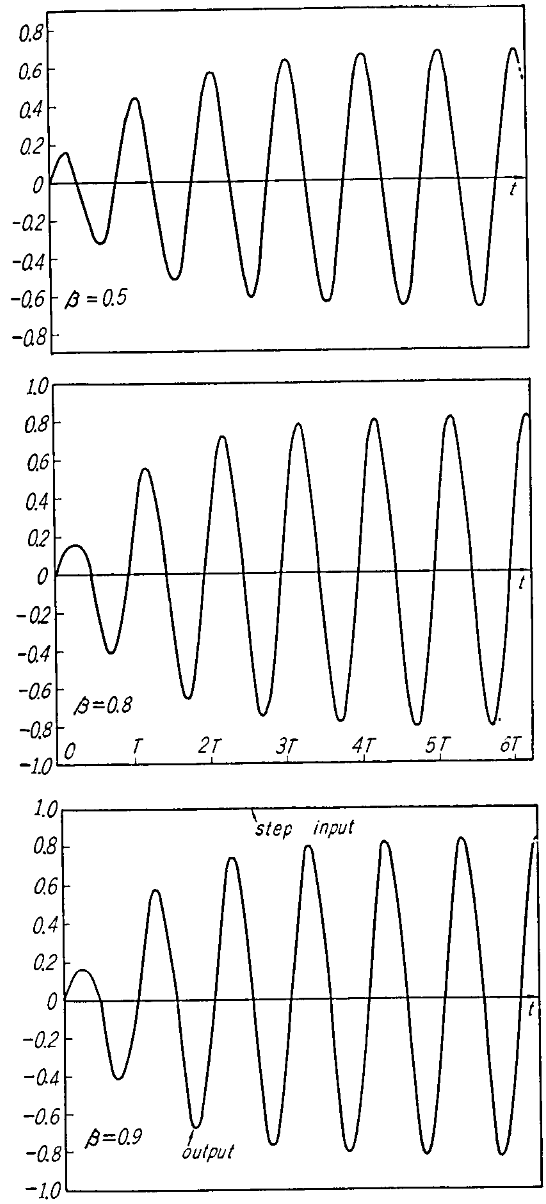

Fig. 18. Transient response to the unit step in the "break before make" type of the chopper where $\beta=0.5$, 0.8 and 0.9 respectively.

Figs. 17 and 18 by means of the Digital Computer (KDC–1), assuming that the constants and conditions are the same one as the previous case, but that in the case of the "make before break" type, the resistance R' is $R'=0.1\Omega$.

Figs. 17 and 18 illustrate the transient responses at three cases of $\beta=0.5$, 0.8 and 0.9 in the "make before break" (M.b.B) and "break before make" (B.b.M) types of the chopper respectively, where $\beta=t_1/(t_1+t_2)$.

From many numerical results of these transient responses, the transient upper envelopes of the modulated outputs to the unit step input are plotted

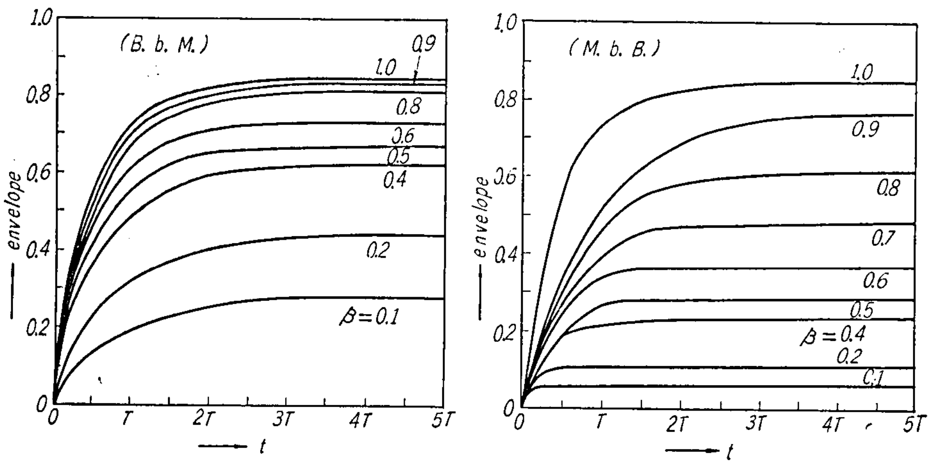

Fig. 19. Transient upper envelopes of the modulated output voltage to the unit step input when the operation of the chopper is (B.b.M) and (M.b.B) types respectively.

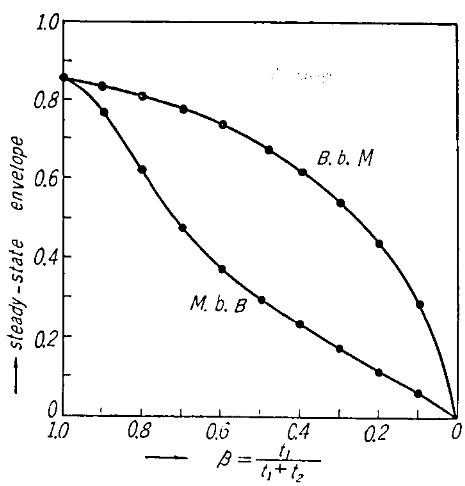

Fig. 20. Relations between the steady-state envelope and duty-ratio β for the *d.c* input signal.

with respect to the parameter of a duty-ratio β as shown in Fig 19 comparing (B.b.M) with (M.b.B) types.

Consequently it is apparent that when the response of envelope of the output becomes the steady-state value, we can obtain the relation between the envelope of the modulated output and duty-ratio β for the d.c input signal to the chopper-modulated circuit as illustrated in Fig. 20, which shows the great difference between (B.b.M) and (M.b.B) types.

From these results, it is concluded that the (B.b.M) type is superior to the (M.b.B) with respect to the performance of the chopper-modulated circuit under discussion.

5. Conclusion

It has been the purpose of this paper to examine the transient and steady-state response of the chopper-modulated circuit to sine wave and step inputs.

First we have introduced in general the analytical method of the periodically interrupted electric circuits of first genus having m circuit modes in complex domain.

On the basis of this new techniques, the transmission characteristics of the chopper-modulated circuits of two types have been clarified by observing the numerical results by means of the Digital Computer (KDC-1).

As the steady-state response of the output, the frequency response of the output, that is, the amplitude and phase characteristics have been obtained clearly only in the case of the "break before make" type of the transformer coupled chopper-modulated circuit, but in another case, not considered here, those performances could be obtained by the similar way of the previous case.

It is found that the transient behaviour of the output to the sinusoidal input is almost diminished in one cycle of the frequency of the input.

While for the unit step input, the transient response of the output have been made clear in both cases of the "break before make" and "make before break" types of the chopper-modulated circuit, and these results have shown the great difference of the characteristics between these two types.

It is hoped that the results given in this paper may serve as a reference to the circuit designer as well as other fields and that this analytical method will be widely available in other fields.

Acknowledgments

The authorse are very grateful to Prof. A. Kishima as well as to the other members of the Department of Electrical Engineering, II for their discussions and valuable comments in this work. Thanks are also due to staff members of the center of the Digital Computer (KDC-1), University of Kyoto, for their helps to our numerical computations.

References

1) S. Hayashi: Periodically Interrupted Electric Circuits; Denki-shoin, (1961).
2) S. Hayashi and K. Mizukami: A Study of the Transfer Function of Chopper Amplifiers; Memoirs of Faculty of Engineering, Kyoto University, Vol. XXVI, part 3, July (1964).
3) S. Hayashi and K. Mizukami: Analysis of the Chopper-Modulated Circuit having *m* Circuit Modes; Convention Records at Joint Meeting of Inst. of Elect. Eng. of Japan, No. 1-7, Nov. (1961).
4) S. Hayashi and K. Mizukami: Frequency Response of the Chopper-Modulated Circuit having *m* Circuit Modes; Convention Records at Joint Meeting of Inst. of Elect. Eng. of Japan, No. 39, April (1962).
5) S. Hayashi and K. Mizukami: Transient Characteristics of the Chopper-Modulated Circuit; Convention Records at Joint Meeting of Inst. of Elect. Eng. of Japan, No. 1-5, Nov. (1962).

33 項欠

CHAPTER III

STATISTICAL ANALYSIS OF CHOPPER-MODULATED CIRCUITS

Statistical Analysis of Chopper-Modulated Circuits

Synopsis.

This paper describes an approach to the statistical analysis of chopper-modulated circuits excited by random inputs.

In general the output response of those networks containing time variable elements such as a periodically operated switch, to say, the chopper, becomes the nonstationary random function, even though the input signal of the random function to networks is stationary, therefore the analytical method has to be considered for the nonstationary random process.

In this paper we introduce the available technique for such process according to Zadeh's methods which are probably the powerful tools for the analysis of linear variable networks.

The two types of practical interest are treated, that is, the transformer coupled chopper-modulated circuit and the resistance-capacitance coupled chopper-modulated circuit which are frequently used to conventional chopper amplifiers. The results obtained in this paper make clear commonly the fundamental statistical characteristics of these circuits.

1. Introduction

The chopper amplifier consists essentially of the chopper-modulated circuit, the a.c conventional amplifier and the synchronizing rectifier circuit.

In recent years this amplifier has been developed in many fields and frequently used in several types of d.c and a.c amplifiers as well as in the control process.

The chopper-modulated circuit containing a periodically operated switch plays an important role in the system of chopper amplifiers to convert input signals to signals which could be amplified in the a.c conventional amplifier.

There has been a significant advance in several studies on the characteristic of the chopper-modulated circuit for regular inputs such as a sine wave signal, but the response of the chopper-modulated circuit to random inputs has been not considered practical on the whole.

It is necessary to make clear the performance of the chopper-modulated circuit to random inputs, because it becomes an availiable element in the control process at the present time.

In the control field the statistical method of the analysis and synthesis of the system has remarkably progressed, but if variable elements are contained in the control system, then it is well known that of which the statistical analysis probably becomes the most difficult problem.

However it should be noted that an attempt to the statistical analysis of linear variable networks has been made in the past notably by L. A. Zadeh who established the theorem[1], that is, the correlation function of the input and output of a variable network N may formally be regarded as the input and output of a variable network N^* whose system function is the correlation function of the system function N.

The present paper will basically develop an approach[2,3] to the analysis of chopper-modulated circuits excited by random inputs by the application of Zadeh's method.

2. Statistical Method of the System Analysis

First we introduce the statistical method of the analysis of variable networks developed by L. A. Zadeh in summary.

Briefly the system function of a variable network N is defined as a function $H(j\omega\,;t)$ such that $H(j\omega\,;t)\varepsilon^{j\omega t}$ is the response of N to the exponential input $\varepsilon^{j\omega t}$. Thus denoting the input and output of N by the symbols $e_1(t)$ and $e_2(t)$, respectively. The definition of $H(j\omega\,;t)$ read

$$H(j\omega\,;t) = \left.\frac{e_2(t)}{e_1(t)}\right]_{e_1(t)=\varepsilon^{j\omega t}}.$$

The most important property of the system function of a variable network N is that it related the output and input signal of N in much the same manner as the system function of a fixed network relates its output and input signals.

Now it will be recalled that the correlation function of a signal $e(t)$ is defined by the relation

$$\Psi(\tau) = \lim_{T\to\infty}\frac{1}{T}\int_0^T e(t)e(t+\tau)dt\,. \tag{1}$$

This definition applies to any random-periodic signal, that is, a signal whose amplitude distribution at any one instant is a periodic function of them. In particular, it applies to the two extreme forms of random-periodic signals, namely, periodic signals and stationary signals. For stationary signals the correlation function may be written as

$$\Psi(\tau) = \overline{e(t)e(t+\tau)}$$

where the bar represents the operation of averaging over the ensemble.

As is well known, the correlation function and the power spectrum of a signal are Fourier transforms of each other. Thus, denoting the power spectrum of a signal by the symbol $S(\omega)$, the relation between $S(\omega)$ and $\Psi(\tau)$ reads

$$S(\omega)=\int_{-\infty}^{\infty}\Psi(\tau)\varepsilon^{-j\omega\tau}d\tau \tag{2}$$

and

$$\Psi(\tau)=\frac{1}{2\pi}\int_{-\infty}^{\infty}S(\omega)\varepsilon^{j\omega\tau}d\omega\,. \tag{3}$$

It is evident that $S(\omega)$ may be found from the knowledge of $\Psi(\tau)$ and vice versa.

Turning to the problems under consideration, it will be assumed that the transmission characteristics of a network N vary with time in a random-periodic manner. In terms of the system function of N this means that $H(j\omega\,;t)$ is a random-periodic function of time involving $j\omega$ as a parameter. The input to N is assumed to be a random-periodic function of time which is uncorrelated with $H(j\omega\,;t)$. The correlation functions of the input and output of N will be denoted by the symbol $\Psi_1(\tau)$ and $\Psi_2(\tau)$, respectively.

The problem is to establish a relation between $\Psi_1(\tau)$, $\Psi_2(\tau)$, and a function describing the pertinent statistical properties of $H(j\omega\,;t)$.

Here, without the proof of the theorem, it may be found that the pertient statistical properties of N are represented by a function which in view of its form might appropriately be called "the correlation function of the system function of the network" or, more simply, the correlation function of N. This function is denoted by the symbol $\Psi_H(\tau\,;\omega)$ and is defined by the relation

$$\Psi_H(\tau\,;\omega)=\lim_{T\to\infty}\frac{1}{T}\int_0^T H(j\omega\,;t)H(-j\omega\,;t+\tau)dt \tag{4}$$

which in the case of stationary system functions equivalent to

$$\Psi_H(\tau\,;\omega)=\overline{H(j\omega\,;t)H(-j\omega\,;t+\tau)}\,. \tag{5}$$

$\Psi_H(\tau\,;\omega)$ has a remarkable property which is that $\Psi_H(\tau\,;\omega)$ may be regarded as the system function of a variable network N^* such that the correlation function $\Psi_1(\tau)$ and $\Psi_2(\tau)$ are the input and output of this network, respectively. Hence it will be recognized, of course, that N^* is not a physical system since its system function $\Psi_H(\tau\,;\omega)$ is an even function of ω.

This result is expressed by the following relation

$$\Psi_2(\tau)=\frac{1}{2\pi}\int_{-\infty}^{\infty}\Psi_H(\tau\,;\omega)S_1(\omega)\varepsilon^{j\omega\tau}d\omega \tag{6}$$

where $S_1(\omega)$ is the power spectrum of the input

$$S_1(\omega)=\int_{-\infty}^{\infty}\Psi_1(\tau)\varepsilon^{-j\omega\tau}d\tau\,, \tag{7}$$

and $\Psi_H(\tau\,;\omega)$ is the correlation function of $H(j\omega\,;t)$.

Comparison of (6) with the relation connecting the output and input of a variable network

$$e_2(t)=\frac{1}{2\pi}\int_{-\infty}^{\infty}H(j\omega\,;t)E_1(j\omega)\varepsilon^{j\omega t}d\omega \tag{8}$$

leads to the interpretation of (6) stated above, where

$$E_1(j\omega)=\int_{-\infty}^{\infty}e_1(t)\varepsilon^{-j\omega\tau}d\tau\,. \tag{9}$$

In addition it is shown that the Fourier transforms of the input and output of a variable network are related to each other by

$$E_2(j\omega)=\int_{-\infty}^{\infty}\Gamma(j\omega'\,;j\omega)E_1(j\omega')d\omega' \tag{10}$$

where the so-called "bifrequency system function", $\Gamma(j\omega'\,;j\omega)$ is the Fourier transform of $H(j\omega'\,;\tau)\varepsilon^{j\omega'\tau}$

$$\Gamma(j\omega'\,;j\omega)=\int_{-\infty}^{\infty}H(j\omega'\,;\tau)\varepsilon^{j\omega'\tau}\varepsilon^{-j\omega\tau}d\tau\,. \tag{11}$$

Now, since the power spectra $S_1(\omega)$ and $S_2(\omega)$ are the Fourier transforms of $\Psi_1(\tau)$ and $\Psi_2(\tau)$, it follows from (10) that

$$S_2(\omega)=\int_{-\infty}^{\infty}\Gamma^*(j\omega'\,;j\omega)S_1(\omega')d\omega' \tag{12}$$

where

$$\Gamma^*(j\omega'\,;j\omega)=\int_{-\infty}^{\infty}\Psi_H(\tau\,;\omega')\varepsilon^{j\omega'\tau}\varepsilon^{-j\omega\tau}d\tau\,. \tag{13}$$

This expression provides the desired relation between the power spectra of the input and output of N.

The theorem established above regarding the relation connecting $\Psi_1(\tau)$, $\Psi_2(\tau)$, and $\Psi_H(\tau\,;\omega)$, has many practical application.

The use of this theorem will be illustrated below by its application to the problems under consideration, namely, the transformer coupled chopper-modulated circuit and the resistance-capacitance coupled chopper-modulated circuit.

3. The Transformer Coupled Chopper-Modulated Circuit

The configuration of this system is shown in Fig. 1. Hence it may be assumed that the equivalent circuit to this system is found as shown in Fig. 2

and the chopper s operates ideally as shown in Fig. 3, which is called the ideal full-wave modulator.

It is now convenient to consider that the time variable system illustrated in Fig. 4 composed of $H(j\omega\,;t)$ and $G(j\omega)$ equivalent to the transformer coupled chopper-modulated circuit, where $H(j\omega\,;t)$ is the system function of the chopper s as defined below and $G(j\omega)$ is the transfer function of the equivalent circuit shown in Fig. 2.

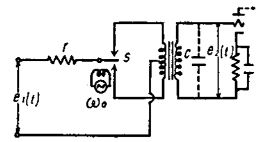

Fig. 1. Transformer coupled chopper-modulated circuit.

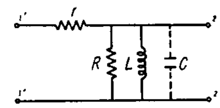

Fig. 2. Equivalent circuit.

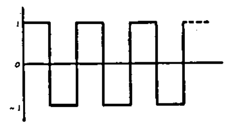

Fig. 3. Operation of chopper.

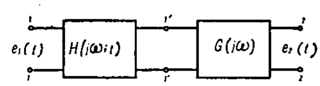

Fig. 4. Time variable system equivalent to Fig. 1.

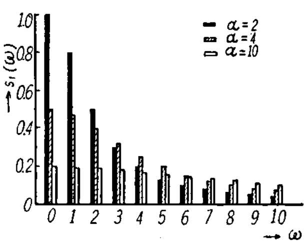

Fig. 5. Power spectrum of the input random signal.

In this case the system function $H(j\omega\,;t)$ is independent of frequency, i.e., it is of the form

$$H(j\omega\,;t)=H(t) \tag{14}$$

and the modulation process as shown in Fig. 3 can be best expressed by the Fourier series as

$$H(t)=\frac{4}{\pi}\sum_{m=0}^{\infty}\frac{1}{2m+1}\sin(2m+1)\omega_0 t \tag{15}$$

where ω_0 is the frequency of the chopper s.

Now it is assumed that the correlation function of the input signal is

$$\Psi_1(\tau)=\varepsilon^{-\alpha|\tau|} \tag{16}$$

and correspondingly its power spectrum is

$$S_1(\omega)=\frac{2\alpha}{\omega^2+\alpha^2} \tag{17}$$

which is shown in Fig. 5.

The correlation function of $H(t)$ in this case becomes

$$\Psi_H(\tau\,;\omega)=\Psi_H(\tau)=\frac{8}{\pi^2}\sum_{m=0}^{\infty}\frac{1}{(2m+1)^2}\cos(2m+1)\omega_0\tau\,. \tag{18}$$

Consequently the expression for the correlation function of the system at points 1′–1′ in Fig. 4 is given by

$$\begin{aligned}\Psi_{1'}(\tau)&=\Psi_H(\tau)\Psi_1(\tau)\\&=\frac{8}{\pi^2}\sum_{m=0}^{\infty}\frac{1}{(2m+1)^2}\cos(2m+1)\omega_0\tau\cdot\varepsilon^{-\alpha|\tau|}\,.\end{aligned} \tag{19}$$

The corresponding power spectrum is readily obtained by applying the

Fourier transforms of $\Psi_1'(\tau)$ as

$$S_1'(\omega)=\int_{-\infty}^{\infty}\Psi_1'(\tau)\varepsilon^{-j\omega\tau}d\tau\ . \tag{20}$$

Therefore the power spectrum of the output of this system is written as

$$S_2(\omega)=|G(j\omega)|^2S_1'(\omega), \tag{21}$$

which is the well-known relation connecting the power spectra of the output and input of a fixed network, in this case, $G(j\omega)$.

From (21), we have

$$S_2(\omega)=\frac{8}{\pi^2}|G(j\omega)|^2\sum_{m=0}^{\infty}\frac{1}{(2m+1)^2}\left\{\frac{a}{a^2+(\omega-\overline{2m+1}\omega_0)^2}+\frac{a}{a^2+(\omega+\overline{2m+1}\omega_0)^2}\right\}. \tag{22}$$

Although the corresponding correlation function $\Psi_2(\tau)$ may be obtained by application of the inverse Fourier transforms of $S_2(\omega)$, or the techniques of the convolution integral, the following method, however, is simpler than the direct methods above for the evaluation of $\Psi_2(\tau)$.

Now assumed that $S_2(\omega)$ can be expressed in the form

$$S_2(\omega)=\frac{P(j\omega)}{Q(j\omega)}, \tag{23}$$

then the evaluation of $\Psi_2(\tau)$ results in

$$\Psi_2(\tau)=\sum_{\mu}\frac{P(j\omega_\mu)}{\dfrac{\partial}{\partial j\omega_\mu}Q(j\omega_\mu)}\varepsilon^{j\omega_\mu t} \tag{24}$$

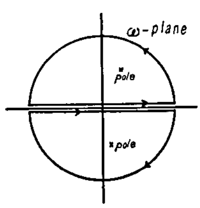

Fig. 6. Integral pass.

where $j\omega_\mu$'s is poles of $S_2(\omega)$, which is the well-known method of Heaviside's expansion.

In applying this techniques to (22), it should be remembered that since the integral pass in ω-plane must be taken as illustrated in Fig. 6, which is different in the upper plane and in the lower plane of ω, the sign of the results for poles in the lower plane should be changed.

The expression for the correlation function of the output of the system in this case reduces finally to

$$\Psi_2(\tau)=\sum_{m=0}^{\infty}\{k_{1,m}\varepsilon^{-a|\tau|}+k_{2,m}\varepsilon^{-\alpha|\tau|}\cos\omega_m\tau+k_{3,m}\varepsilon^{-\alpha|\tau|}\sin\omega_m\tau\} \tag{25}$$

where

$$\left.\begin{aligned}k_{1,m}&=\frac{16}{\pi^2}\cdot\frac{1}{(2m+1)^2}\cdot\frac{K_1a(\omega_m^2-b_1b_2)}{(\omega_m^2+b_1^2)(\omega_m^2+b_2^2)}\\ k_{2,m}&=\frac{8}{\pi^2}\cdot\frac{1}{(2m+1)^2}\cdot\left\{K+\frac{2aK_1(\omega_m^2+b_1b_2)}{(\omega_m^2+b_1^2)(\omega_m^2+b_2^2)}\right.\end{aligned}\right\} \tag{26}$$

$$\left.\begin{aligned}
k_{3,m} &= \frac{16}{\pi^2}\cdot\frac{1}{(2m+1)^2}\cdot\frac{K_1 a\omega_m(b_1-b_2)}{(\omega_m^2+b_1^2)(\omega_m^2+b_2^2)} \\
\omega_m &= (2m+1)\omega_0\,,\ \ b_1 = a+\alpha\,,\ \ b_2 = a-\alpha\,,\ \ a = Rr/L(R+r)\,, \\
K &= R^2/(R+r)^2\,,\ \ K_1 = -aK/2\,.
\end{aligned}\right\}$$

It is the important results in this paper that the statistical response of the system under consideration may be readily determined from Eqs. (22) and (25). The numerical results are illustrated in Fig. 7, which are the normalized correlation function of the output when

$$|G(j\omega)|^2 = \frac{K\omega^2}{a^2+\omega^2}, \tag{27}$$

namely, where the capacitance C is removed in the transformer coupled chopper-modulated circuit.

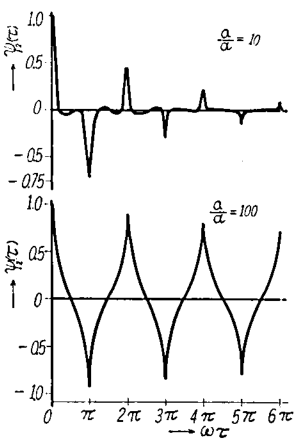

Fig. 7. Correlation function of the output in the case where $R=1000\,\Omega$, $r=50\,\Omega$, $L=1\,H$, and $\omega_0=120$.

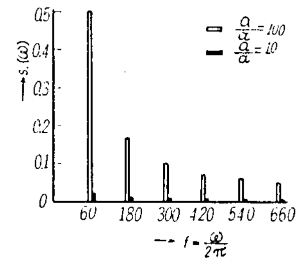

Fig. 8. Power spectrum corresponding to Fig. 7.

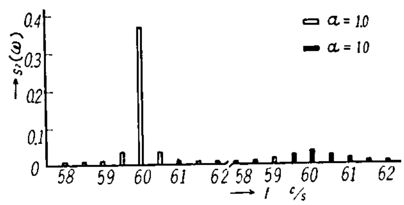

Fig. 9. Power spectra in the vicinity of the chopper frequency in the same case as Fig. 7.

The corresponding power spectrum is shown in Fig. 8 compared with each other, and Fig. 9 illustrates the spectra in the vicinity of the chopper frequency.

While on the other hand we take account of the capacitance C, the transfer function $G(j\omega)$ becomes

$$G(j\omega) = \frac{j\omega LR}{R_0+j\omega LR_1} \tag{28}$$

where

$$R_0 = r(R-\omega^2 LRC)$$
$$R_1 = R+r\,,$$

Hence assume that the following resonant condition is satisfied in the chopper-modulated circuit

$$\omega^2 = \frac{1}{LC}, \tag{29}$$

then we have

$$G(j\omega) = \frac{R}{R+r} \tag{30}$$

Substituting (30) into Eq. (22), the power spectrum $S_2(\omega)$ in this case is obtained as shown in Figs. 10 and 11, where the resonant frequency $\omega/2\pi$ is chosen to be 60 c/s which is equal to the chopper frequency, so that the capacitance C must be

$$C = \frac{1}{\omega^2 L} = \frac{10^{-4}}{1.44\pi^2} F.$$

The numerical results presented in this paper were obtained by making use of the digital computer (KDC-1) for calculating of Eqs. (22) and (25).

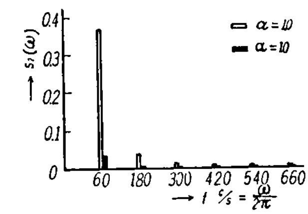

Fig. 10. Power spectrum in the case where $R=1000\Omega$, $r=500\Omega$, $\omega_0=120\pi$, $L=1\,H$ and $C=10^{-4}/1.44\pi^2 F$.

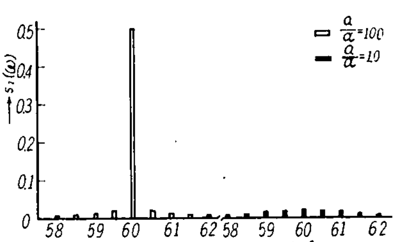

Fig. 11. Power spectra in the vicinity of the chopper frequency in the same case as Fig. 10.

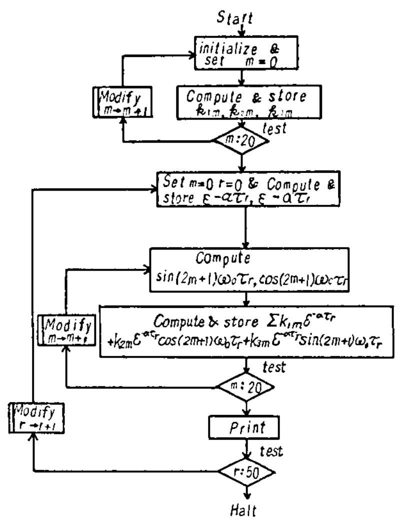

Fig. 12. Digital computer flowchart for the evaluation of the correlation function $\Psi_2(\tau)$.

The flowchart of the evaluation of, for example, the correlation function $\Psi_2(\tau)$ is shown in Fig. 12.

4. The Resistance-Capacitance Coupled Chopper-Modulated Circuit

Now consider that the configuration of this system consists of R.C elements as shown in Fig. 13.

In the same manner as the previous case, we can obtain the same form of the correlation function $\Psi_2(\tau)$ and power spectrum $S_2(\omega)$ of the output as the case of Eqs. (22) and (25) with some different constants, assuming the same random input as the form in the previous case.

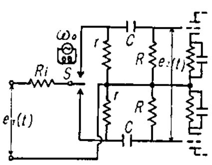

Fig. 13. R.C coupled chopper-modulated circuit.

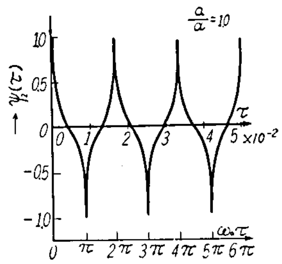

Fig. 14. Correlation function of the output of R.C coupled chopper-modulated circuit.

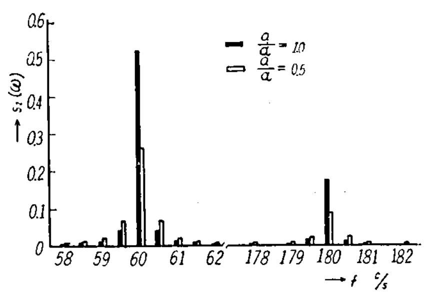

Fig. 15. Power spectra in the vicinity of 60 c/s and 180 c/s.

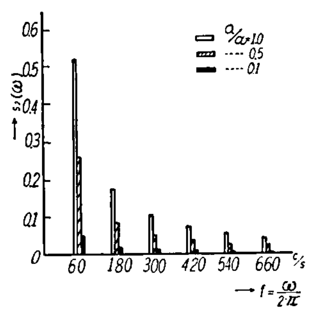

Fig. 16. Power spectrum of the output of R.C coupled chopper-modulated circuit.

The numerical results in this case were obtained by means of use of the digital computer (KDC-1) too and are shown in Figs. 14, 15 and 16 where $R=100\,\mathrm{k}\Omega$, $r=500\,\mathrm{k}\Omega$, $R=1\,\mathrm{M}\Omega$, $C=1\,\mu F$ and $\omega_0=120\pi$. Fig. 15 contains a plot of the power spectrum $S_2(\omega)$ in the vicinity of the chopper frequency as well as three times of one.

5. Conclusion

It has been the purpose of this paper to examine the output response of the chopper-modulated circuits to random inputs. First we have introduced, in general, the statistical method of the analysis of variable networks for input signals of the random function, On the basis of these techniques the transmission characteristics of the chopper-modulated circuits of two types have been clarified by observing the properties of the correlation function and power spectrum.

It is evident that this approach offers the advantages of mathematical simplicity, ease of interpretation, and the fact it is readily calcurable by making use of the digital computer.

The results given in this paper may serve as a reference to the circuit designer as well as to other fields of the random process, for instance, the control process and circuit theory.

Acknowledgements

The authors wish to express their appreciation of the valuable comments given them by Dr. S. Hoshino as well as staff members of the Department of Electrical Engineering, II. Thanks are also due to staff members of the center of the digital computer (KDC-1), University of Kyoto, for their helps to our numerical computations.

References

1) L. A. Zadeh: Correlations Functions and Power Spectra in Variable Networks; Proceedings of the IRE, vol. 38, pp. 1342~1345, Nov. (1950).
2) S. Hayashi and K. Mizukami: Statistical Analysis of Chopper-Modulated Circuits; Proceeding of the general meeting on Automatic Control in Japan, pp. 61~62, Nov. (1961).
3) S. Hayashi and K. Mizukami: Statistical Analysis of Chopper-Modulated Circuits, II; Convention Records at the annual meeting of the Institute of Electrical Engineers of Japan, No. 40, April (1962).

CHAPTER IV

ANALYSIS OF THE HARMONIC PRODUCER CIRCUITS

Analysis of the Harmonic Producer Circuits

Synopsis

This study introduces a mathematical method for the analysis of the harmonic producer circuits with a ferromagnetic saturable core coil, taking the effect of magnetic hysteresis into consideration.

This method is based on the theorems of the Periodically Interrupted Electric Circuits of the Third Genus, and on the application of the Digital Computer (KDC-1).

First we describe in general how to apply this analytical method to the basic circuit of harmonic producers to clarify its behaviour as accurately as possible, and next to the harmonic producer circuit containing an additional capacitor.

One numerical example is presented to show the performance of the harmonic producer circuit in this paper.

1. Introduction

Circuits producing a number of harmonics by means of saturable core coils have been used for the common supply of carrier currents to multi-channel carrier telephone systems. The quality and stability of the carrier current may affect the reliability of each channel of telephone systems, therefore it is important to analyze and to design the circuit generating a group of harmonics as well as possible.

The study on the hamonic producer circuits was done by various workers, such as E. Peterson, J. M. Manley and L. R. Wrathall[1] who, in 1937, investigated the operation of the harmonic generating circuit only considering the discharge pulse from the transient analytical point of view. In 1949, Fourier analysis was worked by T. Kurokawa[2] taking both the discharge and the charge pulse into consideration, and in 1953, S. Hayashi and K. Nishihara[3] applied at first time the theorems of the Periodically Interrupted Electric Circuits to this problem. Recently, in 1961, an investigation for the same systems based on the analytical method of non-linear problems established by L. A. Pipes was attempted by A. Kyogoku, Y. Oohashi and K. Iishi[4].

These investigations, however, could be considered to be established in parctice basing on some assumptions or other, because the analysis of the harmonic producer circuits with a non-linear element such as a saturable core coil might be the most difficult problem from the theoretical point of view.

Therefore the unknown problems exist to be clarified in the harmonic producer circuits. In this paper in order to make clear one of the unknown problems we attempt the analysis of the circuits taking the effect of magnetic hysteresis of the saturable core coil into consideration[5].

2. Harmonic Producer Circuits

The circuit shown in Fig. 1 is the basic circuit of harmonic producers using a saturable core coil. Another circuit containing a capacitance C_1 connected in parallel with the coil will be described in section 6.

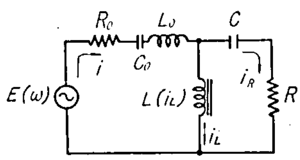

Fig. 1. Harmonic producer circuit with a ferromagnetic core coil.

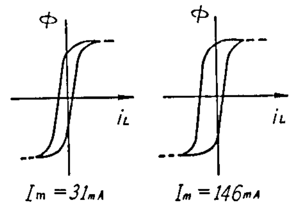

Fig. 2. Observed characteristics of the coil.

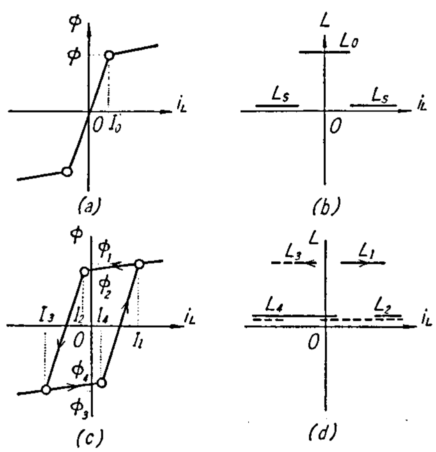

Fig. 3. Approximate characteristics of the coil.

When the current i due to the input source $E(\omega)$ with a fundamental frequency ω flows in R_0, C_0, L_0 and L circuit, the distorted current i_R including the harmonic components is generated in the output circuit of L, C and R by the change of L due to the instantaneous change of the current i.

Now we assume that the input source with a fundamental frequency ω is the current source of sinusoidal wave form and the characteristic of the ferromagnetic core coils is approximately composed of four rectilinear segments as shown in Fig. 3 (c) and of discrete values of L as shown in Fig. 3 (d).

The previous investigations have done to assume the characteristic of the saturable core coils such as in Fi. 3 (a) composed of three rectilinear segments without regard to the magnetic hysteresis. As the results presented in this paper will show later, it is not suitable to consider that the magnetic hysteresis is not taken into consideration, since it will not deform the shape remarkably but only shifts the phase of repeated pulses.

3. Analysis of the Basic Circuit

3.1. Circuit Conditions

The basic circuit of harmonic producers can be rewritten as shown in Fig. 4.

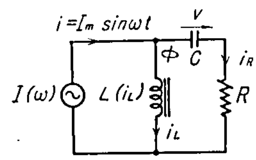

Fig. 4. The basic circuit of a harmonic producer.

The following circuit conditions are assumed:

(a) Input current has a sinusoidal wave form

$$i = I_m \sin \omega t.$$

(b) The total magnetic flux-linkage ϕ of the coil is related to the exciting current i_L by four rectilinear segments as shown in Fig. 3 (c).

Accordingly four kinds of the circuit state as follows can be presumed in the steady state per one cycle.

1. The 1-st circuit mode (in the permeable state of the coil):

$$\phi = \phi_4 + L_1(i_L - I_4), \quad I_4 \leq i_L \leq I_1.$$

2. The 2-nd circuit mode (in the positive saturated state of the coil):

$$\phi = \phi_1 + L_2(i_L - I_1), \quad i_L \geq I_2.$$

3. The 3-rd circuit mode (in the permeable state of the coil):

$$\phi = \phi_2 + L_3(i_L - I_2), \quad I_3 \leq i_L \leq I_2.$$

4. The 4-th circuit mode (in the negative saturated state of the coil):

$$\phi = \phi_3 + L_4(i_L - I_3), \quad i_L \leq I_4.$$

The transient solutions in each rectilinear region are to be found as the elements of certain matrices on applying the Laplace transformation to the basic differential equations expressed in matrix notation.

Supposing that the phenomena in equation ultimately converge to periodic ones, the resulting solutions on adjacent regions are to be equated to each other at the intersection of the rectilinear characteristics in order to determine the instant of transition.

3.2. Transient Solutions

3.2.1. Transient solutions in the 1-st circuit mode.— The circuit equations are written in the forms

$$\left.\begin{aligned} &\frac{d\phi}{dt} = v + Ri_R, \quad i_R = i - i_L, \\ &C\frac{dv}{dt} = i_R, \quad i = I_m \sin(\omega t + \theta_1), \quad i_L = \frac{\phi - \phi_4}{L_1} + I_4, \end{aligned}\right\} \tag{3.1}$$

where θ_1 represents the initial phase angle of the input current, at which the permeable state starts, and the initial conditions are supposed to be

$$\phi = \phi_4 \quad \text{at} \quad t = 0$$

and

$$\phi = \phi_1 \quad \text{at} \quad t = t_1,$$

t_1 being the duration of the state.

Putting

$$\left.\begin{aligned} &y_1(\tau) = \frac{\omega^2 C}{I_m}\phi(\tau), \quad z_1(\tau) = \frac{\omega C}{I_m}v(\tau), \quad \tau = \omega t, \quad K_1 = \frac{I_4}{I_m}, \\ &y_{\bar{1}}^0 = \frac{\omega^2 C}{I_m}\phi_4, \quad \omega CR = k, \quad \delta_1 = \frac{R}{\omega L_1}, \quad \gamma_1 = \frac{1}{\omega^2 CL} = \frac{\delta_1}{k}, \end{aligned}\right\} \tag{3.2}$$

where $y_1(\tau)$ and $z_1(\tau)$ with the subscript "1" belong to the 1-st circuit mode.

Eq. (3.1) reduces to the following dimensionless ones:

$$\left.\begin{aligned} &\left(\frac{d}{d\tau} + \delta_1\right)\{y_1(\tau) - y_{\bar{1}}^0\} - z_1(\tau) = k\{\sin(\tau + \theta_1) - K_1\}, \\ &\gamma_1\{y_1(\tau) - y_{\bar{1}}^0\} + \frac{d}{d\tau}z_1(\tau) = \sin(\tau + \theta_1) - K_1, \\ &i_R/I_m = \sin(\tau + \theta_1) - \gamma_1\{y_1(\tau) - y_{\bar{1}}^0\} - K_1. \end{aligned}\right\} \tag{3.3}$$

Denoting the operational function corresponding to $y_1(\tau)$ and $z_1(\tau)$ by $Y_1(p)$ and $Z_1(p)$ respectively, in view of Eq. (3.3) we have

$$\begin{pmatrix} p+\delta_1, & -1 \\ \gamma_1, & p \end{pmatrix}\begin{pmatrix} Y_1(p) \\ Z_1(p) \end{pmatrix} = \begin{pmatrix} k \\ 1 \end{pmatrix}\frac{\cos\theta_1 + p\sin\theta_1}{p^2+1}p + p\begin{pmatrix} y_{\bar{1}}^0 \\ z_{\bar{1}}^0 \end{pmatrix} - \begin{pmatrix} k \\ 1 \end{pmatrix}K_1. \tag{3.4}$$

Accordingly

$$\begin{pmatrix} Y_1(p) \\ Z_1(p) \end{pmatrix} = \begin{pmatrix} p, & 1 \\ -\gamma_1, & p+\delta_1 \end{pmatrix}\begin{pmatrix} k \\ 1 \end{pmatrix}\frac{(\cos\theta_1 + p\sin\theta_1)p}{(p^2+\delta_1 p+\gamma_1)(p^2+1)} + \frac{p}{p^2+\delta_1 p+\gamma_1}\begin{pmatrix} p, & 1 \\ -\gamma_1, & p+\delta_1 \end{pmatrix}$$
$$\times\begin{pmatrix} y_{\bar{1}}^0 \\ z_{\bar{1}}^0 \end{pmatrix} - \frac{K_1}{p^2+\delta_1 p+\gamma_1}\begin{pmatrix} p, & 1 \\ -\gamma, & p+\delta_1 \end{pmatrix}\begin{pmatrix} k \\ 1 \end{pmatrix}. \tag{3.5}$$

Putting

$$\left.\begin{aligned} &f_{rn}(\tau) = \frac{1}{2\pi j}\int_B \frac{p^n}{(p^2+1)(p^2+\delta_r p+\gamma_r)}\cdot\frac{\varepsilon^{p\tau}}{p}dp, \\ &g_{rn}(\tau) = \frac{1}{2\pi j}\int_B \frac{p^n}{p^2+\delta_r p+\gamma_r}\cdot\frac{\varepsilon^{p\tau}}{p}dp. \end{aligned}\right\} \tag{3.6}$$

$(r = 1, 2, 3, 4,)$

Eq. (3.3) are solved. The result is

$$\begin{pmatrix} y_1(\tau)-y_1^{-0} \\ z_1(\tau) \end{pmatrix} = \begin{pmatrix} F_{11}(\tau), & F_{12}(\tau) \\ f_{12}(\tau), & f_{13}(\tau) \end{pmatrix} \begin{pmatrix} \cos\theta_1 \\ \sin\theta_1 \end{pmatrix} + \begin{pmatrix} g_{11}(\tau), & -G_{11}(\tau) \\ G_{12}(\tau), & -g_{11}(\tau) \end{pmatrix} \begin{pmatrix} z_1^{-0} \\ K_1 \end{pmatrix}, \tag{3.7}$$

where

$$\left. \begin{aligned} F_{11}(\tau) &= kf_{12}(\tau)+f_{11}(\tau), \quad G_{11}(\tau) = kg_{11}(\tau)+g_{10}(\tau), \\ F_{12}(\tau) &= kf_{13}(\tau)+f_{12}(\tau), \quad G_{12}(\tau) = g_{12}(\tau)+\delta_1 g_{11}(\tau) \end{aligned} \right\} \tag{3.8}$$

and

$$\left. \begin{aligned} g_{10}(\tau) &= \frac{1}{\gamma_1}\left\{1-\varepsilon^{-\alpha_1\tau}\left(\cos\beta_1\tau+\frac{\alpha_1}{\beta_1}\sin\beta_1\tau\right)\right\}, \\ g_{11}(\tau) &= \frac{1}{\beta_1}\varepsilon^{-\alpha_1\tau}\sin\beta_1\tau, \\ g_{12}(\tau) &= \varepsilon^{-\alpha_1\tau}\left(\cos\beta_1\tau-\frac{\alpha_1}{\beta_1}\sin\beta_1\tau\right), \\ f_{11}(\tau) &= \frac{1}{\Delta}\left\{a_1\sin\tau-2\alpha_1\cos\tau+\varepsilon^{-\alpha_1\tau}\left(2\alpha_1\cos\beta_1\tau+\frac{1+\alpha_1^2-\beta_1^2}{\beta_1}\sin\beta_1\tau\right)\right\}, \\ f_{12}(\tau) &= \frac{1}{\Delta}\{a_1\cos\tau+\delta_1\sin\tau-\varepsilon^{-\alpha_1\tau}(a_1\cos\beta_1\tau+a_2\sin\beta_1\tau)\}, \\ f_{13}(\tau) &= \frac{1}{\Delta}\{\delta_1\cos\tau-a_1\sin\tau+\varepsilon^{-\alpha_1\tau}(-\delta_1\cos\beta_1\tau+a_3\sin\beta_1\tau)\}, \end{aligned} \right\} \tag{3.9}$$

where

$$\alpha_1 = \frac{\delta_1}{2}, \quad \beta_1 = \sqrt{\gamma_1-\alpha_1^2}, \quad a_1 = \gamma_1 - 1, \quad a_2 = \frac{\alpha_1}{\beta_1}(\alpha_1^2+\beta_1^2+1),$$

$$a_3 = \frac{1}{\beta_1}\{(\alpha_1^2+\beta_1^2)^2+\alpha_1^2-\beta_1^2\}, \quad \Delta = (\alpha_1^2+\beta_1^2)^2+2(\alpha_1^2-\beta_1^2)+1.$$

Here the first subsripts of each quantities in Eqs. (3.8) and (3.9) belong to each circuit mode.

3.2.2. Transient solutions in the 2-nd circuit mode.— When the coil is saturated by an exciting current flowing in the positive direction, the circuit equations are written in the forms

$$\left. \begin{aligned} &\frac{d\phi}{dt} = v+Ri_R, \quad i_R = i-i_L, \\ &C\frac{dv}{dt} = i_R, \quad i = I_m\sin(\omega t+\theta_2), \quad i_L = \frac{\phi-\phi_1}{L_2}+I_1, \end{aligned} \right\} \tag{3.10}$$

where θ_2 represents the initial phase angle of the input current, at which the positive saturated state starts, and the conditions are imposed to be

$$\phi = \phi_1 \quad \text{at} \quad t = 0$$

and

$$\phi = \phi_2 \quad \text{at} \quad t = t_2,$$

t_2 being the duration of the state. Using a similar symbols such as in (3.2), Eq. (3.10) may be written in the forms

$$\left.\begin{aligned}&\left(\frac{d}{d\tau}+\delta_2\right)\{y_2(\tau)-y_{\bar{2}}^0\}-z_2(\tau)=k\{\sin(\tau+\theta_2)-K_2\},\\&\gamma_2\{y_2(\tau)-y_{\bar{2}}^0\}+\frac{d}{d\tau}z_2(\tau)=\sin(\tau+\theta_2)-K_2,\\&i_R/I_m=\sin(\tau+\theta_2)-\gamma_2\{y(\tau)-y_{\bar{2}}^0\}-K_2,\end{aligned}\right\}\tag{3.11}$$

where

$$\delta_2=R/\omega L_2,\quad \gamma_2=\frac{1}{\omega^2CL_2},\quad K_2=I_1/I_m,\quad y_{\bar{2}}^0=\frac{\omega^2C}{I_m}\phi_1.$$

The solutions are obtained in a similar way as before, that is,

$$\begin{pmatrix}y_2(\tau)-y_{\bar{2}}^0\\z_2(\tau)\end{pmatrix}=\begin{pmatrix}F_{21}(\tau), & F_{22}(\tau)\\f_{22}(\tau), & f_{23}(\tau)\end{pmatrix}\begin{pmatrix}\cos\theta_2\\\sin\theta_2\end{pmatrix}+\begin{pmatrix}g_{21}(\tau), & -G_{21}(\tau)\\G_{22}(\tau), & -g_{21}(\tau)\end{pmatrix}\begin{pmatrix}z_{\bar{2}}^0\\K_2\end{pmatrix},\tag{3.12}$$

where the $F_2(\tau)$'s, $f_2(\tau)$'s, $g_2(\tau)$'s and $G_2(\tau)$'s are determined on substituting γ_2, α_2, $j\beta_2$, $\cos\theta_2\tau$, and $\frac{1}{\beta_2}\sinh\beta_2\tau$ for γ_1, α_1, β_1, $\cos\beta_1\tau$ and $\frac{1}{\beta_1}\sin\beta_1\tau$ in the expressions of $F_1(\tau)$'s, $f_1(\tau)$'s, $g_1(\tau)$'s and $G_1(\tau)$'s in Eqs. (3.8) and (3.9) respectively, while $\alpha_2=\delta_2/2$ and $\beta_2=\sqrt{\alpha_2^2-\gamma_2}$.

3.2.3. Transient solutions in the 3-rd mode.— The circuit equations are written in the forms

$$\left.\begin{aligned}&\frac{d\phi}{dt}=v+Ri_R,\quad i_R=i-i_L,\\&C\frac{dv}{dt}=i_R,\quad i=I_m\sin(\omega t+\theta_3),\quad i_L=\frac{\phi-\phi_2}{L_3}+I_2,\end{aligned}\right\}\tag{3.13}$$

where θ_3 represents the initial phase angle of the input current, at which the permeable state begins, and the conditions have to be

$$\phi=\phi_2\quad\text{at}\quad t=0$$

and

$$\phi=\phi_3\quad\text{at}\quad t=t_3,$$

t_3 being the duration of the state.

According to a similar procedure, Eq. (3.13) may be written in the forms

$$\left.\begin{aligned}&\left(\frac{d}{d\tau}+\delta_3\right)\{y_3(\tau)-y_{\bar{3}}^0\}-z_3(\tau)=k\{\sin(\tau+\theta_3)-K_3\},\\&\gamma_3\{y_3(\tau)-y_{\bar{3}}^0\}+\frac{d}{d\tau}z_3(\tau)=\sin(\tau+\theta_3)-K_3,\\&i_R/I_m=\sin(\tau+\theta_3)-\gamma_3\{y(\tau)-y_{\bar{3}}^0\}-K_3,\end{aligned}\right\}\tag{3.14}$$

where

$$\delta_3=\frac{R}{\omega L_3},\quad \gamma_3=\frac{1}{\omega^2CL_3},\quad K_3=\frac{I_2}{I_m},\quad y_{\bar{3}}^0=\frac{\omega^2C}{I_m}\phi_2.$$

The solutions are obtained by a similar procedure, that is,

$$\begin{pmatrix} y_3(\tau)-y_3^{-0} \\ z_3(\tau) \end{pmatrix} = \begin{pmatrix} F_{31}(\tau), & F_{32}(\tau) \\ f_{32}(\tau), & f_{33}(\tau) \end{pmatrix} \begin{pmatrix} \cos\theta_3 \\ \sin\theta_3 \end{pmatrix} + \begin{pmatrix} g_{31}(\tau), & -G_{31}(\tau) \\ G_{32}(\tau), & -g_{31}(\tau) \end{pmatrix} \begin{pmatrix} z_3^{-0} \\ K_3 \end{pmatrix}, \tag{3.15}$$

where the elements of the matrices on the right-hand sides, which are denoted by Eqs. (3.6) and (3.8), can be obtained by substituting γ_3, α_3 and β_3 for γ_1, α_1 and β_1 in the expressions of Eqs. (3.8) and (3.9) respectively, while $\alpha_3=\delta_3/2$ and $\beta_3=\sqrt{\gamma_3-\alpha_3^2}$.

3.2.4. Transient solutions in the 4-th circuit mode.— The circuit equations are written in the forms

$$\left.\begin{aligned} &\frac{d\phi}{dt} = v+Ri_R, \quad i_R = i-i_L, \\ &C\frac{dv}{dt} = i_R, \quad i = I_m\sin(\omega t+\theta_4), \quad i_L = \frac{\phi-\phi_3}{L_4}+I_3, \end{aligned}\right\} \tag{3.16}$$

where θ_4 represented the initial phase angle of the input current, at which the negative saturated state starts, and the conditions have to be

$$\phi = \phi_3 \quad \text{at} \quad t=0$$

and

$$\phi = \phi_4 \quad \text{at} \quad t=t_4,$$

t_4 being the duration of the state.

Eq. (3.16) may be written in the forms as before, that is,

$$\left.\begin{aligned} &\left(\frac{d}{d\tau}+\delta_4\right)\{y_4(\tau)-y_4^{-0}\}-z_4(\tau) = k\{\sin(\tau+\theta_4)-K_4\}, \\ &\gamma_4\{y_4(\tau)-y_4^{-0}\}+\frac{d}{d\tau}z_4(\tau) = \sin(\tau+\theta_4)-K_4, \\ &i_R/I_m = \sin(\tau+\theta_4)-\gamma_4\{y_4(\tau)-y_4^{-0}\}-K_4, \end{aligned}\right\} \tag{3.17}$$

where

$$\delta_4 = \frac{R}{\omega L_4}, \quad \gamma_4 = \frac{1}{\omega^2 CL_4}, \quad K_4 = \frac{I_3}{I_m}, \quad y_4^{-0} = \frac{\omega^2 C}{I_m}\phi_3.$$

Accordingly the solutions may be obtained as follows

$$\begin{pmatrix} y_4(\tau)-y_4^{-0} \\ z_4(\tau) \end{pmatrix} = \begin{pmatrix} F_{41}(\tau), & F_{42}(\tau) \\ f_{42}(\tau), & f_{43}(\tau) \end{pmatrix} \begin{pmatrix} \cos\theta_4 \\ \sin\theta_4 \end{pmatrix} + \begin{pmatrix} g_{41}(\tau), & -G_{41}(\tau) \\ G_{42}(\tau), & -g_{41}(\tau) \end{pmatrix} \begin{pmatrix} z_4^{-0} \\ K_4 \end{pmatrix}, \tag{3.18}$$

where the elements of the matrices on the right-hand sides, which are denoted by Eqs. (3.6) and (3.8), are determined on substituting γ_4, α_4 and β_4 for γ_2, α_2 and β_2 in the expressions of the solutions in the 2-nd circuit mode, while $\alpha_4=\delta_4/2$ and $\beta_4=\sqrt{\alpha_4^2-\gamma_4}$.

4. Steady State Solutions considering the Over-all Characteristics

Next we consider the steady state solutions of the circuit where the phenomena in complete cycle behave as follows.

In the preceding sections we obtained generally the solutions in the case of the unsymmetrical characteristic of the coil. Thus in the unsymmetrical case the conditions for periodic solutions must be imposed to be

$$\left.\begin{aligned}&\tau_1+\tau_2+\tau_3+\tau_4 = 2\pi\,,\\ &y_1(\tau_1) = y_2^{-0}\,,\quad y_2(\tau_2) = y_3^{-0}\,,\quad y_3(\tau_3) = y_4^{-0}\,,\quad y_4(\tau_4) = y_1^{-0}\,,\\ &z_1(\tau_1) = z_2^{-0},\quad z_2(\tau_2) = z_3^{-0},\quad z_3(\tau_3) = z_4^{-0},\quad z_4(\tau_4) = z_1^{-0}.\end{aligned}\right\} \tag{4.1}$$

On the other hand, the conditions in the case of the symmetrical characteristic of the coil, (i.e. $L_1=L_3$ and $L_2=L_4$) that is,

$$\left.\begin{aligned}&\tau_1+\tau_2 = \pi\,,\quad z_1(\tau_1) = z_2^{-0}\,,\quad z_2(\tau_2) = -z_1^{-0}\,,\\ &y_1(\tau_1) = -y_3(\tau_3)=y_2^{-0}\,,\quad y_2(\tau_2) = -y_4(\tau_4) = -y_1^{-0}\,.\end{aligned}\right\} \tag{4.2}$$

These relations of Eq. (4.2) can be induced by the fact as follows.

During the first interval of τ_1 seconds, the coil is kept in unsaturated condition and then is saturated in the positive direction during the subsequent interval of τ_2 seconds, while in the next half cycle, the currents, the magnetic flux and voltage in the circuit become equal to magnitude, but opposite in sign.

Here we will discuss the solutions in the case of the symmetrical characteristic of the coil. The initial values of ϕ, i_L and v in the primary unsaturated state and in the subsequent positive saturated state are equal to the final values of those in the negative saturated state and in the primary unsaturated state respectively, and it is intended to study the steady state phenomena in any one of the two half cycles, which are equal in magnitude, but opposite in sign to each other.

Thus the steady state solutions are given ultimately by the elements of

$$\begin{pmatrix} y_1(\tau)+y_2(\tau_2)\\ z_1(\tau)\end{pmatrix} = \begin{pmatrix} F_{11}(\tau), & F_{12}(\tau)\\ f_{12}(\tau), & f_{13}(\tau)\end{pmatrix}\begin{pmatrix}\cos\theta_1\\ \sin\theta_1\end{pmatrix} - \begin{pmatrix} g_{11}(\tau), & G_{11}(\tau)\\ G_{12}(\tau), & g_{11}(\tau)\end{pmatrix}\begin{pmatrix} z_2(\tau_2)\\ K_1\end{pmatrix},\quad 0\leq\tau\leq\tau_1 \tag{4.3}$$

and

$$\begin{pmatrix} y_2(\tau)-y_1(\tau_1)\\ z_2(\tau)\end{pmatrix} = \begin{pmatrix} F_{21}(\tau), & F_{22}(\tau)\\ f_{22}(\tau) & f_{23}(\tau)\end{pmatrix}\begin{pmatrix}\cos(\tau_1+\theta_1)\\ \sin(\tau_1+\theta_1)\end{pmatrix} + \begin{pmatrix} g_{21}(\tau), & -G_{21}(\tau)\\ G_{22}(\tau), & -g_{21}(\tau)\end{pmatrix}\begin{pmatrix} z_1(\tau_1)\\ K_2\end{pmatrix}$$
$$0\leq\tau\leq\tau_2\,. \tag{4.4}$$

τ_1, τ_2, θ_1, $z_1(\tau_1)$ and $z_2(\tau_2)$ in the above equations are so far unknown, and we have to find their values so that these equations must satisfy the relations in Eq. (4.2) for the given values of ϕ_1 and ϕ_2 or $y_1(\tau_1)$ and $y_2(\tau_2)$.

Putting $\tau=\tau_1$ in Eq. (4.3) and $\tau=\tau_2$ in Eq. (4.4), we can obtain the following equations respectively which will determine the unknown equantities.

$$\begin{pmatrix}1, & 1\\ 0, & 0\end{pmatrix}\begin{pmatrix}y_1(\tau_1)\\ y_2(\tau_2)\end{pmatrix}+\begin{pmatrix}0, & g_{11}(\tau_1)\\ 1, & G_{12}(\tau_1)\end{pmatrix}\begin{pmatrix}z_1(\tau_1)\\ z_2(\tau_2)\end{pmatrix}=\begin{pmatrix}F_{11}(\tau), & F_{12}(\tau_1)\\ f_{12}(\tau_1), & f_{13}(\tau)\end{pmatrix}\begin{pmatrix}\cos\theta_1\\ \sin\theta_1\end{pmatrix}-\begin{pmatrix}G_{11}(\tau_1)\\ g_{11}(\tau_1)\end{pmatrix}K_1 \tag{4.5}$$

and

$$\begin{pmatrix}-1, & 1\\ 0, & 0\end{pmatrix}\begin{pmatrix}y_1(\tau_1)\\ y_2(\tau_2)\end{pmatrix}+\begin{pmatrix}-g_{21}(\tau_2), & 0\\ -G_{22}(\tau_2), & 1\end{pmatrix}\begin{pmatrix}z_1(\tau_1)\\ z_2(\tau_2)\end{pmatrix}=\begin{pmatrix}E_{21}(\tau_2), & E_{22}(\tau_2)\\ E_{23}(\tau_2), & E_{24}(\tau_2)\end{pmatrix}\begin{pmatrix}\cos\theta_1\\ \sin\theta_1\end{pmatrix}-\begin{pmatrix}G_{21}(\tau_2)\\ g_{21}(\tau_2)\end{pmatrix}K_2, \tag{4.6}$$

where

$$\begin{pmatrix}E_{21}(\tau_2), & E_{22}(\tau_2)\\ E_{23}(\tau_2), & E_{24}(\tau_2)\end{pmatrix}=\begin{pmatrix}F_{21}(\tau_2), & F_{22}(\tau_2)\\ f_{22}(\tau_2), & f_{23}(\tau_2)\end{pmatrix}\begin{pmatrix}\cos\tau_1, & -\sin\tau_1\\ \sin\tau_1, & \cos\tau_1\end{pmatrix}. \tag{4.7}$$

Eliminating $z_1(\tau_1)$ and $z_2(\tau_2)$ from Eqs. (4.5) and (4.6), first by Eq. (4.5) we have

$$\begin{pmatrix}z_1(\tau_1)\\ z_2(\tau_2)\end{pmatrix}=\begin{pmatrix}0, & g_{11}(\tau_1)\\ 1, & G_{12}(\tau_1)\end{pmatrix}^{-1}\left\{\begin{pmatrix}F_{11}(\tau_1), & F_{12}(\tau_1)\\ f_{12}(\tau_1), & f_{13}(\tau_1)\end{pmatrix}\begin{pmatrix}\cos\theta_1\\ \sin\theta_1\end{pmatrix}-\begin{pmatrix}G_{11}(\tau_1)\\ g_{11}(\tau_1)\end{pmatrix}K_1-\begin{pmatrix}1, & 1\\ 0, & 0\end{pmatrix}\begin{pmatrix}y_1(\tau_1)\\ y_2(\tau_2)\end{pmatrix}\right\} \tag{4.8}$$

and then substituting Eq. (4.8) into Eq. (4.6), we have

$$\begin{pmatrix}h_{11}(\tau_1), & h_{12}(\tau_1)\\ h_{21}(\tau_1), & h_{22}(\tau_1)\end{pmatrix}\begin{pmatrix}y_1(\tau_1)\\ y_2(\tau_2)\end{pmatrix}+\begin{pmatrix}u_{11}(\tau_1), & u_{12}(\tau_1)\\ u_{21}(\tau_1), & u_{22}(\tau_1)\end{pmatrix}\begin{pmatrix}K_2\\ K_1\end{pmatrix}=\begin{pmatrix}d_{11}(\tau_1), & d_{12}(\tau_1)\\ d_{21}(\tau_1), & d_{22}(\tau_1)\end{pmatrix}\begin{pmatrix}\cos\theta_1\\ \sin\theta_1\end{pmatrix}, \tag{4.9}$$

where

$$\left.\begin{aligned}
\begin{pmatrix}h_{11}(\tau_1), & h_{12}(\tau_1)\\ h_{21}(\tau_1), & h_{22}(\tau_1)\end{pmatrix}&=\begin{pmatrix}-1, & 1\\ 0, & 0\end{pmatrix}-\begin{pmatrix}-g_{21}(\tau_2), & 0\\ -G_{22}(\tau_2), & 1\end{pmatrix}\begin{pmatrix}0, & g_{11}(\tau_1)\\ 1, & G_{12}(\tau_1)\end{pmatrix}^{-1}\begin{pmatrix}1, & 1\\ 0, & 0\end{pmatrix},\\
\begin{pmatrix}u_{11}(\tau_1), & u_{12}(\tau_1)\\ u_{21}(\tau_1), & u_{22}(\tau_1)\end{pmatrix}&=\begin{pmatrix}G_{21}(\tau_2), & 0\\ g_{21}(\tau_2), & 0\end{pmatrix}-\begin{pmatrix}-g_{21}(\tau_2), & 0\\ -G_{22}(\tau_2), & 1\end{pmatrix}\begin{pmatrix}0, & g_{11}(\tau_1)\\ 1, & G_{12}(\tau_1)\end{pmatrix}^{-1}\begin{pmatrix}0, & G_{11}(\tau_1)\\ 0, & g_{11}(\tau_1)\end{pmatrix},\\
\begin{pmatrix}d_{11}(\tau_1), & d_{12}(\tau_1)\\ d_{21}(\tau_1), & d_{22}(\tau_1)\end{pmatrix}&=\begin{pmatrix}E_{21}(\tau_2), & E_{22}(\tau_2)\\ E_{23}(\tau_2), & E_{24}(\tau_2)\end{pmatrix}-\begin{pmatrix}-g_{21}(\tau_2), & 0\\ -G_{22}(\tau_2), & 1\end{pmatrix}\begin{pmatrix}0, & g_{11}(\tau_1)\\ 1, & G_{12}(\tau_1)\end{pmatrix}^{-1}\begin{pmatrix}F_{11}(\tau_1), & F_{12}(\tau_1)\\ f_{12}(\tau_1), & f_{13}(\tau_1)\end{pmatrix}.
\end{aligned}\right\} \tag{4.10}$$

Now the first equation of Eq. (4.9) is

$$h_{11}(\tau_1)y_1(\tau_1)+h_{12}(\tau_1)y_2(\tau_2)+u_{11}(\tau_1)K_2+u_{12}(\tau)K_1=d_{11}(\tau_1)\cos\theta_1+d_{12}(\tau_1)\sin\theta_1. \tag{4.11}$$

In view of Eq. (4.11) we can obtain the phase angle θ_1 as follows.
Putting

$$\left.\begin{aligned}\sqrt{d_{11}^2(\tau_1)+d_{12}^2(\tau_1)}&=d_0(\tau_1),\\ \theta_0&=\tan^{-1}\frac{d_{12}(\tau_1)}{d_{11}(\tau_1)},\end{aligned}\right\} \tag{4.12}$$

then, Eq. (4.11) may be written in the forms

$$d_0\cos(\theta_1-\theta_0)=f_n\{y_1(\tau_1),\ y_2(\tau_2),\ \tau_1\}. \tag{4.13}$$

Consequently we have

$$\theta_1 = \theta_0 + \cos^{-1}\frac{1}{d_0} f_n\{y_1(\tau_1),\ y_2(\tau_2),\ \tau_1\}, \tag{4.14}$$

where

$$f_n\{y_1(\tau),\ y_2(\tau_2),\ \tau_1\} = h_{11}(\tau_1)y_1(\tau_1) + h_{12}(\tau_1)y_2(\tau_2) + u_{11}(\tau_1)K_2 + u_{12}(\tau_1)K_1. \tag{4.15}$$

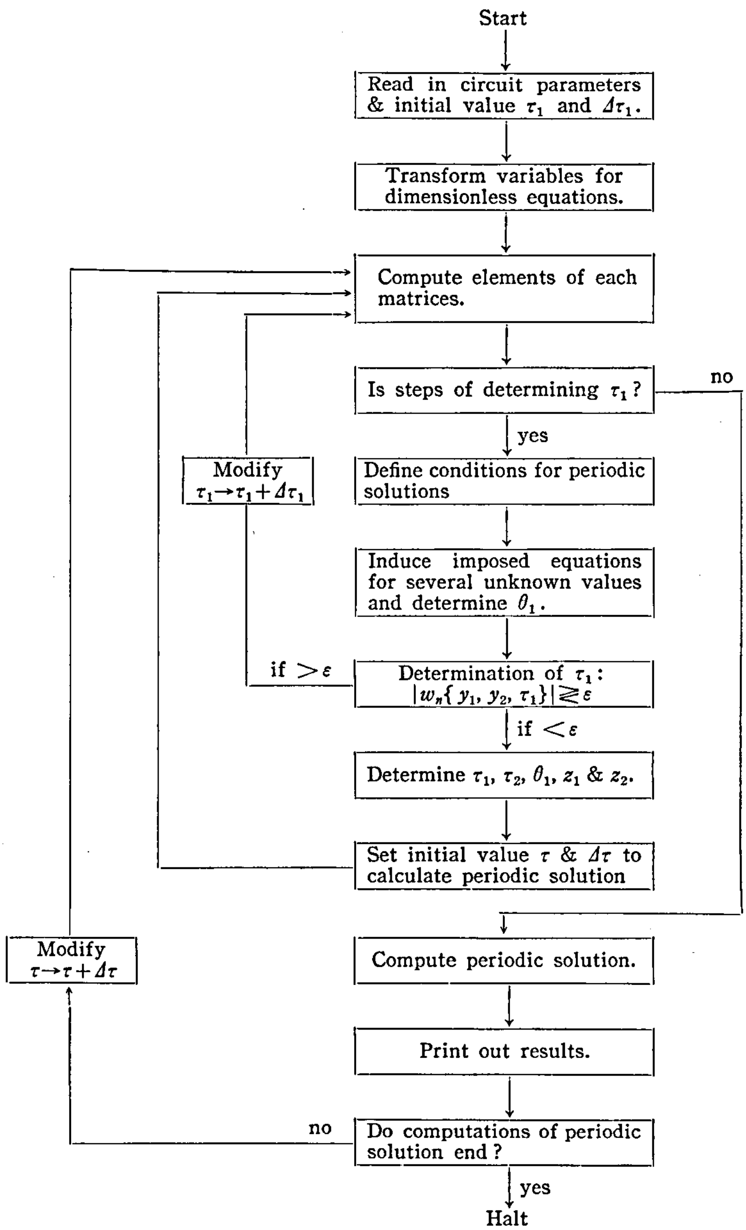

Fig. 5. Digital Computer flowchart for the steady state solutions.

Next to obtain τ_1, substituting θ_1 of Eq. (4.14) into the second equation of Eq. (4.9), i.e.

$$h_{21}(\tau_1)y_1(\tau_1)+h_{22}(\tau_1)y_2(\tau_2)+u_{21}(\tau_1)K_2+u_{22}(\tau_1)K_1 = d_{21}(\tau_1)\cos\theta_1+d_{22}(\tau_1)\sin\theta_1, \quad (4.16)$$

we have the following transcendental equation with regard to the given values of $y_1(\tau_1)$, $y_2(\tau_2)$ and to the unknown values τ_1, and then τ_1 can be determined by solving this equation with respect to the function τ_1.

$$w_n\{y_1(\tau_1),\ y_2(\tau_2),\ \tau_1\}=0, \quad (4.17)$$

where

$$w_n\{y_1(\tau_1),\ y_2(\tau_2),\ \tau_1\}=h_{21}(\tau_1)y_1(\tau_1)+h_{22}(\tau_1)y_2(\tau_2)+u_{21}(\tau_1)K_2. \quad (4.18)$$

Since θ_1, τ_1 and τ_2 have been found, $z_1(\tau_1)$ and $z_2(\tau_2)$ can be easily found by substituting θ_1, τ_1 and τ_2 into Eq. (4.8).

5. Determination of τ_1 by Digital Computer

It is the most difficult problem to determine τ_1 in the preceding procedure and to obtain the steady state solution.

Since τ_1 cannot be written in the explicit forms because of the complicated transcendental equation, it is comparatively easy to solve this equation by making use of the digital computer for some numerical examples.

Here we can determine τ_1 and the periodic solutions by means of the Digital Computer (KDC-1) according to the procedures as shown in Fig. 5, where approximately the determination τ_1 is confined to solve the following equation

$$|w_n\{y_1(\tau_1),\ y_2(\tau_2),\ \tau_1\}|<\varepsilon, \quad (5.1)$$

ε being a given infinitesimal value.

6. Analysis of the Producer Circuit with a Shunt Condenser

In this section we study the circuit shown in Fig. 6 involving an additional capacitor C_1, which will intensify the generation of several desired components of harmonic currents. This capacitor may, of course, include the effective stray capacitor of the coil. The characteristic of the coil, i.e. the symmetrical characteristic, and other circuit modes are assumed to be just the same as those discussed in the preceding sections.

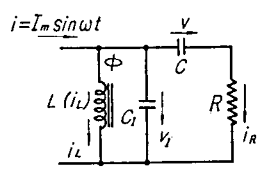

Fig. 6. Harmonic producer circuit involving an additional capacitor.

6.1. Transient Solutions in the 1-st Circuit Mode

The circuit equations are

$$\left.\begin{aligned} &\frac{d\phi}{dt} = v_1\,, \quad v_1 = v + Ri_R\,, \\ &C\frac{dv}{dt} = i_R\,, \quad i_L = \frac{\phi-\phi_4}{L_1} + I_4\,, \\ &i_L + C_1\frac{dv_1}{dt} + C\frac{dv}{dt} = I_m \sin(\omega t + \theta_1)\,, \end{aligned}\right\} \tag{6.1}$$

where θ_1 represents the initial phase angle of the input current, at which the state starts, and the conditions are supposed to be

$$\phi = \phi_4 \quad \text{at} \quad t = 0$$

and

$$\phi = \phi_1 \quad \text{at} \quad t = t_1\,,$$

t_1 being the duration of the state.

Putting

$$\left.\begin{aligned} &y_1(\tau) = \frac{\omega^2 C\phi}{I_m}\,, \quad x_1(\tau) = \frac{\omega C_1 v_1}{I_m}\,, \quad z_1(\tau) = \frac{\omega C v}{I_m}\,, \ \tau = \omega t\,, \\ &\delta = \frac{1}{\omega CR}\,, \quad \mu = \frac{C}{C_1}\,, \quad \delta_1 = \frac{1}{\omega RC_1}\,, \end{aligned}\right\} \tag{6.2}$$

where $y_1(\tau)$, $x_1(\tau)$ and $z_1(\tau)$ with the subscript "1" belong to the 1-st circuit mode.

The following dimensionless equations are obtained from Eq. (6.1), that is,

$$\left.\begin{aligned} &\frac{d}{d\tau}x_1(\tau) + \frac{d}{d\tau}z_1(\tau) + \gamma_1 y_1(\tau) - \gamma_1 y_1^{-0} + K_1 = \sin(\tau+\theta_1)\,, \\ &\frac{d}{d\tau}y_1(\tau) - \mu x_1(\tau) = 0\,, \\ &\left(\frac{d}{d\tau}+\delta\right) z_1(\tau) - \delta_1 x_1(\tau) = 0\,, \end{aligned}\right\} \tag{6.3}$$

where

$$\gamma_1 = \frac{1}{\omega^2 CL_1}\,, \quad K_1 = \frac{I_4}{I_m}\,, \quad y_1^{-0} = \frac{\omega^2 C\phi_4}{I_m}\,.$$

The corresponding operational equations which determine the operational functions $X_1(p)$, $Y_1(p)$ and $Z_1(p)$ corresponding to $x_1(\tau)$, $y_1(\tau)$ and $z_1(\tau)$ are written in the matrix form

$$\begin{pmatrix} p, & \gamma_1, & p \\ -\mu, & p, & 0 \\ -\delta, & 0, & p+\delta \end{pmatrix} \begin{pmatrix} X_1(p) \\ Y_1(p) \\ Z_1(p) \end{pmatrix} = \begin{pmatrix} 1 \\ 0 \\ 0 \end{pmatrix} \frac{\cos\theta_1 + p\sin\theta_1}{p^2+1}\,p + p\begin{pmatrix} 1 & 0 & 1 \\ 0 & 1 & 0 \\ 0 & 0 & 1 \end{pmatrix} \begin{pmatrix} x_1^{-0} \\ y_1^{-0} \\ z_1^{-0} \end{pmatrix} + \begin{pmatrix} -K_1 \\ 0 \\ 0 \end{pmatrix}. \tag{6.4}$$

Hence we have

$$\begin{aligned} \begin{pmatrix} X_1(p) \\ Y_1(p) \\ Z_1(p) \end{pmatrix} &= \frac{p\cos\theta_1 + p^2\sin\theta_1}{(p^2+1)(p^3+p^2\delta_0+p\gamma_{10}+a_1)} \begin{pmatrix} p(p+\delta) \\ \mu(p+\delta) \\ \delta_1 p \end{pmatrix} + \frac{p}{p^3+p^2\delta_0+p\gamma_{10}+a_1} \\ &\times \begin{pmatrix} p(p+\delta), & -\gamma_1(p+\delta), & \delta p \\ \mu(b+\delta), & p(p+\delta_0), & \delta_1 \\ \delta_1 p, & -a_1, & p^2+\delta_1 p+\gamma_{10} \end{pmatrix} \begin{pmatrix} x_1^{-0} \\ y_1^{-0} \\ z_1^{-0} \end{pmatrix} + \frac{-K_1}{p^3+p^2\delta_0+p\gamma_{10}+a_1} \begin{pmatrix} p(p+\delta) \\ \mu(p+\delta) \\ \delta_1 p \end{pmatrix}, \end{aligned} \tag{6.5}$$

where

$$\delta_0=\delta+\delta_1\,,\quad \gamma_{10}=\mu\gamma_1\,,\quad a_1=\gamma_1\delta_1\,.$$

The solution of Eq. (6.3) become

$$\begin{pmatrix} x_1(\tau) \\ y_1(\tau)-y_1^{-0} \\ z_1(\tau) \end{pmatrix} = \begin{pmatrix} F_{111}(\tau), & F_{112}(\tau) \\ F_{121}(\tau), & F_{122}(\tau) \\ F_{131}(\tau), & F_{132}(\tau) \end{pmatrix} \begin{pmatrix} \cos\theta_1 \\ \sin\theta_1 \end{pmatrix} + \begin{pmatrix} \chi_{111}(\tau), & \chi_{112}(\tau), & \chi_{113}(\tau) \\ \chi_{121}(\tau), & \chi_{122}(\tau), & \chi_{123}(\tau) \\ \chi_{131}(\tau), & \chi_{132}(\tau), & \chi_{133}(\tau) \end{pmatrix} \begin{pmatrix} x_1^{-0} \\ 0 \\ z_1^{-0} \end{pmatrix} - K_1 \begin{pmatrix} \chi_{11}(\tau) \\ \chi_{12}(\tau) \\ \chi_{13}(\tau) \end{pmatrix}, \tag{6.6}$$

where $F(\tau)$'s and $\chi(\tau)$'s are tabulated in Table 1, provided that $f_{rn}(\tau)$ and $g_{rn}(\tau)$ be given by

$$\left.\begin{aligned} f_{rn}(\tau) &= \frac{1}{2\pi j}\int_B \frac{p^n}{(p^2+1)(p^3+p^2\delta_0+p\gamma_{r0}+a_r)}\cdot\frac{\varepsilon^{p\tau}}{p}\,dp\,, \\ g_{rn}(\tau) &= \frac{1}{2\pi j}\int_B \frac{p^n}{p^3+p^2\delta_0+p\gamma_{r0}+a_r}\cdot\frac{\varepsilon^{p\tau}}{p}\,dp\,. \end{aligned}\right\} \tag{6.7}$$

$(r=1, 2, 3, 4)$

Table 1.

$F_{111}(\tau)$	$f_{12}(\tau)+\delta f_{12}(\tau)$	$\chi_{111}(\tau)$	$g_{13}(\tau)+\delta g_{12}(\tau)$
$F_{112}(\tau)$	$f_{14}(\tau)+\delta f_{13}(\tau)$	$\chi_{112}(\tau)$	$-\gamma_1\{g_{12}(\tau)+\delta g_{11}(\tau)\}$
$F_{121}(\tau)$	$\mu\{f_{12}(\tau)+\delta f_{11}(\tau)\}$	$\chi_{113}(\tau)$	$\delta g_{12}(\tau)$
$F_{122}(\tau)$	$\mu\{f_{13}(\tau)+\delta f_{12}(\tau)\}$	$\chi_{121}(\tau)$	$\mu\{g_{12}(\tau)+\delta g_{11}(\tau)\}$
$F_{131}(\tau)$	$\delta_1 f_{12}(\tau)$	$\chi_{122}(\tau)$	$g_{13}(\tau)+\delta_0 g_{12}(\tau)$
$F_{132}(\tau)$	$\delta_1 f_{13}(\tau)$	$\chi_{123}(\tau)$	$\delta_1 g_{11}(\tau)$
$\chi_{11}(\tau)$	$g_{12}(\tau)+\delta g_{11}(\tau)$	$\chi_{131}(\tau)$	$\delta_1 g_{12}(\tau)$
$\chi_{12}(\tau)$	$\mu\{g_{11}(\tau)+\delta g_{10}(\tau)\}$	$\chi_{132}(\tau)$	$-a_1 g_{11}(\tau)$
$\chi_{13}(\tau)$	$\delta_1 g_{11}(\tau)$	$\chi_{133}(\tau)$	$g_{13}(\tau)+\delta_1 g_{12}(\tau)+\gamma_{10}g_{11}(\tau)$

6.2. Transient Solutions in the 2-nd Circuit Mode

The circuit equations are

$$\left.\begin{aligned} &\frac{d\phi}{dt}=v_1\,,\quad v_1=v+Ri_R\,, \\ &C\frac{dv}{dt}=i_R\,,\quad i_L=\frac{\phi-\phi_1}{L_2}+I_1\,, \\ &i_L+C_1\frac{dv_1}{dt}+C\frac{dv}{dt}=I_m\sin(\omega t+\theta_2)\,, \end{aligned}\right\} \tag{6.8}$$

where θ_2 represents the initial phase angle of the input current, at which the positive saturated state begins, and the conditions are supposed to be

$$\phi = \phi_1 \quad \text{at} \quad t = 0$$

and
$$\phi = \phi_2 \quad \text{at} \quad t = t_2,$$

t_2 being the duration of the state.

Using a similar symbol such as in (6.2), Eq. (6.8) may be written in the dimensionless forms

$$\left.\begin{aligned}
&\frac{d}{d\tau} x_2(\tau)+\frac{d}{d\tau} z_2(\tau)+\gamma_2\{y_2(\tau)-y_2^{-0}\}+K_2 = \sin(\tau+\theta_2),\\
&\frac{d}{d\tau}\{y_2(\tau)-y_2^{-0}\}-\mu x_2(\tau) = 0,\\
&\left(\frac{d}{d\tau}+\delta\right) z_2(\tau)-\delta_1 x_2(\tau) = 0,
\end{aligned}\right\} \tag{6.9}$$

where

$$\gamma_2 = \frac{1}{\omega^2 CL_2}, \quad K_2 = \frac{I_1}{I_m}, \quad y_2^{-0} = \frac{\omega^2 C\phi}{I_m}, \quad \gamma_{20} = \mu\gamma_2, \quad a_2 = \gamma_2\delta_1.$$

The solutions are obtained in a similar may as before, that is,

$$\begin{pmatrix} x_2(\tau) \\ y_2(\tau)-y_2^{-0} \\ z_2(\tau) \end{pmatrix} = \begin{pmatrix} F_{211}(\tau), & F_{212}(\tau) \\ F_{221}(\tau), & F_{222}(\tau) \\ F_{231}(\tau), & F_{232}(\tau) \end{pmatrix}\begin{pmatrix} \cos\theta_2 \\ \sin\theta_2 \end{pmatrix} + \begin{pmatrix} \chi_{211}(\tau), & \chi_{212}(\tau), & \chi_{213}(\tau) \\ \chi_{221}(\tau), & \chi_{222}(\tau), & \chi_{223}(\tau) \\ \chi_{231}(\tau), & \chi_{232}(\tau), & \chi_{233}(\tau) \end{pmatrix}\begin{pmatrix} x_2^{-0} \\ 0 \\ z_2^{-0} \end{pmatrix} - K_2\begin{pmatrix} \chi_{21}(\tau) \\ \chi_{22}(\tau) \\ \chi_{23}(\tau) \end{pmatrix}, \tag{6.10}$$

where $F(\tau)$'s and $\chi(\tau)$'s are tabulated in Table 2.

Table 2.

$F_{211}(\tau)$	$f_{23}(\tau)+\delta f_{22}(\tau)$	$\chi_{211}(\tau)$	$g_{23}(\tau)+\delta g_{22}(\tau)$
$F_{212}(\tau)$	$f_{24}(\tau)+\delta f_{23}(\tau)$	$\chi_{212}(\tau)$	$-\gamma_2\{g_{22}(\tau)+\delta g_{21}(\tau)\}$
$F_{221}(\tau)$	$\mu\{f_{22}(\tau)+\delta f_{21}(\tau)\}$	$\chi_{213}(\tau)$	$\delta g_{22}(\tau)$
$F_{222}(\tau)$	$\mu\{f_{23}(\tau)+\delta f_{22}(\tau)\}$	$\chi_{221}(\tau)$	$\mu\{g_{22}(\tau)+\delta g_{21}(\tau)\}$
$F_{231}(\tau)$	$\delta_1 f_{22}(\tau)$	$\chi_{222}(\tau)$	$g_{23}(\tau)+\delta_0 g_{22}(\tau)$
$F_{232}(\tau)$	$\delta_1 f_{23}(\tau)$	$\chi_{223}(\tau)$	$\delta_1 g_{21}(\tau)$
$\chi_{21}(\tau)$	$g_{22}(\tau)+\delta f_{21}(\tau)$	$\chi_{231}(\tau)$	$\delta_1 g_{22}(\tau)$
$\chi_{22}(\tau)$	$\mu\{g_{21}(\tau)+\delta g_{20}(\tau)\}$	$\chi_{232}(\tau)$	$-a_2 g_{21}(\tau)$
$\chi_{23}(\tau)$	$\delta_1 g_{21}(\tau)$	$\chi_{233}(\tau)$	$g_{23}(\tau)+\delta_1 g_{22}(\tau)+\gamma_{20} g_{21}(\tau)$

Although we can easily obtain the solutions in the 3-rd and 4-th circuit mode by a similar produre, it is unnecessary to get one for considering the steady state of the circuit with the symmetrical characteristic of the coil.

7. Steady State Solutions

Since the duration of the steady state is 2π, and at the transition points of the characteristic curve, the transient solutions in adjacent region should be equated to each other, we have

$$\left.\begin{array}{l}\tau_1+\tau_2=\pi, \quad z_1(\tau_1)=z_{\bar{2}}^{0}, \quad z_2(\tau_2)=-z_{\bar{1}}^{0}, \\ x_1(\tau_1)=x_{\bar{2}}^{0}, \quad x_2(\tau)=-x_{\bar{1}}^{0}, \quad y_1(\tau_1)=y_{\bar{2}}^{0}, \quad y_2(\tau_2)=-y_{\bar{1}}^{0}.\end{array}\right\} \tag{7.1}$$

Substituting these relations into Eqs. (6.6) and (6.10) yields

$$\begin{pmatrix} x_1(\tau) \\ y_1(\tau)-y_{\bar{1}}^{0} \\ z_1(\tau) \end{pmatrix} = \begin{pmatrix} F_{111}(\tau), & F_{112}(\tau) \\ F_{121}(\tau), & F_{122}(\tau) \\ F_{131}(\tau), & F_{132}(\tau) \end{pmatrix} \begin{pmatrix} \cos\theta_1 \\ \sin\theta_1 \end{pmatrix} - \begin{pmatrix} \chi_{111}(\tau), & \chi_{113}(\tau) \\ \chi_{121}(\tau), & \chi_{123}(\tau) \\ \chi_{131}(\tau), & \chi_{133}(\tau) \end{pmatrix} \begin{pmatrix} x_2(\tau_2) \\ z_2(\tau_2) \end{pmatrix} - K_1 \begin{pmatrix} \chi_{11}(\tau) \\ \chi_{12}(\tau) \\ \chi_{13}(\tau) \end{pmatrix} \tag{7.2}$$

$$0 \leq \tau \leq \tau_1$$

and

$$\begin{pmatrix} x_2(\tau) \\ y_2(\tau)-y_{\bar{2}}^{0} \\ z_2(\tau) \end{pmatrix} = \begin{pmatrix} F_{211}(\tau), & F_{212}(\tau) \\ F_{221}(\tau), & F_{222}(\tau) \\ F_{231}(\tau), & F_{232}(\tau) \end{pmatrix} \begin{pmatrix} \cos(\theta_1+\tau_1) \\ \sin(\theta_1+\tau_1) \end{pmatrix} + \begin{pmatrix} \chi_{211}(\tau), & \chi_{213}(\tau) \\ \chi_{221}(\tau), & \chi_{223}(\tau) \\ \chi_{231}(\tau), & \chi_{233}(\tau) \end{pmatrix} \begin{pmatrix} x_1(\tau_1) \\ z_1(\tau_1) \end{pmatrix} - K_2 \begin{pmatrix} \chi_{21}(\tau) \\ \chi_{22}(\tau) \\ \chi_{23}(\tau) \end{pmatrix} \tag{7.3}$$

$$0 \leq \tau \leq \tau_2$$

Next to determine τ_1. θ_1, $z_1(\tau_1)$, $z_2(\tau_2)$, $x_1(\tau_1)$ and $x_2(\tau_2)$, putting $\tau=\tau_1$ in Eq. (7.2) and $\tau=\tau_2$ in Eq. (7.3), we can obtain the following equations respectively,

$$\begin{pmatrix} 1, & 0, & \chi_{111}(\tau_1), & \chi_{113}(\tau_1) \\ 0, & 0, & \chi_{121}(\tau_1), & \chi_{123}(\tau_1) \\ 0, & 1, & \chi_{131}(\tau_1), & \chi_{133}(\tau_1) \end{pmatrix} \begin{pmatrix} x_1(\tau_1) \\ z_1(\tau_1) \\ x_2(\tau_2) \\ z_2(\tau_2) \end{pmatrix} + \begin{pmatrix} 0, & 0 \\ 1, & 1 \\ 0, & 0 \end{pmatrix} \begin{pmatrix} y_2(\tau_2) \\ y_1(\tau_1) \end{pmatrix} = \begin{pmatrix} F_{111}(\tau_1), & F_{112}(\tau_1) \\ F_{121}(\tau_1), & F_{122}(\tau_1) \\ F_{131}(\tau_1), & F_{132}(\tau_1) \end{pmatrix} \begin{pmatrix} \cos\theta_1 \\ \sin\theta_1 \end{pmatrix} - K_1 \begin{pmatrix} \chi_{11}(\tau_1) \\ \chi_{12}(\tau_1) \\ \chi_{13}(\tau_1) \end{pmatrix}, \tag{7.4}$$

$$\begin{pmatrix} -\chi_{211}(\tau_2), & -\chi_{213}(\tau_2), & 1, & 0 \\ -\chi_{221}(\tau_2), & -\chi_{223}(\tau_2), & 0, & 0 \\ -\chi_{231}(\tau_2), & -\chi_{233}(\tau_2), & 0, & 1 \end{pmatrix} \begin{pmatrix} x_1(\tau_1) \\ z_1(\tau_1) \\ x_2(\tau_2) \\ z_2(\tau_2) \end{pmatrix} + \begin{pmatrix} 0, & 0 \\ 1, & -1 \\ 0, & 0 \end{pmatrix} \begin{pmatrix} y_2(\tau_2) \\ y_1(\tau_1) \end{pmatrix} = \begin{pmatrix} E_{211}(\tau_2), & E_{212}(\tau_2) \\ E_{221}(\tau_2), & E_{222}(\tau_2) \\ E_{231}(\tau_2), & E_{232}(\tau_2) \end{pmatrix} \begin{pmatrix} \cos\theta_1 \\ \sin\theta_1 \end{pmatrix} - K_2 \begin{pmatrix} \chi_{21}(\tau_2) \\ \chi_{22}(\tau_2) \\ \chi_{23}(\tau_2) \end{pmatrix}, \tag{7.5}$$

where

$$\begin{pmatrix} E_{211}(\tau_2), & E_{212}(\tau_2) \\ E_{221}(\tau_2), & E_{222}(\tau_2) \\ E_{231}(\tau_2), & E_{232}(\tau_2) \end{pmatrix} = \begin{pmatrix} F_{211}(\tau_2), & F_{212}(\tau_2) \\ F_{221}(\tau_2), & F_{222}(\tau_2) \\ F_{231}(\tau_2), & F_{232}(\tau_2) \end{pmatrix} \begin{pmatrix} \cos\tau_1, & -\sin\tau_1 \\ \sin\tau_1, & \cos\tau_1 \end{pmatrix}. \tag{7.6}$$

The first and third equations of Eq. (7.4) are

$$\begin{pmatrix} x_1(\tau_1) \\ z_1(\tau_1) \end{pmatrix} + \begin{pmatrix} \chi_{111}(\tau_1), & \chi_{113}(\tau_1) \\ \chi_{131}(\tau_1), & \chi_{133}(\tau_1) \end{pmatrix} \begin{pmatrix} x_2(\tau_2) \\ z_2(\tau_2) \end{pmatrix} = \begin{pmatrix} F_{111}(\tau_1), & F_{112}(\tau_1) \\ F_{131}(\tau_1), & F_{132}(\tau_1) \end{pmatrix} \begin{pmatrix} \cos\theta_1 \\ \sin\theta_1 \end{pmatrix} - K_1 \begin{pmatrix} \chi_{11}(\tau_1) \\ \chi_{13}(\tau_1) \end{pmatrix} \tag{7.7}$$

and the first and third equations of Eq. (7.5) are

$$-\begin{pmatrix} \chi_{211}(\tau_2), & \chi_{213}(\tau_2) \\ \chi_{231}(\tau_2), & \chi_{233}(\tau_2) \end{pmatrix} \begin{pmatrix} x_1(\tau_1) \\ z_1(\tau_1) \end{pmatrix} + \begin{pmatrix} x_2(\tau_2) \\ z_2(\tau_2) \end{pmatrix} = \begin{pmatrix} E_{211}(\tau_2), & E_{212}(\tau_2) \\ E_{231}(\tau_2), & E_{232}(\tau_2) \end{pmatrix} \begin{pmatrix} \cos\theta_1 \\ \sin\theta_1 \end{pmatrix} - K_2 \begin{pmatrix} \chi_{21}(\tau_2) \\ \chi_{23}(\tau_2) \end{pmatrix}. \tag{7.8}$$

Accordingly

$$\begin{pmatrix} x_2(\tau_2) \\ z_2(\tau_2) \end{pmatrix} = \begin{pmatrix} \chi_{211}(\tau_2), & \chi_{213}(\tau_2) \\ \chi_{231}(\tau_2), & \chi_{233}(\tau_2) \end{pmatrix} \begin{pmatrix} x_1(\tau_1) \\ z_1(\tau_1) \end{pmatrix} + \begin{pmatrix} E_{211}(\tau_2), & E_{212}(\tau_2) \\ E_{231}(\tau_2), & E_{232}(\tau_2) \end{pmatrix} \begin{pmatrix} \cos\theta_1 \\ \sin\theta_1 \end{pmatrix} - K_2 \begin{pmatrix} \chi_{21}(\tau_2) \\ \chi_{23}(\tau_2) \end{pmatrix}. \tag{7.9}$$

Substituting Eq. (7.9) into Eq. (7.7) yields

$$\begin{aligned} \begin{pmatrix} k_{11}(\tau_1), & k_{12}(\tau_1) \\ k_{13}(\tau_1), & k_{14}(\tau_1) \end{pmatrix} \begin{pmatrix} x_1(\tau_1) \\ z_1(\tau_1) \end{pmatrix} &= \begin{pmatrix} c_{11}(\tau_1), & c_{12}(\tau_1) \\ c_{13}(\tau_1), & c_{14}(\tau_1) \end{pmatrix} \begin{pmatrix} \cos\theta_1 \\ \sin\theta_1 \end{pmatrix} - K_1 \begin{pmatrix} \chi_{11}(\tau_1) \\ \chi_{13}(\tau_1) \end{pmatrix} \\ &\quad + K_2 \begin{pmatrix} \chi_{111}(\tau_1), & \chi_{113}(\tau_1) \\ \chi_{131}(\tau_1), & \chi_{133}(\tau_1) \end{pmatrix} \begin{pmatrix} \chi_{21}(\tau_2) \\ \chi_{23}(\tau_2) \end{pmatrix}, \end{aligned} \tag{7.10}$$

where

$$\begin{pmatrix} k_{11}(\tau_1), & k_{12}(\tau_1) \\ k_{13}(\tau_1), & k_{14}(\tau_1) \end{pmatrix} = \begin{pmatrix} 1, & 0 \\ 0, & 1 \end{pmatrix} + \begin{pmatrix} \chi_{111}(\tau_1), & \chi_{113}(\tau_1) \\ \chi_{131}(\tau_1), & \chi_{133}(\tau_1) \end{pmatrix} \begin{pmatrix} \chi_{211}(\tau_2), & \chi_{213}(\tau_2) \\ \chi_{231}(\tau_2), & \chi_{233}(\tau_2) \end{pmatrix} \tag{7.11}$$

and

$$\begin{pmatrix} c_{11}(\tau_1), & c_{12}(\tau_1) \\ c_{13}(\tau_1), & c_{14}(\tau_1) \end{pmatrix} = \begin{pmatrix} F_{111}(\tau_1), & F_{112}(\tau_1) \\ F_{131}(\tau_1), & F_{132}(\tau_1) \end{pmatrix} - \begin{pmatrix} \chi_{111}(\tau_1), & \chi_{113}(\tau_1) \\ \chi_{131}(\tau_1), & \chi_{133}(\tau_1) \end{pmatrix} \begin{pmatrix} E_{211}(\tau_2), & E_{212}(\tau_2) \\ E_{231}(\tau_2), & E_{232}(\tau_2) \end{pmatrix}. \tag{7.12}$$

Eq. (7.10) gives the following equations for obtaining the unknown values $x_1(\tau_1)$ and $z_1(\tau_1)$,

$$\begin{pmatrix} x_1(\tau_1) \\ z_1(\tau_1) \end{pmatrix} = \begin{pmatrix} x_{11}(\tau_1), & x_{12}(\tau_1) \\ z_{11}(\tau_1), & z_{12}(\tau_1) \end{pmatrix} \begin{pmatrix} \cos\theta_1 \\ \sin\theta_1 \end{pmatrix} + \begin{pmatrix} q_{11}(\tau_1) \\ q_{12}(\tau_1) \end{pmatrix}, \tag{7.13}$$

where

$$\begin{pmatrix} x_{11}(\tau_1), & x_{12}(\tau_1) \\ z_{11}(\tau_1), & z_{12}(\tau_1) \end{pmatrix} = \begin{pmatrix} k_{11}(\tau_1), & k_{12}(\tau_1) \\ k_{13}(\tau_1), & k_{14}(\tau_1) \end{pmatrix}^{-1} \begin{pmatrix} c_{11}(\tau_1), & c_{12}(\tau_1) \\ c_{13}(\tau_1), & c_{14}(\tau_1) \end{pmatrix} \tag{7.14}$$

and

$$\begin{pmatrix} q_{11}(\tau_1) \\ q_{12}(\tau_1) \end{pmatrix} = \begin{pmatrix} k_{11}(\tau_1), & k_{12}(\tau_1) \\ k_{13}(\tau_1), & k_{14}(\tau_1) \end{pmatrix}^{-1} \left\{ -K_1 \begin{pmatrix} \chi_{11}(\tau_1) \\ \chi_{13}(\tau_1) \end{pmatrix} + K_2 \begin{pmatrix} \chi_{111}(\tau_1), & \chi_{113}(\tau_1) \\ \chi_{131}(\tau_1), & \chi_{133}(\tau_1) \end{pmatrix} \begin{pmatrix} \chi_{21}(\tau_2) \\ \chi_{23}(\tau_2) \end{pmatrix} \right\}. \tag{7.15}$$

From Eq. (7.7), we have

$$\begin{pmatrix} x_1(\tau_1) \\ z_1(\tau_1) \end{pmatrix} = -\begin{pmatrix} \chi_{111}(\tau_1), & \chi_{113}(\tau_1) \\ \chi_{131}(\tau_1), & \chi_{133}(\tau_1) \end{pmatrix} \begin{pmatrix} x_2(\tau_2) \\ z_2(\tau_2) \end{pmatrix} + \begin{pmatrix} F_{111}(\tau_1), & F_{112}(\tau_1) \\ F_{131}(\tau_1), & F_{132}(\tau_1) \end{pmatrix} \begin{pmatrix} \cos\theta_1 \\ \sin\theta_1 \end{pmatrix} - K_1 \begin{pmatrix} \chi_{11}(\tau_1) \\ \chi_{13}(\tau_1) \end{pmatrix}. \tag{7.16}$$

Substituting Eq. (7.16) into Eq. (7.8) gives

$$\begin{aligned} \begin{pmatrix} k_{21}(\tau_2), & k_{22}(\tau_2) \\ k_{23}(\tau_2), & k_{24}(\tau_2) \end{pmatrix} \begin{pmatrix} x_2(\tau_2) \\ z_2(\tau_2) \end{pmatrix} &= \begin{pmatrix} c_{21}(\tau_2), & c_{22}(\tau_2) \\ c_{23}(\tau_2), & c_{24}(\tau_2) \end{pmatrix} \begin{pmatrix} \cos\theta_1 \\ \sin\theta_1 \end{pmatrix} - K_2 \begin{pmatrix} \chi_{21}(\tau_2) \\ \chi_{23}(\tau_2) \end{pmatrix} \\ &\quad - K_1 \begin{pmatrix} \chi_{211}(\tau_2), & \chi_{213}(\tau_2) \\ \chi_{231}(\tau_2), & \chi_{233}(\tau_2) \end{pmatrix} \begin{pmatrix} \chi_{11}(\tau_1) \\ \chi_{13}(\tau_1) \end{pmatrix}, \end{aligned} \tag{7.17}$$

where

$$\begin{pmatrix} k_{21}(\tau_2), & k_{22}(\tau_2) \\ k_{23}(\tau_2), & k_{24}(\tau_2) \end{pmatrix} = \begin{pmatrix} 1, & 0 \\ 0, & 1 \end{pmatrix} + \begin{pmatrix} \chi_{211}(\tau_2), & \chi_{213}(\tau_2) \\ \chi_{231}(\tau_2), & \chi_{233}(\tau_2) \end{pmatrix} \begin{pmatrix} \chi_{111}(\tau_1), & \chi_{113}(\tau_1) \\ \chi_{131}(\tau_1), & \chi_{133}(\tau_1) \end{pmatrix} \tag{7.18}$$

and

$$\begin{pmatrix} c_{21}(\tau_2), & c_{22}(\tau_2) \\ c_{23}(\tau_2), & c_{24}(\tau_2) \end{pmatrix} = \begin{pmatrix} \chi_{211}(\tau_2), & \chi_{213}(\tau_2) \\ \chi_{231}(\tau_2), & \chi_{233}(\tau_2) \end{pmatrix} \begin{pmatrix} F_{111}(\tau_1), & F_{112}(\tau_1) \\ F_{131}(\tau_1), & F_{132}(\tau_1) \end{pmatrix} + \begin{pmatrix} E_{211}(\tau_2), & E_{212}(\tau_2) \\ E_{231}(\tau_2), & E_{232}(\tau_2) \end{pmatrix}. \tag{7.19}$$

Similarly Eq. (7.17) gives the following equations for obtaining the unknown values $x_2(\tau_2)$ and $z_2(\tau_2)$,

$$\begin{pmatrix} x_2(\tau_2) \\ z_2(\tau_2) \end{pmatrix} = \begin{pmatrix} x_{21}(\tau_2), & x_{22}(\tau_2) \\ z_{21}(\tau_2), & z_{22}(\tau_2) \end{pmatrix} \begin{pmatrix} \cos\theta_1 \\ \sin\theta_1 \end{pmatrix} + \begin{pmatrix} q_{21}(\tau_2) \\ q_{22}(\tau_2) \end{pmatrix}, \tag{7.20}$$

where

$$\begin{pmatrix} x_{21}(\tau_2), & x_{22}(\tau_2) \\ z_{21}(\tau_2), & z_{22}(\tau_2) \end{pmatrix} = \begin{pmatrix} k_{21}(\tau_2), & k_{22}(\tau_2) \\ k_{23}(\tau_2), & k_{24}(\tau_2) \end{pmatrix}^{-1} \begin{pmatrix} c_{21}(\tau_2), & c_{22}(\tau_2) \\ c_{23}(\tau_2), & c_{24}(\tau_2) \end{pmatrix} \tag{7.21}$$

and

$$\begin{pmatrix} q_{21}(\tau_2) \\ q_{22}(\tau_2) \end{pmatrix} = \begin{pmatrix} k_{21}(\tau_2), & k_{22}(\tau_2) \\ k_{23}(\tau_2), & k_{24}(\tau_2) \end{pmatrix}^{-1} \left\{ -K_2 \begin{pmatrix} \chi_{21}(\tau_2) \\ \chi_{23}(\tau_2) \end{pmatrix} - K_1 \begin{pmatrix} \chi_{211}(\tau_2), & \chi_{213}(\tau_2) \\ \chi_{231}(\tau_2), & \chi_{233}(\tau_2) \end{pmatrix} \begin{pmatrix} \chi_{11}(\tau_1) \\ \chi_{13}(\tau_1) \end{pmatrix} \right\}. \tag{7.22}$$

Next the second equation of Eq. (7.5) is

$$-\chi_{221}(\tau_2)x_1(\tau_1) - \chi_{223}(\tau_2)z_1(\tau_1) + y_2(\tau_2) - y_1(\tau_1) = E_{221}(\tau_2)\cos\theta_1 + E_{222}(\tau_2)\sin\theta_1 - K_2\chi_{22}(\tau_2). \tag{7.23}$$

Substituting of Eq. (7.13) into Eq. (7 23) yields

$$y_{10}(\tau_1) = F_{1c}(\tau_1)\cos\theta_1 + F_{1s}(\tau_1)\sin\theta_1, \tag{7.24}$$

where

$$\left.\begin{aligned} y_{10}(\tau_1) &= K_2\chi_{22}(\tau_2) - \chi_{221}(\tau_2)q_{11}(\tau_1) - \chi_{223}(\tau_2)q_{12}(\tau_1) + y_2(\tau_2) - y_1(\tau_1), \\ F_{1c}(\tau_1) &= E_{221}(\tau_2) + \chi_{221}(\tau_2)x_{11}(\tau_1) + \chi_{223}(\tau_2)z_{11}(\tau_1), \\ F_{1s}(\tau_1) &= E_{222}(\tau_2) + \chi_{221}(\tau_2)x_{12}(\tau_1) + \chi_{223}(\tau_2)z_{12}(\tau_1). \end{aligned}\right\} \tag{7.25}$$

By this equation, θ_1 can be obtained as follows

$$\theta_1 = \theta_0 + \cos^{-1}\frac{y_{10}(\tau_1)}{F_{10}(\tau_1)}, \tag{7.26}$$

where

$$\theta_0 = \tan^{-1}\frac{F_{1s}(\tau_1)}{F_{1c}(\tau_1)}, \quad F_{10}(\tau_1) = \sqrt{F_{1c}^2(\tau_1) + F_{1s}^2(\tau_1)}. \tag{7.27}$$

The second equation of Eq. (7.4) is

$$\chi_{121}(\tau_1)x_2(\tau_2) + \chi_{123}(\tau_1)z_2(\tau_2) + y_2(\tau_2) + y_1(\tau_1) = F_{121}(\tau_1)\cos\theta_1 + F_{122}(\tau_1)\sin\theta_1 - K_1\chi_{12}(\tau_1). \tag{7.28}$$

Substitution of Eq. (7.20) in Eq. (7.28) yields

$$y_{20}(\tau_1) = F_{2c}(\tau_1)\cos\theta_1 + F_{2s}\sin(\tau_1)\theta_1, \tag{7.29}$$

where

$$\left.\begin{aligned} y_{20}(\tau_1) &= K_1\chi_{12}(\tau_1)+\chi_{121}(\tau_1)q_{21}(\tau_2)+\chi_{123}(\tau_1)q_{22}(\tau_2)+y_2(\tau_2)+y_1(\tau_1), \\ F_{2c}(\tau_1) &= F_{121}(\tau_1)-\chi_{121}(\tau_1)x_{21}(\tau_2)-\chi_{123}(\tau_1)z_{21}(\tau_2), \\ F_{2s}(\tau_1) &= F_{122}(\tau_1)-\chi_{121}(\tau_1)x_{22}(\tau_2)-\chi_{123}(\tau_1)z_{22}(\tau_2) \end{aligned}\right\}. \tag{7.30}$$

Consequently, substituting of Eqs. (7.14), (7.15), (7.21), (7.22) and (7.26) into Eq. (7.29), the transcendental equation can be obtained as follows, which containing unexplicitly the unknown function τ_1,

$$w_n'\{y_1(\tau_1),\ y_2(\tau_2),\ \tau_1\}=0, \tag{7.31}$$

then we can determine τ_1 by solving this equation.

8. $f_{rn}(\tau)$ and $g_{rn}(\tau)$

(a) When the equation $p^3+\delta_0 p^2+p\gamma_{10}+a_1=0$ has three distinct roots.
Putting

$$p^3+\delta_0 p^2+p\gamma_{10}+a_1=(p+\alpha_1)(p+\alpha_2)(p+\alpha_3), \tag{8.1}$$

$f_{rn}(\tau)$'s and $g_{rn}(\tau)$'s are tabulated in Tables 3, 4 and 5, when $r=1$,

Table 3.

$g_{10}(\tau)$	$\frac{1}{a_1}+\frac{1}{\alpha_1 A_1}\varepsilon^{-\alpha_1\tau}+\frac{1}{\alpha_2 A_2}\varepsilon^{-\alpha_2\tau}+\frac{1}{\alpha_3 A_3}\varepsilon^{-\alpha_3\tau}$
$g_{11}(\tau)$	$-\frac{1}{A_1}\varepsilon^{-\alpha_1\tau}-\frac{1}{A_2}\varepsilon^{-\alpha_2\tau}-\frac{1}{A_3}\varepsilon^{-\alpha_3\tau}$
$g_{12}(\tau)$	$\frac{\alpha_1}{A_1}\varepsilon^{-\alpha_1\tau}+\frac{\alpha_2}{A_2}\varepsilon^{-\alpha_2\tau}+\frac{\alpha_3}{A_3}\varepsilon^{-\alpha_3\tau}$
$g_{13}(\tau)$	$-\frac{d_1^2}{A_1}\varepsilon^{-\alpha_1\tau}-\frac{d_2^2}{A_2}\varepsilon^{-\alpha_2\tau}-\frac{\alpha_3^2}{A_3}\varepsilon^{-\alpha_3\tau}$

Table 4.

$f_{11}(\tau)$	$b_0\cos\tau+b_1\sin\tau-\frac{1}{B_1}\varepsilon^{-\alpha_1\tau}-\frac{1}{B_2}\varepsilon^{-\alpha_2\tau}-\frac{1}{B_3}\varepsilon^{-\alpha_3\tau}$
$f_{12}(\tau)$	$b_0\sin\tau+b_1\cos\tau+\frac{\alpha_1}{B_1}\varepsilon^{-\alpha_1\tau}+\frac{\alpha_2}{B_2}\varepsilon^{-\alpha_2\tau}+\frac{\alpha_3}{B_3}\varepsilon^{-\alpha_3\tau}$
$f_{13}(\tau)$	$-b_0\cos\tau-b_1\sin\tau-\frac{\alpha_1^2}{B_1}\varepsilon^{-\alpha_1\tau}-\frac{\alpha_2^2}{B_2}\varepsilon^{-\alpha_2\tau}-\frac{\alpha_3^2}{B_3}\varepsilon^{-\alpha_3\tau}$
$f_{14}(\tau)$	$b_0\sin\tau-b_1\cos\tau+\frac{\alpha_1^3}{B_1}\varepsilon^{-\alpha_1\tau}+\frac{\alpha_2^3}{B_2}\varepsilon^{-\alpha_2\tau}+\frac{\alpha_3^3}{B_3}\varepsilon^{-\alpha_3\tau}$

Table 5.

b_1	$\frac{a_1-\delta_0}{(\alpha_1^2+1)(\alpha_2^2+1)(\alpha_3^2+1)}$	b_0	$\frac{1-\gamma_0}{(\alpha_1^2+1)(\alpha_2^2+1)(\alpha_3^2+1)}$
B_1	$(1+\alpha_1^2)A_1$	A_1	$(\alpha_1-\alpha_2)(\alpha_3-\alpha_1)$
B_2	$(1+\alpha_2^2)A_2$	A_2	$(\alpha_2-\alpha_3)(\alpha_1-\alpha_2)$
B_3	$(1+\alpha_3^2)A_3$	A_3	$(\alpha_3-\alpha_1)(\alpha_2-\alpha_3)$

The values of $f_{2n}(\tau)$'s and $g_{2n}(\tau)$'s are obtained by replacing γ_{10} and a_1 by γ_{20} and a_2 in the expressions of $f_{1n}(\tau)$'s and $g_{1n}(\tau)$'s.

(b) When the equation $p^3+\delta_0 p^2+\gamma_{10}p+a_1=0$ has one root and a pair of conjugate roots.

Putting

$$p^3+\delta_0 p^2+\gamma_{10}p+a_1=(p+\alpha_1)(p+\alpha+j\beta)(p+\alpha-j\beta), \tag{8.2}$$

we have Tables 6, 7 and 8.

Table 6.

$g_{10}(\tau)$	$\frac{1}{a_1}-\frac{e_0}{\alpha_1}\varepsilon^{-\alpha_1\tau}+\varepsilon^{-\alpha\tau}(e_1\cos\beta-e_2\sin\beta\tau)$
$g_{11}(\tau)$	$e_0\varepsilon^{-\alpha_1\tau}+\varepsilon^{-\alpha\tau}(-e_3\cos\beta\tau+e_4\sin\beta\tau)$
$g_{12}(\tau)$	$-\alpha_0 e_0\varepsilon^{-\alpha_1\tau}+\varepsilon^{-\alpha\tau}(e_5\cos\beta\tau-e_6\sin\beta\tau)$
$g_{13}(\tau)$	$\alpha_1^2 e_0\varepsilon^{-\alpha_1\tau}+\varepsilon^{-\alpha\tau}(-e_7\cos\beta\tau+e_8\sin\beta\tau)$

Table 7.

$f_{11}(\tau)$	$b_0\cos\tau+b_1\sin\tau+d_0\varepsilon^{-\alpha_1\tau}+\varepsilon^{-\alpha\tau}(-d_1\cos\beta\tau+d_2\sin\beta\tau)$
$f_{12}(\tau)$	$b_1\cos\tau-b_0\sin\tau-\alpha_1 d_0\varepsilon^{-\alpha_1\tau}+\varepsilon^{-\alpha\tau}(d_3\cos\beta\tau-d_4\sin\beta\tau)$
$f_{13}(\tau)$	$-b_0\cos\tau-b_1\sin\tau+\alpha_1^2 d_0\varepsilon^{-\alpha_1\tau}+\varepsilon^{-\alpha\tau}(-d_5\cos\beta\tau+d_6\sin\beta\tau)$
$f_{14}(\tau)$	$-b_1\cos\tau+b_0\sin\tau-\alpha_1^3 d_0{}^{-\alpha_1\tau}+\varepsilon^{-\alpha\tau}(d_7\cos\beta\tau-d_8\sin\beta\tau)$

Table 8.

e_0	$\frac{1}{(\alpha_1-\alpha)^2+\beta^2}$	d_0	$\frac{e_0}{\alpha_1^2+1}$	d_1	$\frac{e_0}{\Delta}(3\alpha^2-\beta^2+1-2\alpha_1\alpha)$
e_2	$\frac{\alpha_1}{a_1\beta}\{\alpha(\alpha_1-\alpha)+\beta^2\}e_0$	e_1	$\frac{e_0}{\alpha_1}-\frac{1}{a_1}$	d_2	$\frac{e_0}{\beta\Delta}\{(\alpha_1-\alpha)(\alpha^2-\beta^2+1)+2\alpha\beta^2\}$
e_3	e_0	e_5	$\alpha_1 e_0$	d_3	$\alpha d_1+\beta d_2$
e_6	$\frac{e_0}{\beta}\{\alpha(\alpha_1-\alpha)-\beta^2\}$	e_4	$e_0\cdot\frac{\alpha_1-\alpha}{\beta}$	d_4	$\alpha d_2-\beta d_1$
				d_5	$\alpha d_3+\beta d_4$
e_8	$\alpha e_6-\beta e_5$	e_7	$-e_0(\alpha-\beta)^2$	d_6	$\alpha d_4-\beta d_3$
b_0	$\frac{1-\gamma_{10}}{(\alpha_1^2+1)\cdot\Delta}$	b_1	$\frac{a_1-\delta_0}{(\alpha_1^2+1)\cdot\Delta}$	d_7	$\alpha d_5+\beta d_6$
Δ	$(\alpha^2-\beta^2+1)^2+4\alpha^2\beta^2$	a_1	$\alpha_1(\alpha^2+\beta^2)$	d_8	$\alpha d_6-\beta d_5$

As in the previous case, the values $f_{2n}(\tau)$'s and $g_{2n}(\tau)$'s are obtained on replacing γ_{10} and a_1 by γ_{20} and a_2 in the expressions of $f_{1n}(\tau)$'s and $g_{1n}(\tau)$'s respectively.

9. Numerical Example

In the present section a numerical example of the basic circuit is illustrated, and the results of this example were obtained by making use of the Digital Computer (KDC-1). Here, for the sake of comparing with those of Reference (3) we assume that the circuit constants are the same ones in Reference (3) as follows:

$$L_1 = L_3 = 1.17\,H, \quad L_2 = L_4 = 1.7\,mH,$$

$$C = 0.002\,\mu F, \quad R = 2000\,\Omega, \quad f = \frac{\omega}{2\pi} = 1000\,c/s.$$

In the numerical calculation of determing τ_1, we take

$$\Delta\tau_1 = 0.001, \quad \varepsilon = 0.0001.$$

The results are shown in Figs. 7, 8, 9, 10 and 11.

Fig. 7 shows the determined values τ_1 with respect to a measure of the hysteresis of the coil, i.e.

$$\Delta y\,\% = \frac{y_1(\tau_1) - y_2(\tau_2)}{y_1(\tau_1)} \times 100\%$$

for some parameters K', i.e. $K' = 1/K_2 = I_m/I_1$.

From this result, we can find that the pulse width τ_1 increases in proportion to increasing of the measure of the hysteresis, and that the values τ_1 are equal to those of Reference (3) when $\Delta y\% = 0$, without the hysteresis.

Fig. 8 shows the values of θ_1 which also increase in accordance with increasing $\Delta y\%$. The peak value of $E_L(t)$ is shown in Figs. 9 and 10, from which, the effect of the hysteresis of the coil makes the peak voltake decrease. Fig. 11

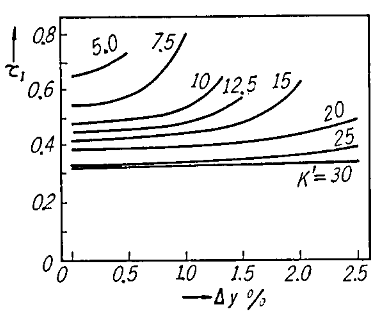

Fig. 7. Durations of the 1-st circuit mode (Widths of pulse voltages across the coil).

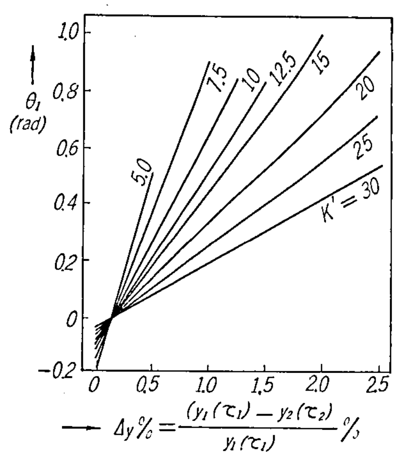

Fig. 8. Phase angles θ_1.

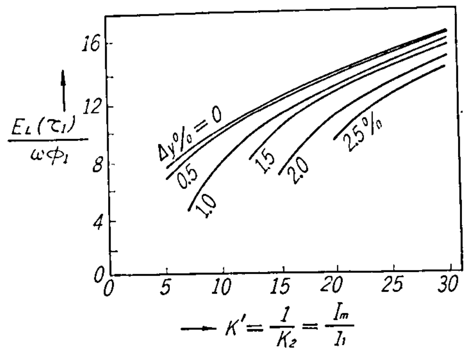

Fig. 9. Peak pulse voltage across the coil.

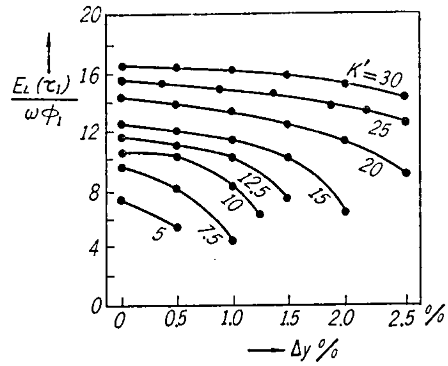

Fig. 10. Peak pulse voltage across the coil.

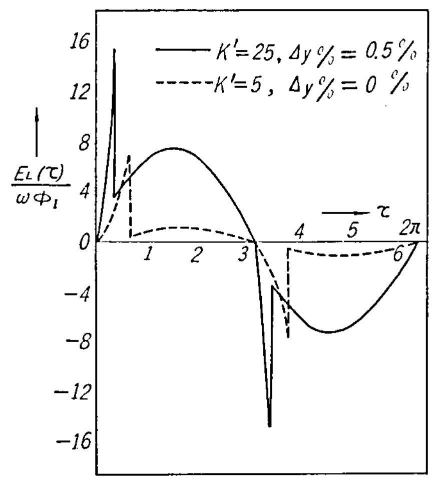

Fig. 11. Wave forms of voltage across the coil.

shows the wave forms of the steady state voltage across the coil, in this case we can find that the wave form was remarkably distorted by the effect of the hysteresis, comparing with the case without the hysteresis.

10. Conclusion

In this paper, the study on the harmonic producer circuits is presented by the use of the analytical method based on the theorems of the Periodically Interrupted Electric Circuits of the Third Genus.

Taking the effect of magnetic hysteresis of the coil into consideration, we can make clear the behaviour of the producer circuits as accurately as possible, and show the numerical results of one example.

It is evident that this analytical method is useful for the analysis of the non-linear problems such as those containing the hysteresis or other non-linearity in order to obtain the steady state solutions, but it is difficult to determine the periods which decided by the natural phenomena in the considered problems, in that case, by means of the digital computer we can easily determine these values for the case of some numerical examples.

Acknowledgment

The authors wish to thank Prof. H. Nishihara and Prof. A. Kishima as well as other members of the Department of Electrical Engineering II for their valuable discussions in this work.

References

1) E. Peterson, J. M. Manley & L. R. Wrathall: B.S.T.J., 16, 4, p. 88, (1949).
2) T. Kurokawa: Jour. of Inst. of Elect. Comm. Eng. of Japan, 32, 4, p. 88, (1949).
3) S. Hayashi & H. Nishihara: Tech. Rep. of Eng. Res. Inst. Kyoto Uni., vol III, 2, (1953).
4) A. Kyogoku, Y. Oohashi & K. Ishii: Jour. of Inst. of Elect. Comm. Eng. of Japan, 44, 10, p. 79, (1961).
5) S. Hayashi & K. Mizukami: Convention Records at Joint Meeting of Inst. of Elect. Eng. of Japan, No. 11, (1962), No. 1-7, (1962) and No. 68, (1963).
6) S. Hayashi: Periodically Interrupted Electric Circuits, Denki-Shoin, (1961).

68 項欠

CHAPTER V

AN ANALYSIS OF NON-LINEAR SAMPLED-DATA FEEDBACK CONTROL SYSTEMS

70 項欠

An Analysis of Non-Linear Sampled-Data Feedback Control Systems

Synopsis

Higher order sampled-data feedback systems which contain a saturating element or a backlash element are investigated in this paper.

This study introduces a new approach to the analysis of non-linear sampled-data control systems. At first the authors describe a new analytlcal method for such systems using the theorem of Periodically Interrupted Electric Circuits and how to apply the Digital Computer (KDC-1) to this theorem. The method presented here can be applied to any higher order systems with any non-linear elements by making use of the digtal computer simulation of the above theorem and the non-linear element. Some illustrative examples are given to clarify the method involved. One example of the third order sampled-data feedback system wlth a saturating element is investigated in case of initial conditions being given without external forces, a unit step function and sine wave inputs being given. The examples show that in the case of a step input as well as initial conditions existing, slight variations of initial values result in diferent modes of periodic oscillations, while in the case of a sinusoidal input, a slight modification of non-linear characteristics results in forced oscillations in one case and in sub-harmynic oscillations in another.

Two illustrative examples of the second order system with a backlash element are considered in the case where the linear system is followed by the backlash or follows the backlash.

Some results obtained by numerical computations are presented to show the performance of the system dynamics on the basis of the new analytical method presented here.

1. Introduction

To feedback control systems belongs a sampled-data feedback system for which the input signal is represented by samples at regular intervals of time as a discontinious waveform, for example, the control system with contactor relay mechanism, the radar system and the digital computer control system. There are two types in the sampled-data feedback systems, one of which is a linear sampled-data feedback system containing linear elements and another is a non-linear sampled-data feedback system containing non-linear elements.

The theory of the former has progressed and been well constructed by means of the techniques of the z transform and the modified z transform. However the theory of the latter containing non-linear elements, for example, a saturating element, a backlash element, and a hysteresis or deadzone element, has hardly been established because of difficulties of analyzing the complicated phenomena arising between the discontinious signal and nonlinearity. However C.K. Chow[1] has recently studied about the self-sustained oscillations in relay servomechanisms with sampling by using the describing function method. R.E. Kalman[2], on the other hand, has investigated the initial condition problems for the same system by the phase plane method and has obtained unexpected results from the theoretical point of view.

The approach to the analysis of the transient behavior of the low order relay sampled-data feedback system has been introduced in the past by F.J. Mullin, E.I. Jury[3], K. Izawa and L.E. Weaver[4] by use of the phase plane method. Especially F.J. Mullin[5] has studied the stability and the compensation of the saturating sampled-data feedback systems and S. Kodama[6], from a different point of view, investigated the stability of a non-linear sampled-data feedback system and he gave the counter theory for the stability to F.J. Mullin's study. These investigations based on various assumptions of non-linear elements as well as the dynamic chracteristic of the feedback systems have not been established generally for the non-linear sampled-data feedback systems.

In this paper we introduce a new approach to the analysis of the higher order sampled-data feedback systems containing non-linear elements. This analytical technique for the transient and steady state behavior of the systems is based on the theorem of Periodically Interrupted Electrical Circuits[7] applying the digital computer[8][9]. Although only saturating and backlash elements are here taken into account as non-linear elements, the analytical method presented here may serve as a useful tool in the system with other non-linear elements.

2. Application of the Theorem of Periodically Interrupted Electric Circuits

The system under consideration is shown in Fig. 1. The non-linearity of the memory or the zero-memory type follows a zero-order hold network.

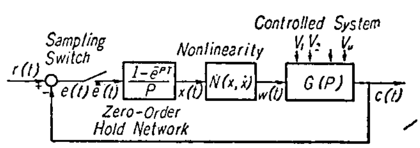

Fig. 1 Nonlinear sampled-data control system

The controlled system is considered

generally as an m-th order linear element and subject to the disturbances $v(t)$'s which are applied to points of the cascaded output elements.

When the input to the nonlinearity is $x(t)$, the output $w(t)$ of the nonlinearity is written as

$$\begin{aligned} w(t) &= N\{x(t),\ \dot{x}(t)\} \\ &= w_n \qquad\qquad t = \overline{n-1}T+0 \end{aligned} \tag{1}$$

where $N(x, \dot{x})$ is the non-linear function representing the non-linearity, T is the sampling period, $\dot{x}(t)=\frac{d}{dt}x(t)$ and $n=1, 2, \cdots$. This output $w(t)$ becomes constant during one sampling period as shown in Fig. 2.

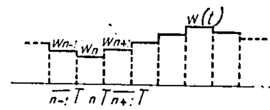

Fig. 2 Output of the nonlinearity

The system equation can be set up, in general, in the matrix form as follows during some (n) sampling period

$$\begin{pmatrix} D+a_{11} & \lambda_{12} \cdots\cdots & \lambda_{1m} \\ \lambda_{21} & D+a_{22} & \vdots \\ \vdots & \ddots & \vdots \\ \vdots & \ddots & \lambda_{m-1,m} \\ \lambda_{m1}\cdots\lambda_{m,m-1} & & D+a_{mm} \end{pmatrix} \begin{pmatrix} c_1(t) \\ c_2(t) \\ \vdots \\ c_{m-1}(t) \\ c(t) \end{pmatrix} = \begin{pmatrix} w_n \\ v_1(t)+v_{1n} \\ v_2(t)+v_{2n} \\ \vdots \\ v_u(t)+v_{un} \end{pmatrix} \quad 0 \leqq t \leqq T \tag{2}$$

where

$$D = \frac{d}{dt},\ v_{un} = v_u(t)],\qquad t = \overline{n-1}T \qquad \lambda_{12}, \cdots, \lambda_{m,m-1}, = 0 \text{ or } \pm 1$$

and $a_{11}, \cdots, a_{mm}$ are constants determined by the controlled system, $c_1(t), \cdots, c_{m-1}(t)$ are outputs at points of the cascaded first order output elements of the controlled system.

Now we rewrite Eq. (2) in the abbreviated form as

$$[Z(D)][g_n(t)] = [y_n(t)] \qquad 0 \leqq t \leqq T \tag{3}$$

and Eq. (3) can be replaced by the operational form (the second kind Laplace transform)

$$[Z(p)][g_n(p)] = [y_n(p)] + p[L][g_{n-1}(T)] \tag{4}$$

where $[L]$ is a constant determined by $[Z(D)]$ and generally this matrix is a unit matrix.

Premultiplying both sides of Eq. (4) by $[Z(p)]^{-1}$, the following equation can be obtained

$$[g_n(p)] = [Z(p)]^{-1}[y_n(p)] + p[Z(p)]^{-1}[L][g_{n-1}(T)] \tag{5}$$

Hence the corresponding time function to Eq. (5) can be derived by taking the inverse transform of Eq. (5) directly

$$[g_n(t)] = [\varphi_n(t)]+[\chi(t)][g_{n-1}(T)] \qquad 0 \leqq t \leqq T \tag{6}$$

where

$$[\varphi_n(t)] = \mathfrak{H}^*[Z(p)]^{-1}[y_n(p)]$$
$$[\chi(t)] = \mathfrak{H}p[Z(p)]^{-1}[L]$$

This result is the solution of the system Eq. (2) under consideration during n-th sampling period and corresponds to the solution obtaind by the modified Z trasform used in the linear sampled-data feedback system.

Now the initial matrix $[g_{n-1}(T)]$ of Eq. (6) is evaluated by the following reccurrence formulae in matrix notation as

$$\begin{aligned}[g_{n-1}(T)] &= [\varphi_{n-1}(T)]+[\chi(T)][g_{n-2}(T)] \\ &= [\varphi_{n-1}(T)]+[\chi(T)][\varphi_{n-2}(T)]+[\chi(T)]^2[\varphi_{n-3}(T)]+\cdots\cdots \\ &\qquad +[\chi(T)]^{n-2}[\varphi_1(T)]+[\chi(T)]^{n-1}[g_0^{-0}]\end{aligned} \tag{7}$$

then, substituting Eq. (7) into Eq. (6) results in the solution during any sampling interval.

If the disturbances $v_1(t), \cdots, v_u(t)$ in Fig. 1 were not applied, then $[\varphi_n(t)]$ in Eq. (6) would be replaced and deduced easily in the form of the product of two matrices, that is, $[y_n(t)]$ becomes equal to $[y_n]$ composed of the constant elements being indifferent to time t during one sampling interval, therefore in such a case Eq. (6) can be written as

$$[g_n(t)] = [\varphi(t)][y_n]+[\chi(t)][g_{n-1}(T)] \qquad 0 \leqq t \leqq T \tag{8}$$

where

$$\left.\begin{aligned}[\varphi(t)] &= \mathfrak{H}[Z(p)]^{-1} \\ [y_n] &= [N\{[R_n]+[T]'g[_{n-1}(T)]\}]\end{aligned}\right\} \tag{9}$$

In Eq. (9), $[R_n]$ is determined by the $r(t)$ input to the feedback system and includes $r(\overline{n-1}T)$ component, $[(T)]'$ is the so-called transfer matrix whose components of 0 or ± 1. In this case the initial matrix $[g_{n-1}(T)]$ can be written as

$$\begin{aligned}[g_{n-1}(T)] &= [\varphi(T)][y_{n-1}]+[\chi(T)][g_{n-2}(T)] \\ &= [\varphi(T)][y_{n-1}]+[\chi(T)][\varphi(T)][y_{n-2}]+[\chi(T)]^2[\varphi(T)][y_{n-3}]+\cdots\cdots \\ &\qquad +[\chi(T)]^{n-2}[\varphi(T)][y_1]+[\chi(T)]^{n-1}[g_0^{-0}]\end{aligned} \tag{10}$$

Next we shall induce the condition of the self-sustained oscillations. In the case where the $r(t)$ input to the system exists, it is possible to obtain its conditions, though we now consider the case where the $r(t)$ input is not given.

If the self-sustained oscillations of period $rT(r=1, 2, \cdots)$ are to exist in the system when $r(t)=0$, we can put, from Eq. (9)

---

* $\mathfrak{H}\{f(p)\} = \frac{1}{2\pi j}\lim_{\beta\to\infty}\int_{r-j\beta}^{r+j\beta}\frac{f(p)}{p}e^{pt}dp$

$$[N\{[T]'[g_{n-1}(T)]\}] = [\varepsilon_{n-1}] \tag{11}$$

and substituting Eq. (11) into Eq. (8) yields the following matrix according to the condition that Eq. (8) should have the same value at the r-th sampling instant as the value at the previous r-th sampling instant, that is,

$$\begin{aligned}[B_\mu] = &\{[\varphi(T)][\varepsilon_{\mu-1}]+[\chi(T)]\}\{[\varphi(T)][\varepsilon_{\mu-2}]+[\chi(T)]\}\cdots \\ &\{[\varphi(T)][\varepsilon_1]+[\chi(T)]\}\{[\varphi(T)][\varepsilon_r]+[\chi(T)]\}\cdots\{[\varphi(T)][\varepsilon_n]+[\chi(T)]\}\end{aligned} \tag{12}$$

where

$$\mu = 1, 2, \cdots, r.$$

Hence we can obtain the β's latent roots of the matrix $[B_\mu]$ by solving the characteristic equation of the form

$$\delta\{\beta[U]-[B_\mu]\} = 0 \tag{13}$$

Then we know that the necessary and sufficient condition* where the system would generate the self-sustained oscillations is that the absolute values of all the latent roots $\beta_1, \beta_2, \cdots, \beta_m$ should be equal to unity respectively. If there is only one latent root which is more than unity, the system is unstable and if all the latent roots are less than unity, the system is stable because the solution becomes infinitesimal as time goes.

3. Simulation by the Digital Computer and Numerical Examples

In practice it is difficult to clarify theoreticaly the dynamic characteristics of the system according to the above theorem, but it is easily possible to place the characteristics more clearly in sight by using the digital computer to simutate this analytical method applied to some examples.

Now consider the case where the controlled system is the 3rd order system without disturbances and the non-linearity is a saturaing element shown in Fig. 3.

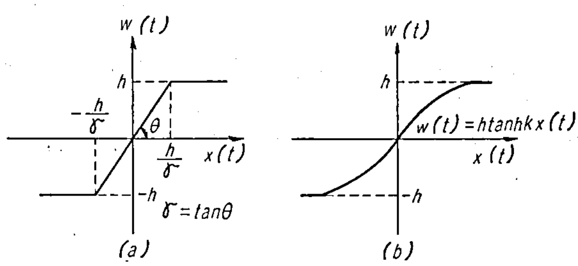

Fig. 3 Nonlinarity (saturating element)

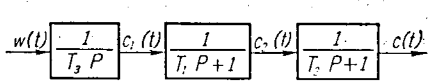

Fig. 4 Controlled system $G(p)$

Eq. (8) represents the solution during n-th sampling interval when the saturating element is given

* When r is a rational number, similarly we consider the self-sustained oscillation, therefore the condition of the self-sustained oscillatlons could be established in general.

by Fig. 3(a), where $[y_n]$ of Eq. (9) can be determined by the following three regions denoted such that

(1), if the linear region exists;

$$|x_n| \equiv |\{r(t)-c(t)\}| \leq h/r \qquad t=\overline{n-1}T+0$$

then Eq. (9) becomes

$$[y_n] = r\{[r(\overline{n-1}T)]+[T]'[g_{n-1}(T)]\} \\ = \begin{pmatrix} rx_n \\ 0 \\ 0 \end{pmatrix}, \tag{14}$$

(2), if the positive saturate region exists;

$$x_n > \frac{h}{r}$$

then Eq. (9) becomes

$$[y_n] = \begin{pmatrix} h \\ 0 \\ 0 \end{pmatrix}, \tag{15}$$

(3), and if the negative saturating region exists;

$$x_n < \frac{h}{r}$$

then Eq. (9) becomes

$$[y_n] = \begin{pmatrix} -h \\ 0 \\ 0 \end{pmatrix}. \tag{16}$$

In the case of this example, the digital computer flowchart is shown in Fig. 5.

When the saturating element whose characteristic is represented by the following Eq. (17) is given in Fig. 3(b), $[y_n]$ can be more easily determined rather than in the above case.

$$w(t) = h \tanh kx(t) \tag{17}$$

Fig. 6 and Fig. 7 show the numerical results in the case of these examples. Fig. 6(a) shows the response to a unit step function input in which the different modes of periodic oscillation occurring depend on a slight variations of initial values.

Other different modes of periodic oscillation depending on other initial conditions in the same system was generated.

Fig. 6(b) shows the response of the system with various saturating elements to a unit step function input in the case where the γ of the non-linearity is only changed at same initial conditions.

The modes (2), (3) and (4) in Fig. 6(b) illustrate the periodic oscillation, therefore we know that it is possible for one value of the γ of the non-linearity that the periodic oscillation should exist in the system, but for another value

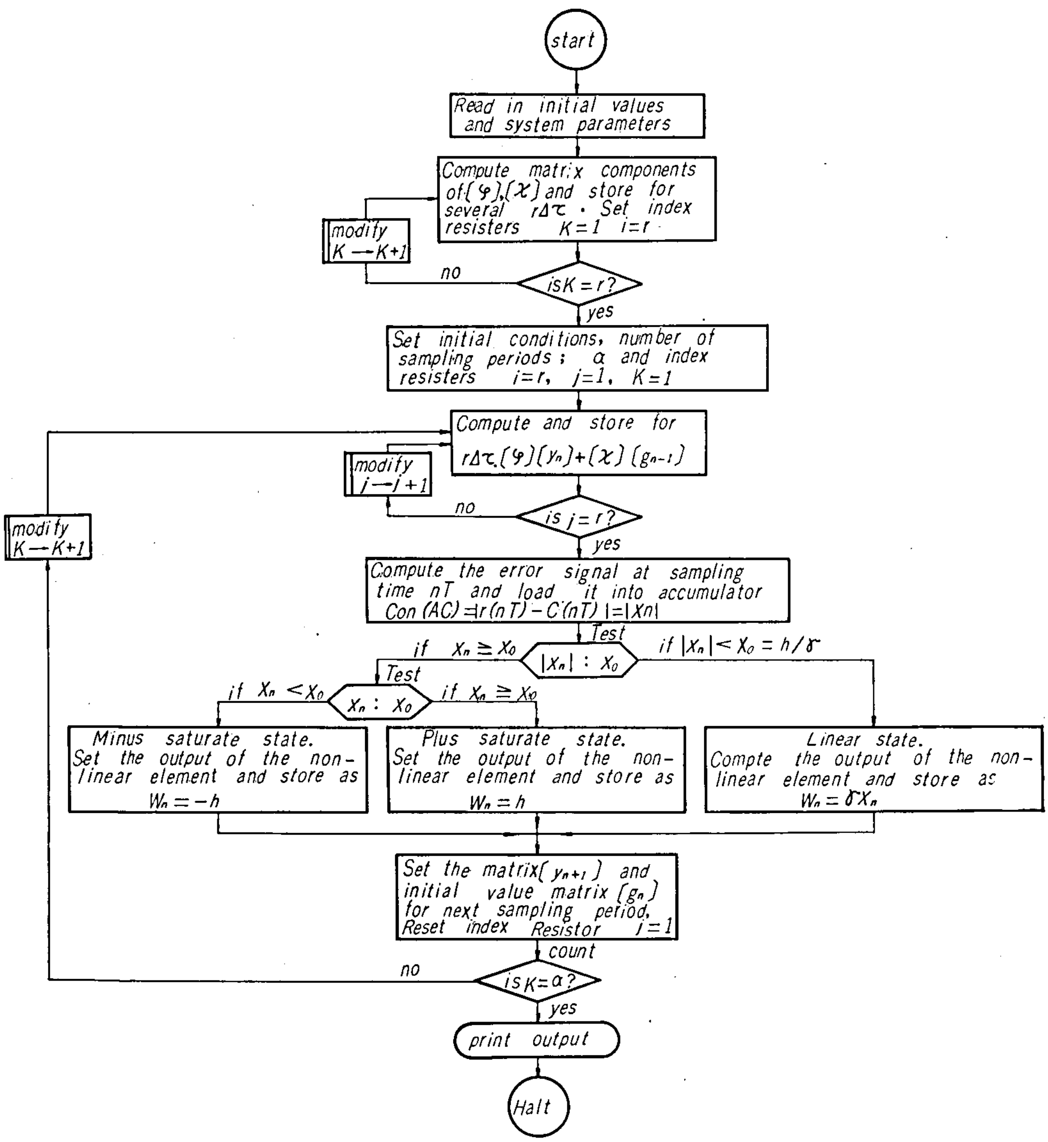

Fig. 5 Digital computer flowchart for the higher order sampled-data control system with a saturating element

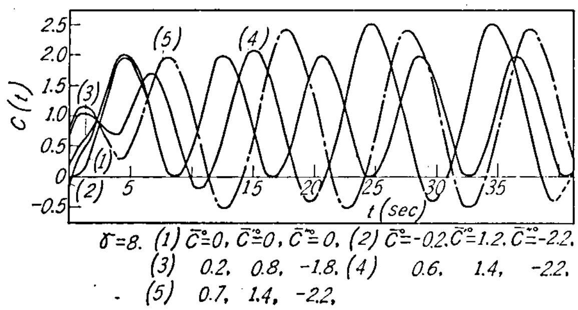

(a) Different modes of periodic oscillations in response to a unit step function input

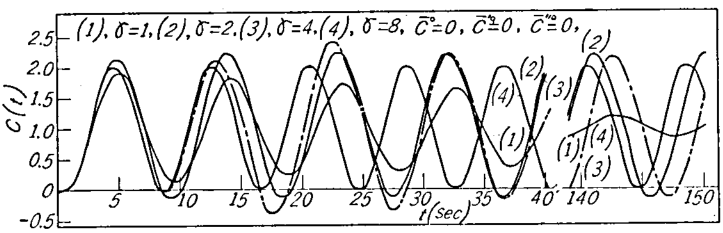

(b) The time response of the system with various saturating elements to a unit step function input

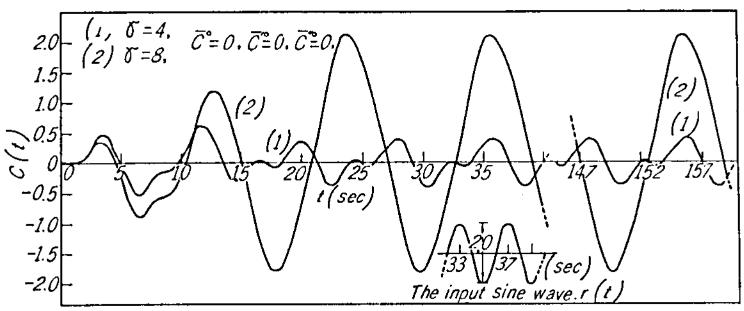

(c) Forced oscillations in the system with a saturating element for $r(t)=\sin 0.5\pi t$

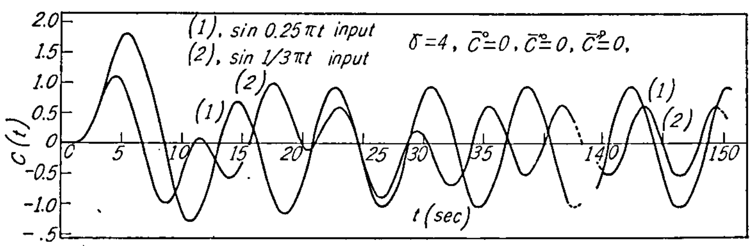

(d) The transient response of the system with a saturating element to sinusoidal inputs

Fig. 6 Response of the system with a saturating element, $h=1.0$, $T=1.0$ (sec) and $G(p)=\dfrac{1}{p(p+1)^2}$ to a unit step function and sinusoidal inputs

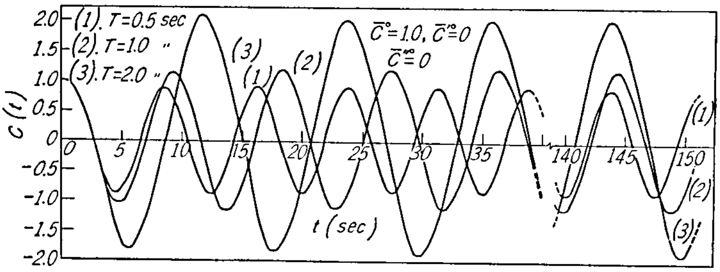

(a) The response of the system with a saturating element ($w(t)=\tanh 3x(t)$) to $r(t)=0$

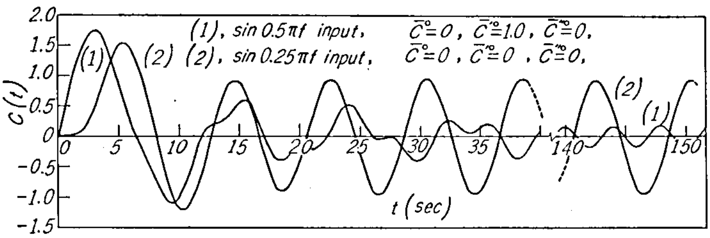

(b) The response of the system with a saturating element ($w(t)=\tanh 2x(t)$) and $T=1.0$ to sinusoidal inputs

Fig. 7 Response of the system with a saturating element described $w(t)=h \tanh kx(t)$ and $G(p)=\dfrac{1}{p(p+1)^2}$ to sine wave inputs and no input but only initial values

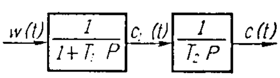

(a) Controlled system $G(p)$

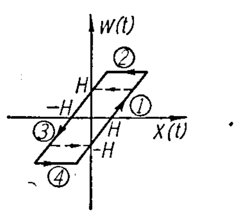

(b) Nonlinearity (backlash)

Fig. 8 Controlled system and backlash element

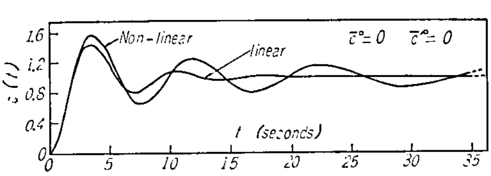

Fig. 9 The response of the second order system of $G(p)=\dfrac{1}{p(p+1)}$, $T=1.0$ with a backlash element $H=0.1$ and without (linear) to a unit step function input

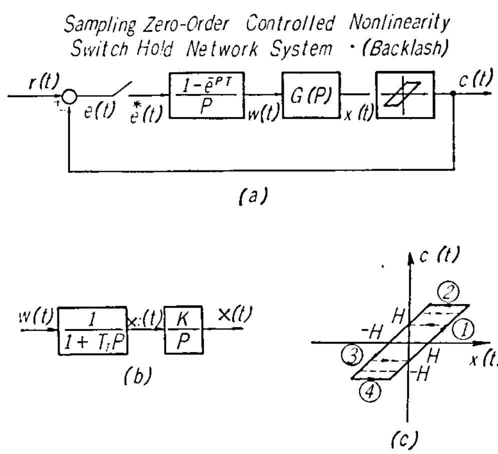

(a) Sampled-data sarvo with backlash element
(b) Controlled system, $G(p)$
(c) Nonlinearity (backlash)

Fig. 10 Non-linear sampled data control system

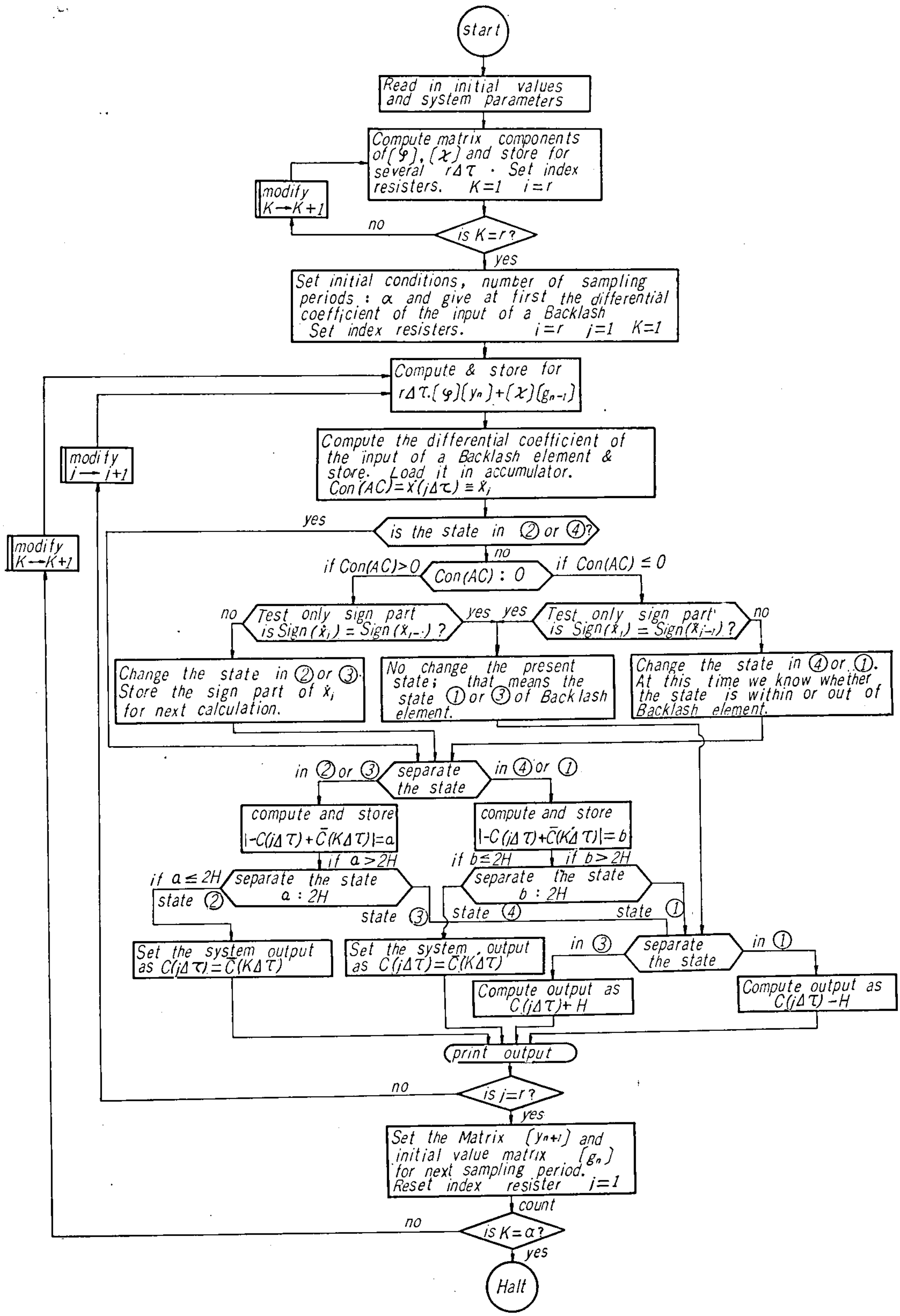

Fig. 11 Digital computer flowchart for the second order sampled-data control system with a backlash element

it is impossible.

Fig. 6(c) and (d) show the response of the system to a sine wave input. The forced oscillations shown in Fig. 6(c) are the subharmonic oscillation of order 1/2 illustrated by curve 1 and order 1/3 by curve 2, however in the case shown in Fig. 6(d) the subharmonic oscillation don't occur under the same condition as in Fig. 6(c).

Fig. 7(a) shows the response of the system to no inputs only due to the given initial value for changing the sampling period and Fig. 7(b) indicates the response of the same system to a sine wave input under the same conditions in Fig. 7(a).

Next we show the numerical examples of the system with a backlash element as the non-linearity shown in Fig. 8(b).

At first we consider that the controlled system is the 2nd order system without disturbances and a backlash element follows the zero-order hold network as shown in Fig. 1.

In such a case, $[y_n]$ of Eq. (9) is determined by the following separete regions, thus

$$[y_n] = \begin{pmatrix} w(\overline{n-1}T+0) \\ 0 \end{pmatrix}$$

here $w(t)$ is found to be

① $w(t) = x(t) - H, \ (x'(t) = 0)$

② $w(t) = \{x(t) - H\} \quad t = \overline{n-2}T+0$ (within backlash)

③ $w(t) = x(t) + H, \ (x'(t) < 0)$

④ $w(t) = \{x(t) + H\} \quad t = \overline{n-2}T+0$ (within backlash)

where

H: half of the backlash width, $t = \overline{n-1}T+0$ (at n-th sampling instant).

Fig. 9 shws the response of the system containing a backlash element to a unit step function input which is compared with the response of the linear system.

When the backlash element follows the controlled system as shown in Fig. 10, one numerical results in such a case is illustrated in Fig. 12 which gives the response of the system to a unit step

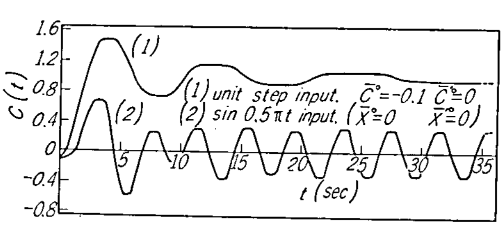

Fig. 12 The transient response of the system of Fig. 10 with $T=1.0$, $T_1=1.0$, $K=1.0$ and $H=0.1$ to a unit step function and sine wave input

function input and to a sine wave input.

The digital computer flowchart for numerical calculation of the feedback system shown in Fig. 10 is illustrated in Fig. 11.

4. Conclusion

An attempt has been made to analyze the higher order sampled-data feedback systems with non-linear element by appling the theorem of Periodically Interrupted Electric Circuits.

The application of this analytical method to some non-linear sampled-data system can be useful in practice only by making use of the digital computer simulation.

In this paper we consider the 3rd order sampled-data feedback system with a saturating element and the 2nd order sampled-data feedback system with a backlash, however it may be possible to analyzed the higher order sampled-dat feedback system with other non-linear elements by means of the analytical method presented here.

It is evident that this approach will be useful to clarify the performance of the sampled-data feedback system with non-linear elements, which has hardly been analyzed by other methods.

Acknowledgments

The authors are very grateful to Dr. A. Kishima, Dr. Y. Umoto, Dr. S. Hoshino and Dr. T. Okada as well as to the other members of the Department of Electrical Engineering II for their discussions and valuable comments in this work. Particular thanks are due to Prof. H. Nishihara in making the programing and to Prof. T. Kiyono and other staff members of the center of the Digital Computer KDC-1 at the University of Kyoto.

References

1) C. K. Chow : Contactor Servomechanisms Employing Sampled Data; AIEE Trans., Vol. 73, II, pp. 51~64 (1954)
2) R. E. Kalman : Nonlinear Aspects of Sampled-Data Control System; Proceeding of the Symposium on Nonlinear Circuit Analysis, Vol. 6, Polytechnic Institute of Brooklyn, April (1956)
3) F. J. Mullin & E. I. Jury : A Phase-Plane Approach to Relay Sampled-Data Feedback Systems; AIEE Trans., Application & Industry, pp. 517~524, Jan. (1957)
4) K. Izawa & L. E. Weaver : Relay-Type Feedback Control System with Dead Time and Sampling; AIEE Trans., Application & Industry, pp. 49~53, May (1959)
5) F. J. Mullin : The Stability and Compensation of Staurating Sampled-Data Systems; AIEE Trans., Application & Industry, pp. 270~278, July (1959)
6) S. Kodama : Stability of Nonlinear Sampled-Data Control Systems; IRE Trans. on Automatic Control, pp. 15~23, Jan. (1962)

7) S. Hayashi : Periodically Interrupted Electric Circuits ; Denki-Shoin (1961)
8) S. Hayashi, K. Mizukami : An analysis of the nonlinear sampled-data Feedback control system ; Proceeding of the general meeting on Automatic Control in Japan (1961)
9) S. Hayashi, K. Mizukami & K. Tamuro : An analysis of the nonlinear sample-data feedback control system, II ; Proceeding of the annual meeting of the Institute of Electrical Engineers of Japan, (1962).

84 項欠

85 項欠

CHAPTER VI

ANALYSIS OF SAMPLED-DATA FEEDBACK CONTROL SYSTEMS WITH FINITE PULSE WIDTH

Analysis of Sampled-Data Feedback Control Systems with Finite Pulse Width

Synopsis

A method for analysis of sampled-data feedback control systems with finite pulse width is presented in this work.

The analysis is based on introducing a new technique with some approximations by the theories of the Periodically Interrupted Electric Circuits.

The results make it possible to obtain the transient and steady-state response of such systems containing a sampler with any pulse width. Furthermore, by utilizing this method, the stability criterion is readily developed and its application to systems under consideration make clear the effects of the sampler with finite pulse width on the performance of sampled-data feedback control systems, which are of considerable importance in view of its engineering applications.

Some illustrative examples are given to clarify the method involved and its numerical results are presented to show the performance of the system dynamics. Moreover the results in this investigation are examined by the simulation of the control system in question by means of the analog computer.

1. Introduction

Analysis and design of sampled-data control systems have been developed after considerable investigation during the past decade. Especially, the development of the z-transform and modified z-transform in recent years has become an important tool in the analysis and synthesis of sampled-data systems.

However, in almost all cases the sampled version of a given signal has continued to be regarded idealistically as a train of impulses of infinitesimal duration.

More recently, efforts have been made to deal more realistically with the sampling problem by recognizing that in practice the duration of a pulse formed by sampling a function of time is not only not infinitesimal, but often appreciable.

Farmanfarma[1] introduced the p-transform to allow consideration of pulse width, and Tou[2] introduced the τ-transform for the same purpose. These efforts led to the establishment of methods of analysis and synthesis of open-loop sampled-data systems with appreciable pulse width.

Furthermore, Farmanfarma[3] has published an exact method for the analysis and synthesis of closed-loop sampled-data systems with finite pulse width. However, the exact method is very tedious. Murphy and Kennedy[4] developed an approximate method for such systems from a different point of view.

The purpose of this paper is to present a method which allows the treatment of sampled-data systems with pulse width ranging from zero to the sampling period[5,6]. The technique presented here, which is based on the theories of the Periodically Interrupted Electric Circuits, yields approximately the correct value of the system response at all instants and also develops the valuable stability criterion for systems under consideration.

Investigating the stability of sampled-data feedback control systems with finite pulse width is of considerable importance to examine the effects of pulse width on the system dynamics.

Numerical examples are worked out to show the application of the method presented in this paper, and also the results are examined by means of analog computer simulation.

2. General Analytical Method Based on the Theories of the Periodically Interrupted Electric Circuits

The sampled-data system with finite pulse width under consideration is shown in Fig. 1.

As is well-known, the basic difference between a continuous system and a finite pulsed sampled-data system is due to the presence of the sampler in the latter. Thus any general investigation of the pulsed system must start with the study of the sampler, and the relation between its input and output time functions.

Fig. 2 illustrates the input and output of a sampler with pulse width h and sampling period T.

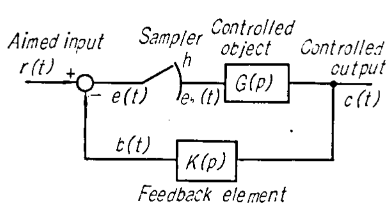

Fig. 1. Sampled-data feedback control system with finite pulse with.

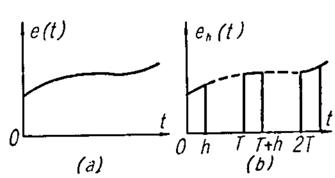

Fig. 2. (a)–Input signal to sampler. (b)–Sampler output.

Hence, the relation between input $e(t)$ and output $e_h(t)$ in the time domain may be written as:

$$e_h(t) = e(t)\{u(t)-u(t-h)\}+e(t)\{u(t-T)-u(t-T-h)\}+\cdots$$
$$= e(t)\sum_{n=0}^{\infty}\{u(t-nT)-u(t-nT-h)\} \quad (2.1)$$

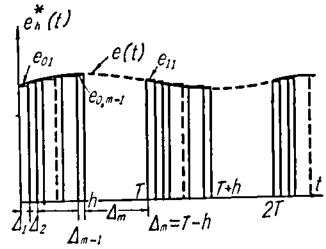

Fig. 3. Pulse width h of sampler output is subdivided into $m-1$ narrow pulses with each different width Δi $(i=1, 2, \cdots, m-1)$.

where $u(t)$ is a unit step function.

Now if pulse width h of sampler output is subdivided into $m-1$ narrow pulses with each different width Δ_i, $(i=1, 2, \cdots, m-1)$ as shown in Fig. 3, then the output $e_h(t)$ is expressed in the form, too

$$\begin{aligned} e_h(t) &= e(t)\{u(t)-u(t-\Delta_1)\}+e(t)\{u(t-\Delta_1)-u(t-\Delta_1-\Delta_2)\}+\cdots \\ &\quad +e(t)\{u(t-\sum_{i=1}^{m-2}\Delta_i)-u(t-\sum_{i=1}^{m-1}\Delta_i)\}+e(t)\{u(t-T)-u(t-T-\Delta_1)\}+\cdots \\ &\quad +e(t)\{u(t-nT)-u(t-nT-\Delta_1)\}+\cdots \\ &\quad +e(t)\{u(t-nT-\sum_{i=1}^{m-2}\Delta_i)-u(t-nT-\sum_{i=1}^{m-1}\Delta_i)\}+\cdots \\ &= \sum_{n=0}^{\infty}\sum_{j=0}^{m-2}e(t)\{u(t-nT-\sum_{i=0}^{j}\Delta_i)-u(t-nT-\sum_{i=0}^{j+1}\Delta_i)\} \end{aligned} \quad (2.2)$$

where $\Delta_0=0$.

For the application of our new technique to the system under discussion, we first assume that the output pulse $e_h(t)$ may be expressed approximately by staircase functions as indicated in Fig. 3, in other words, that it is flat-topped pulses during each different width Δ_i, then we have

$$\begin{aligned} e_h^*(t) &= e(0)\{u(t)-u(t-\Delta_1)\}+e(\Delta_1)\{u(t-\Delta_1)-u(t-\Delta_1-\Delta_2)\}+\cdots \\ &\quad +e(nT)\{u(t-nT)-u(t-nT-\Delta_1)\}+\cdots \\ &\quad +e(nT+\sum_{i=1}^{m-2}\Delta_i)\{u(t-nT-\sum_{i=1}^{m-2}\Delta_i)-u(t-nT-\sum_{i=1}^{m-1}\Delta_i)\}+\cdots \\ &= \sum_{n=0}^{\infty}\sum_{j=0}^{m-2}e(nT+\sum_{i=0}^{j}\Delta_i)\{u(t-nT-\sum_{i=0}^{j}\Delta_i)-u(t-nT-\sum_{i=1}^{j+1}\Delta_i)\} \end{aligned} \quad (2.3)$$

Accordingly, it may be obviously said, from inspection of Eq. (2.3), that the sampler with finite pulse width h in practice is replaced by an idealized cyclic sampler approximately equivalent to it. This ideal periodic sampler with sampling period T is illustrated in Fig. 4 (B), which is followed by zero order hold networks with different holding time Δ_i, that is

$$H_i(p) = \frac{1-\varepsilon^{-p\Delta_i}}{p}, \qquad i = 1, 2, \cdots, m-1. \quad (2.4)$$

Thus the system under consideration as shown in Fig. 1 can be evidently

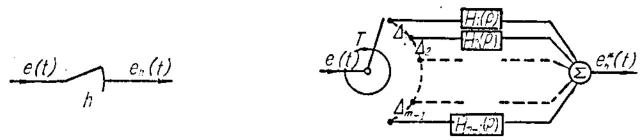

(A) Sampler with finite pulse width h in practice.

(B) An idealized cyclic sampler approximately equivalent to the sampler in Fig. 4 (A).

Fig. 4. Cyclic ideal sampler with sampling period T followed by zero order hold networks $H_i(p)=(1-\varepsilon^{-p\Delta_i})/p$.

rewitten as illustrated in Fig. 5 according to replacement of the cyclic ideal sampler and zero order hold networks. Hereafter, we consider this approximate equivalent system in the following analysis by means of the present method in this paper.

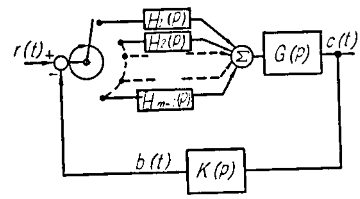

Fig. 5. Equivalent block diagram of the sampled-data feedback control system with finite pulse width h.

Now assume that a linear controlled object with transfer function $G(p)$, as shown in Fig. 5, is generally an α-th order element and subjects to the sampled output $e_h^*(t)$, and that a feedback element with transfer function $K(p)$ is generally a β-th order element.

For brevity, we introduce a new symbol such that

$$e_h^*(nT)\equiv e_{n1}, \quad e_h^*(nT+\Delta_1)\equiv e_{n2}, \quad e^*(nT+\sum_{i=1}^{r-1}\Delta_i)\equiv e_{nr} \tag{2.5}$$

where $n=0,1,2,\cdots$ and $r=1,2,\cdots,m$.

During from $t=nT$ to $t=nT+\Delta_1$, that is, its interval is said so as the 1st circuit mode on the n-th stage, the controlled output $c_n(t)$ may be obtained by solving the differential equation of the form

$$\frac{d^\alpha}{d\tau^\alpha}c_n(\tau)+a_1\frac{d^{\alpha-1}}{d\tau^{\alpha-1}}c_n(\tau)+\cdots+a_{\alpha-1}\frac{d}{d\tau}c_n(\tau)+a_\alpha c_n(\tau)=e_{n1} \qquad 0\leq\tau\leq\Delta_1 \tag{2.6}$$

where $a_1,\cdots,a_\alpha$ are constants of the controlled object.

Here it is convenient to express Eq. (2.6) in the matrix notation as

$$\begin{pmatrix} D & a_1D & a_2D\cdots\cdots a_{\alpha-1} & D+a_\alpha \\ -1 & D & 0\cdots\cdots\cdots & 0 \\ 0 & -1 & D\cdots\cdots\cdots & 0 \\ \vdots & \cdots\cdots\cdots & \cdots\cdots\cdots & \vdots \\ \vdots & \cdots\cdots\cdots & \cdots\cdots\cdots & \vdots \\ 0 & \cdots\cdots\cdots 0 & -1 & D \end{pmatrix} \begin{pmatrix} c_n^{\alpha-1}(\tau) \\ \vdots \\ \vdots \\ \vdots \\ c_n'(\tau) \\ c_n(\tau) \end{pmatrix} = \begin{pmatrix} e_{n1} \\ 0 \\ \vdots \\ \vdots \\ \vdots \\ 0 \end{pmatrix} \qquad 0\leq\tau\leq\Delta_1 \tag{2.7}$$

where $D=\frac{d}{d\tau}$, and $c_n^i(\tau)=\frac{d^i}{d\tau^i}c_n(\tau)$, $(1=1,2,\cdots,\alpha-1)$.

In feedback loop, the differential equation is written in the form

$$\frac{d^\beta}{d\tau^\beta}b_n(\tau)+d_1\frac{d^{\beta-1}}{d\tau^{\beta-1}}b_n(\tau)+\cdots+d_{\beta-1}\frac{d}{d\tau}b_n(t)+d_\beta b_n(\tau)=c_n(\tau)\quad 0\leq\tau\leq\Delta_1 \tag{2.8}$$

where $b_n(\tau)$ is the output of the feedback element in the 1st circuit mode on the n-th stage, and $d_1,\cdots,d_\beta$ are constants of the feedback element.

Similarly Eq. (2.8) is expressed in matrix notation

$$\begin{pmatrix} D & d_1D & d_2D\cdots\cdots d_{\beta-1} & D+d_\beta \\ -1 & D & 0\cdots\cdots & 0 \\ 0 & -1 & \cdots\cdots & \vdots \\ \vdots & \cdots\cdots & & \vdots \\ \vdots & \cdots\cdots & & 0 \\ 0 & \cdots\cdots 0 & -1 & D \end{pmatrix}\begin{pmatrix} b_n^{\beta-1}(\tau) \\ \vdots \\ \\ \vdots \\ b_n'(\tau) \\ b_n(\tau)\end{pmatrix}=\begin{pmatrix} c_n(\tau) \\ 0 \\ \vdots \\ \\ \vdots \\ 0\end{pmatrix}\quad 0\leq\tau\leq\Delta_1 \tag{2.9}$$

where $D=\frac{d}{d\tau}$, and $b_n^i(\tau)=\frac{d^i}{d\tau^i}b_n(\tau)$, $(i=1,2,\cdots,\beta-1)$.

While the relation between $e(t)$ and $b(t)$ is represented as follows, clearly by inspection of the system under discussion

$$\begin{aligned} e_{n1} &= \{r(t)-b(t)\}_{t=nT} \\ &\vdots \\ e_{nr} &= \{r(t)-b(t)\}_{t=nT+\sum_{i=1}^{r-1}\Delta_i}\,. \end{aligned} \tag{2.10}$$

Now, for simplicity, Eqs. (2.7) and (2.9) are rewritten in the abbreviate matrix forms, respectively

$$[z_G(D)][y_{n1}(\tau)]=[w_{n1}] \tag{2.11}$$

and

$$[z_K(D)][x_{n1}(\tau)]=[T'][y_{n1}(\tau)] \tag{2.12}$$

where $[T']$ is a transformation matrix whose elements consist of 0 or ± 1.

While, $[w_{n1}]$ is expressed as

$$\begin{aligned}[w_{n1}] &= \{[R(t)]-[T'][x(t)]\}_{t=nT} \\ &= [R_{n1}]-[T'][x_{n1}]\end{aligned} \tag{2.13}$$

where $[x_{n1}]=[x_{n-1,m}(\Delta_m)]$, and $[R_{n1}]=[R_{n-1,m}(\Delta_m)]$ consists of the aimed input $r(t)$.

Then substituting Eq. (2.13) into Eq. (2.11) yields

$$[z_G(D)][y_{n1}(\tau)]=[R_{n1}]-[T'][x_{n1}]. \tag{2.14}$$

Hence it is first necessary to obtain $[x_{n-1,m}(\tau)]$ from Eq. (2.12) for determination of $[x_{n1}]=[x_{n-1,m}(\Delta m)]$.

By the use of the Laplace transformation*, Eq. (2.12) becomes

---

* $F(p)=p\int_0^\infty f(t)\,\varepsilon^{-pt}\,dt$,

$$[Z_K(p)][X_{n-1,m}(p)] = [T'][Y_{n-1,m}(p)] + p[L_K][x^{+0}_{n-1,m}] \tag{2.15}$$

where elements of $[L_K]$ consist of elements l_{ij} when elements of $[Z_K(p)]$ have the form of $l_{ij}p + r_{ij}$.

Premultiplying each term on the both-hand side of Eq. (2.15) by $[Z_K(p)]^{-1}$, we have

$$[X_{n-1,m}(p)] = [Z_K(p)]^{-1}[T'][Y_{n-1,m}(p)] + p[Z_K(p)]^{-1}[L_K][x^{+0}_{n-1,m}]. \tag{2.16}$$

Transforming Eq. (2.16) into time function by the use of the inverse Laplace transformation**, we get

$$\begin{aligned}[x_{n-1,m}(\tau)] &= [\varphi_K(\tau)]*[T'][y_{n-1,m}(\tau)] + [\chi_K(\tau)][x^{+0}_{n-1,m}] \\ &= [\varphi_K \cdot y_{n-1,m}(\tau)] + [\chi_K(\tau)][x_{n-1,m-1}(\varDelta_{m-1})] \qquad 0 \leq \tau \leq \varDelta_m\end{aligned} \tag{2.17}$$

where a symbol "$*$" means the convolution integral, and its result is written of the form $[\varphi_K \cdot y_{n-1,m}(\tau)]$, for brevity,

while

$$\left.\begin{aligned}[\varphi_K(\tau)] &= \mathfrak{H}[Z_K(p)]^{-1}, \\ [\chi_K(\tau)] &= \mathfrak{H}p[Z_K(p)]^{-1}[L_K].\end{aligned}\right\} \tag{2.18}$$

Similarly, Eq. (2.14) is expressed in the form of p-function as

$$[Z_G(p)][Y_{n1}(p)] = [R_{n1}] - [T'][x_{n1}] + p[L_G][y^{+0}_{n1}]. \tag{2.19}$$

By a similar way, Eq. (2.19) becomes

$$[Y_{n1}(p)] = [Z_G(p)]^{-1}\{[R_{n1}] - [T'][x_{n1}]\} + p[Z_G(p)]^{-1}[L_G][y^{+0}_{n1}] \tag{2.20}$$

then, the solution in time domain is given by

$$\begin{aligned}[y_{n1}(\tau)] &= [\varphi_G(\tau)]\{[R_{n1}] - [T'][x_{n1}]\} + [\chi_G(\tau)][y^{+0}_{n1}] \\ &= [\varphi_G(\tau)][R_{n1}] + [\chi_G(\tau)][y_{n-1,m}(\varDelta_m)] - [\varphi_G(\tau)][T'][x_{n-1,m}(\varDelta_m)] \\ &\qquad 0 \leq \tau \leq \varDelta_1\end{aligned} \tag{2.21}$$

where

$$[\varphi_G(\tau)] = \mathfrak{H}[Z_G(p)]^{-1} \tag{2.22}$$

$$[\chi_G(\tau)] = \mathfrak{H}p[Z_G(p)]^{-1}[L_G] \tag{2.23}$$

and the unknown matrices $[x_{n-1,m}(\varDelta_m)]$ and $[y_{n-1,m}(\varDelta_m)]$ are readily determined by the following recurrence formulae in matrix notation

$$[x_{n-1,m}(\varDelta_m)] = [\varphi_K \cdot y_{n-1,m}(\varDelta_m)] + [\chi_K(\varDelta_m)][x_{n-1,m-1}(\varDelta_{m-1})] \tag{2.24}$$

and

$$\begin{aligned}[y_{n-1,m}(\varDelta_m)] &= [\varphi_G(\varDelta_m)][R_{n-1,m}(\varDelta_m)] + [\chi_G(\varDelta_m)][y_{n-1,m-1}(\varDelta_{m-1})] \\ &\quad - [\varphi_G(\varDelta_m)][T'][x_{n-1,m-1}(\varDelta_{m-1})].\end{aligned} \tag{2.25}$$

** $f(t) = \mathfrak{H}F(p) = \dfrac{1}{2\pi i}\lim\limits_{\beta\to\infty}\displaystyle\int_{r-i\beta}^{r+i\beta}\frac{F(p)}{p}\varepsilon^{pt}dp.$

It is evident in the end from these recurrence formulae that these two values on the left-hand side of Eqs. (2.24) and (2.25) are given by the given initial value matrices $[y_{11}^{+0}]$ and $[x_{11}^{+0}]$ respectively.

Therefore, Eq. (2.21) is the general solution of the system under discussion in the 1st circuit mode on the n-th stage, in other words, during from $t=nT$ to $t=nT+\Delta_1$.

Consequently, with above relations in mind, the solution in the i-th circuit mode on the n-th stage can be written as

$$[y_{ni}(\tau)] = [\varphi_G(\tau)][R_{ni}]+[\chi_G(\tau)][y_{n,i-1}(\Delta_{i-1})]-[\varphi_G(\tau)][T'][x_{n,i-1}(\Delta_{i-1})]$$
$$0\leq\tau\leq\Delta_i \qquad (i=1,2,\cdots,m. \quad n=0,1,\cdots) \tag{2.26}$$

while

$$[x_{n,i-1}(\Delta_{i-1})] = [\varphi_K\cdot y_{n,i-1}(\Delta_{i-1})]+[\chi_K(\Delta_{i-1})][x_{n,i-2}(\Delta_{i-2})] \tag{2.27}$$

and

$$[y_{n,i-1}(\Delta_{i-1})] = [\varphi_G(\Delta_{i-1})][R_{n,i-1}]+[\chi_G(\Delta_{i-1})][y_{n,i-2}(\Delta_{i-2})] -[\varphi_G(\Delta_{i-1})][T'][x_{n,i-1}(\Delta_{i-2})]. \tag{2.28}$$

Since the matrices on the left-hand side of Eqs. (2.27) and (2.28) can be finally determined by the given initial matrices $[y_{11}^{+0}]$ and $[x_{11}^{+0}]$ according to the recurrence formulae, Eq. (2.26) results in the general solution in any circuit mode on any stage.

3. Numerical Examples and The Effects of Pulse Width on the Stability of the Control System

First we consider the control system under discussion with unity feedback $K(p)=1$.

In this case, the solution is reduced to the more simple form as follows, putting $[x_{n,i-1}(\Delta_{i-1})]$ on the right-hand side of Eq. (2.26) into $[y_{n,i-1}(\Delta_{i-1})]$,

$$[y_{ni}(\tau)] = [\varphi_G(\tau)][R_{ni}]+[\chi(\tau)][y_{n,i-1}(\Delta_{i-1})] \qquad 0\leq\tau\leq\Delta_i \tag{3.1}$$

where $[\chi(\tau)]=[\chi_G(\tau)]-[\varphi_G(\tau][T']$

and the initial matrix $[y_{n,i-1}(\Delta_{i-1})]$ is written of the recurrence formula, but in a more compact form, as

$$[y_{n,i-1}(\Delta_{i-1})] = [\varphi_G(\Delta_{i-1})][R_{n,i-1}]+[\chi(\Delta_{i-1})][\varphi_G(\Delta_{i-2})][R_{n,i-2}] +[\chi(\Delta_{i-1})][\chi(\Delta_{i-2})][\varphi_G(\Delta_{i-3})][R_{n,i-3}]+\cdots +[\chi(\Delta_{i-1})][\chi(\Delta_{i-2})]\cdots[\chi(\Delta_1)][y_{n-1,m}(\Delta_m)] \tag{3.2}$$

and

$$[y_{n-1,m}(\Delta_m)] = [\Phi_{n-1,m}]+[B_m][\Phi_{n-2,m}]+[B_m]^2[\Phi_{n-3,m}]+\cdots +[B_m]^{n-2}[\Phi_{1m}]+[B_m]^{n-1}[y_{11}^{+0}] \tag{3.3}$$

where

$$[B_m] = [\chi(\Delta_m)][\chi(\Delta_{m-1})]\cdots[\chi_1(\Delta_1)] \tag{3.4}$$

$$[\Phi_{rm}] = [\varphi_G(\Delta_m)][R_{rm}]+[\chi(\Delta_m)][\varphi_G(\Delta_{m-1})][R_{r,m-1}]+\cdots$$
$$+[\chi(\Delta_m)][\chi(\Delta_{m-1})]\cdots[\chi(\Delta_2)][\varphi_G(\Delta_1)][R_{r1}]. \tag{3.5}$$

Therefore, substituting Eq. (3.3) into Eq. (3.2) yields

$$[y_{n,i-1}(\Delta_{i-1})] = [\Phi_{n,i-1}]+[B_{i-1}]\{[\Phi_{n-1,m}]+[B_m][\Phi_{n-2,m}]+\cdots$$
$$+[B_m]^{n-2}[\Phi_{1m}]+[B_m]^{n-1}[y_{11}^{+0}]\}. \tag{3.6}$$

Furtheremore, when the pulse width h is subdivided into $m-1$ narrow pulses with each equal width Δ, that is,

$$\Delta_i = \Delta = h/(m-1),\quad (i=1,2,\cdots,m-1)\quad \text{and}\quad \Delta_m = T-h. \tag{3.7}$$

$[B_m]$ and $[\Phi_{rm}]$ become, respectively

$$[B_m] = [\chi(\Delta_m)][\chi(\Delta)]^{m-1} \tag{3.8}$$

and

$$[\Phi_{rm}] = [\varphi_G(\Delta_m)][R_{rm}]+[\chi(\Delta_m)][\varphi_G(\Delta)][R_{r,m-1}]+\cdots$$
$$+[\chi(\Delta_m)][\chi(\Delta)]^{m-2}[\varphi_G(\Delta)][R_{r1}]. \tag{3.9}$$

Consequently, Eq. (3.6) is substituted into Eq. (3.1), then we get finally the solution of the system with unity feedback in question in the i-th circuit mode on the n-th stage.

Now let us apply the above established method to an example of a third-order system as shown in Fig. 6.

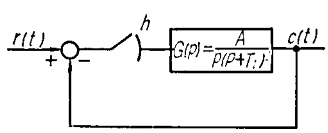

Fig. 6. An example of a third-order system with unity feedback.

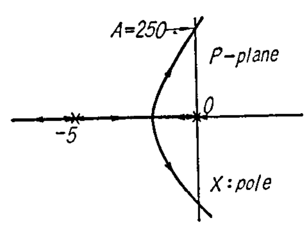

Fig. 7. Root loci of $G(p)$ with $T_1=5.0$.

Here assume that the controlled object is of the form

$$G(p) = \frac{A}{p(p+T_1)^2} \tag{3.10}$$

whose root loci are illustrated in Fig. 7, and that the pulse width h of the sampler is subdivided into $m-1$ narrow pulses with each equal width Δ as shown in Eq. (3.7).

The response to a unit step input for the system illustrated in Fig. 6 can be readily evaluated by the use of Eqs. (3.1), (3.8), (3.9) and following relations of Eqs. (3.12) and (3.13), since in this case it is satisfied that

$$[\Phi_{rm}] = [\Phi_{r-1,m}] = \cdots = [\Phi_{1m}] = [\Phi_{r+1,m}] \equiv [\Phi_m], \tag{3.11}$$

then

$$\begin{aligned}[y_{n-1,m}(\Delta_m)] &= \{[U]+[B_m]+[B_m]^2+\cdots+[B_m]^{n-2}\}[\Phi_m]+[B_m]^{n-1}[y_{11}^{+0}] \\ &= \{[U]-[B_m]\}^{-1}\{[U]-[B_m]^{n-1}\}[\Phi_m]+[B_m]^{n-1}[y_{11}^{+0}]\end{aligned} \tag{3.12}$$

and

$$[y_{n,i-1}(\Delta_{i-1})] = [\Phi_{i-1}]+[B_{i-1}](\{[U]-[B_m]\}^{-1}\{[U]-[B_m]^{n-1}\}[\Phi_m]+[B_m]^{n-1}[y_{11}^{+0}]) \tag{3.13}$$

where $[U]$ is a unit matrix and $[B_m]^{n-1}$ is calculable by the use of the Sylvester expansion theorem of the form

$$[B_m]^{n-1} = \sum_{r=1}^{l} \alpha_r^{n-1} \frac{\prod\limits_{\substack{s=1,2,\cdots,l \\ r\neq s}} \{\alpha_s[U]-[B_m]\}}{\prod\limits_{\substack{s=1,2,\cdots,l \\ r\neq s}} (\alpha_s-\alpha_r)}$$

where $\alpha_1, \cdots, \alpha_l$ are the distinct latent roots of $[B_m]$.

In the case where the controlled object is given by Eq. (3.10), the several fundamental matrices in the solution of the example shown in Fig. 6 are expressed as follows,

$$[y_{ni}(\tau)] = \begin{pmatrix} \ddot{c}_{ni}(\tau) \\ \dot{c}_{ni}(\tau) \\ c_{ni}(\tau) \end{pmatrix} \tag{3.14}$$

where $\ddot{c}_{ni}(\tau)=\frac{d^2}{d\tau^2}c_{ni}(\tau)$ and $\dot{c}_{ni}(\tau)=\frac{d}{d\tau}c_{ni}(\tau)$.

$$[R_{ni}] = \begin{pmatrix} 1 \\ 0 \\ 0 \end{pmatrix}, \tag{3.15}$$

$$[T'] = \begin{pmatrix} 0 & 0 & 1 \\ 0 & 0 & 0 \\ 0 & 0 & 0 \end{pmatrix}, \tag{3.16}$$

$$[\varphi_G(\tau)] = \begin{pmatrix} \varphi_{11}(\tau) & \varphi_{12}(\tau) & \varphi_{13}(\tau) \\ \varphi_{21}(\tau) & \varphi_{22}(\tau) & \varphi_{23}(\tau) \\ \varphi_{31}(\tau) & \varphi_{32}(\tau) & \varphi_{33}(\tau) \end{pmatrix} \tag{3.17}$$

where

$$\left.\begin{aligned} &\varphi_{11}(\tau) = A\tau\varepsilon^{-T_1\tau}, \quad \varphi_{12}(\tau) = -1+\varepsilon^{-T_1\tau}-T_1\tau\varepsilon^{-T_1\tau}, \quad \varphi_{13}(\tau) = -T_1^2\tau\varepsilon^{-T_1\tau}, \\ &\varphi_{21}(\tau) = \frac{A}{T_1^2}\{1-(1+T_1\tau)\varepsilon^{-T_1\tau}\}, \quad \varphi_{22}(\tau) = \tau\varepsilon^{-T_1\tau}, \quad \varphi_{23}(\tau) = -\{1-(1+T_1\tau)\varepsilon^{-T_1\tau}\}, \end{aligned}\right|$$

$$\left.\begin{aligned}&\varphi_{31}(\tau)=\frac{2A}{T_1^3}(\varepsilon^{-T_1\tau}-1)+\frac{A}{T_1^2}(\tau+\tau\varepsilon^{-T_1\tau}),\\&\varphi_{32}(\tau)=\frac{1}{T_1^2}\{1-(1+T_1\tau)\varepsilon^{-T_1\tau}\},\quad \varphi_{33}(\tau)=\frac{2A}{T_1}(1-\varepsilon^{-T_1\tau})-\tau\varepsilon^{-T_1\tau}.\end{aligned}\right\}\tag{3.18}$$

$$[\chi_G(\tau)]=\begin{pmatrix}\chi_{11}(\tau) & \chi_{12}(\tau) & \chi_{13}(\tau)\\ \chi_{21}(\tau) & \chi_{22}(\tau) & \chi_{23}(\tau)\\ \chi_{31}(\tau) & \chi_{32}(\tau) & \chi_{33}(\tau)\end{pmatrix}\tag{3.19}$$

where

$$\left.\begin{aligned}&\chi_{11}(\tau)=(1+T_1\tau)\varepsilon^{-T_1\tau},\quad \chi_{12}(\tau)=-T_1^2\tau\varepsilon^{-T_1\tau},\quad \chi_{13}(\tau)=0,\\&\chi_{21}(\tau)=\tau\varepsilon^{-T_1\tau},\quad \chi_{22}(\tau)=(1+T_1\tau)\varepsilon^{-T_1\tau},\quad \chi_{23}(\tau)=0,\\&\chi_{31}(\tau)=\frac{1}{T_1^2}\{1-(1+T_1\tau)\varepsilon^{-T_1\tau}\},\quad \chi_{32}(\tau)=\tau\varepsilon^{-T_1\tau}+\frac{2}{T_1}\{1-(1+T_1\tau)\varepsilon^{-T_1\tau}\},\\&\chi_{33}(\tau)=1.\end{aligned}\right\}\tag{3.20}$$

and $[\chi(\tau)]=[\chi_G(\tau)]-[\varphi_G(\tau)][T']$ is of the form, from (3.17) and (3.19),

$$[\chi(\tau)]=\begin{pmatrix}\chi_{11}(\tau), & \chi_{12}(\tau), & \chi_{13}(\tau)-\varphi_{11}(\tau)\\ \chi_{21}(\tau), & \chi_{22}(\tau), & \chi_{23}(\tau)-\varphi_{21}(\tau)\\ \chi_{31}(\tau), & \chi_{32}(\tau), & \chi_{33}(\tau)-\varphi_{31}(\tau)\end{pmatrix}\tag{3.21}$$

whose elements are given by Figs. (3.18) and (3.20).

The results based on Eq. (3.1) are easily calculated by means of the Digital Computer (KDC-1) as illustrated in Fig. 8, where $G(p)=100/p(p+5)^2$ ($A=100$, $T_1=5.0$) and $h/T=0.25$, on three cases of initial conditions and sampling periods.

Next we consider the stability criterion for the sampled-data feedback

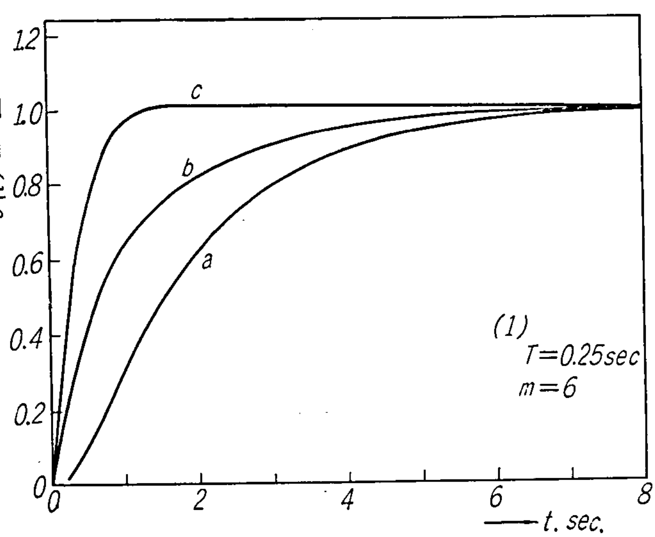

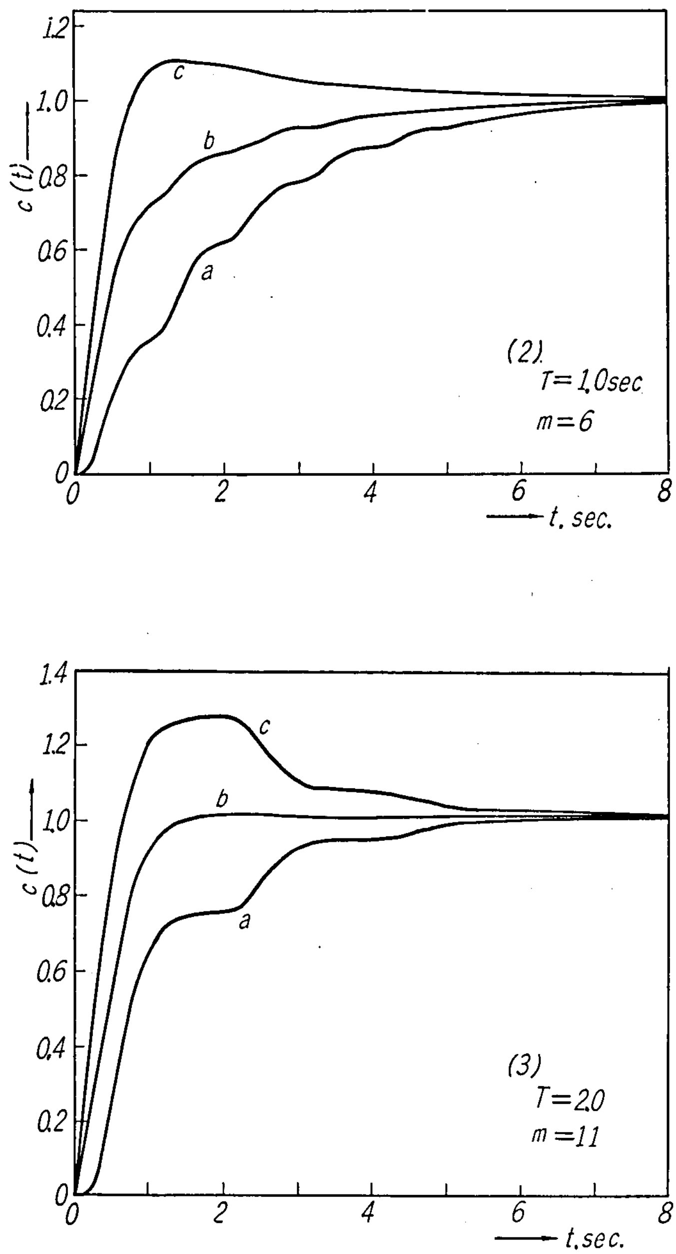

Fig. 8. Response to a unit step input for a system of the type illustrated in Fig. 6, with $G(p)=100/p(p+5)^2$ and $h/T=0.25$, where initial conditions, i.e. a: $c^{+0}=0$, $\dot{c}^{+0}=0$, $\ddot{c}^{+0}=0$, b: 0, 1.0, 0, c: 0, 2.0, 0.

control system with finite pulse width in question and examine the effects of finite sampling on the performance of the system.

The criterion is established under the presumption that the system should be supposed stable so long as the factors containing the initial values of the system variable vanish away gradually from the solution as time goes.

Accordingly, in our case, the stability criterion for the system may be achieved by examining the initial matrices of Eqs. (3.12) or (3.13), whose values must be limited one for the stable system.

As was well-defined in References (7), by the use of the Sylvester expansion theorem, it is evident that the necessary and sufficient condition that the system should be stable is that the absolute values of all the latent roots of $[B_m]$ should be less than unity, or in other words, that all the latent roots should lie inside the unit circle on the complex domain with its center at the origin.

In general, assuming $[B_m]$ to be the n-th order matrix, the characteristic equation of $[B_m]$ is of the form

$$\delta\{\alpha[U]-[B_m]\} = 0 \tag{3.22}$$

and this determinant reduces to an algebraic equation of the form

$$a_0\alpha^n + a_1\alpha^{n-1} + \cdots + a_{n-1}\alpha + a_n = 0 \tag{3.23}$$

where $a_0, a_1, \cdots, a_n$ are constants.

The solutions $\alpha_1, \alpha_2, \cdots, \alpha_n$ of this equation result in the latent roots of $[B_m]$.

Here, it is convenient to do the bilinear transformation such as $\alpha=(\lambda+1)/(\lambda-1)$ in Eq. (3.23), and its results become

$$b_0\lambda^n + b_0\lambda^{n-1} + \cdots + b_{n-1}\lambda + b_n = 0 \tag{3.24}$$

where $b_0, b_1, \cdots, b_n$ are constants determined by constants $a_0, a_1, \cdots, a_n$.

Then, we can immediately apply a stability criterion of the Hurwitz type to Eq. (3.24), because that the points inside the unit circle on the α-plane can be transformed to those lying on the left half region of the complex λ-plane by this bilinear transformation.

Now based on these stability criterion, we examine the stability of the example system shown in Fig. 6.

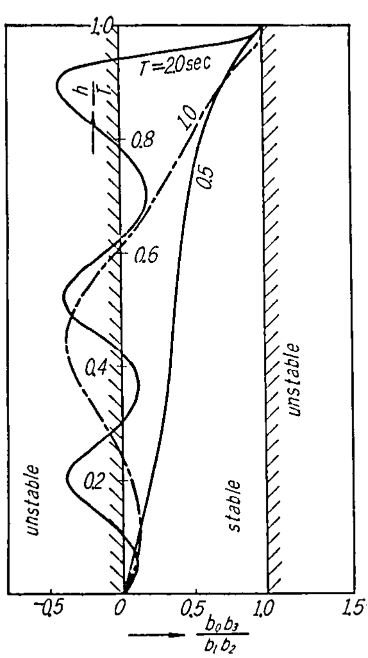

Fig. 9. Region for stability.

The numerical results illustrated in Fig. 9 make clear the relations between the finite pulse width h with respect to the sampling period T and the stability of the control system under discussion, where the controlled system $G(p)=250/p(p+5)^2$, ($A=250$, $T_1=5.0$), that is, a value of $A=250$ is a critical point between the stable and unstable regions of the system in linear continuous cases as shown in Fig. 7.

In this case, the analogue form to Eq. (3.24) is written as

$$b_0\lambda^3+b_1\lambda^2+b_2\lambda+b_3=0 \tag{3.25}$$

therefore, the following conditions are the necessary and sufficient one for the stable system by the Hurwitz's criterion

$$\begin{gathered} b_0,\ b_1,\ b_2,\ b_3>0 \\ \begin{vmatrix} b_1 & b_3 \\ b_0 & b_2 \end{vmatrix} = b_1b_2-b_0b_3>0 \end{gathered} \tag{3.26}$$

These numerical evalutions are done by means of the Digital Computer (KDC-1), whose flowchart is shown in Fig. 10.

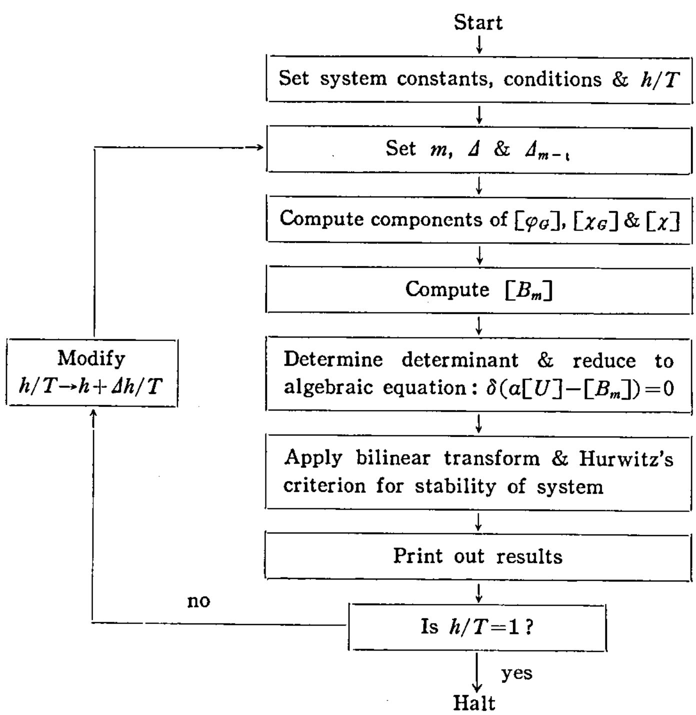

Fig. 10. Digital computer flowchart for calculating the stability of the system.

From inspection of Fig. 9, when the sampling period $T=0.5$, the system is stable for any value of h/T, while on the other hand, when the sampling period becomes large such as $T=1.0$ or $T=2.0$, the stability of the system is variable with respect to the change of h/T.

It is now of interest to clarify the performance of the system under consideration due to the change of pulse width of the sampler when the control system is naturally unstable in continuous systems.

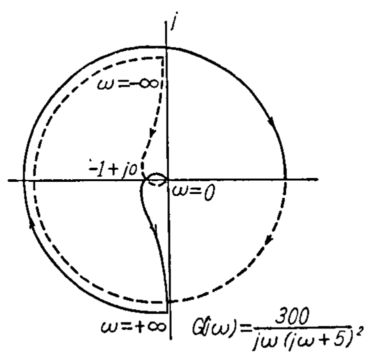

Fig. 11. Inverse transfer function of an unstable control system.

For instance, we take $A=300$, $T_1=5.0$ in our example system of Fig. 6 which is unstable as its inverse transfer function is plotted in Fig. 11.

The numerical results in this example are illustrated in Fig. 12 which demonstrate that the pulse width of the sampler affects remarkably the stability of the

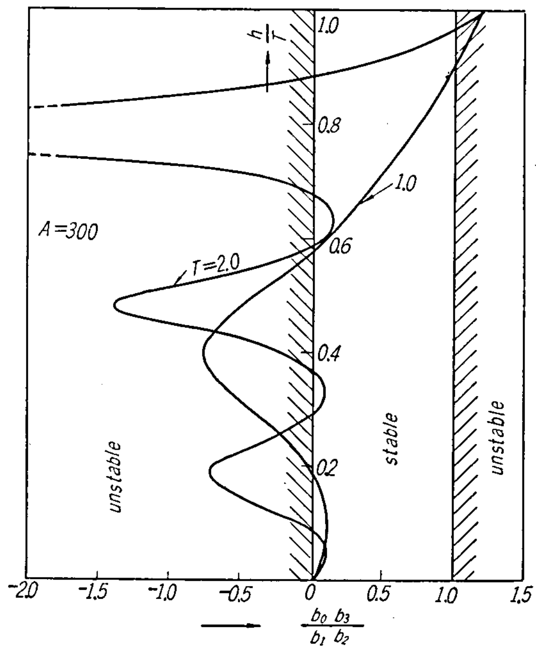

Fig. 12. Region for stability.

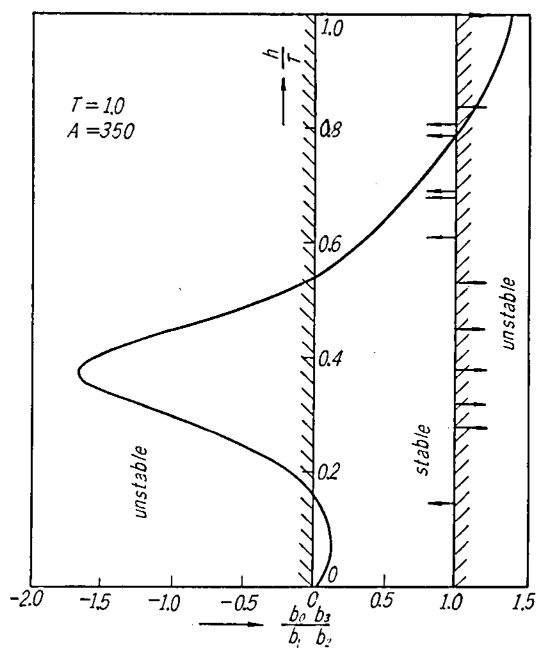

Fig. 13. Region for stability where arrow symbols "← and →" show results by the analog computer.

control system, and that the unstable controlled object becomes stable by the use of the sampler with finite pulse width.

Another result when $A=350$, $T_1=5.0$ is shown in Fig. 13 comparing the theoretical result with the simulated one by means of an analog computer.

Both results indicate a close coincidence as might be expected, and one result by the analog computer is illustrated in Fig. 14 when the sampling period $T=1$ sec and $h/T=0.45$, which shows an unstable response.

The analogue simulation of this example may take the form shown in Fig. 15 where the sampler with finite pulse width is simulated by electronic elements as shown in Fig. 16.

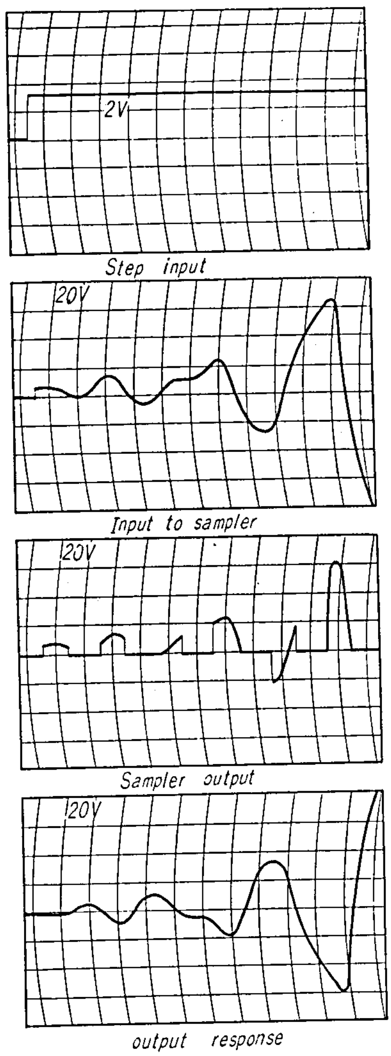

Fig. 14. A simulated result by the analog computer when $G(p)=350/p(p+5)^2$, $T=1$ sec and $h/T=0.45$.

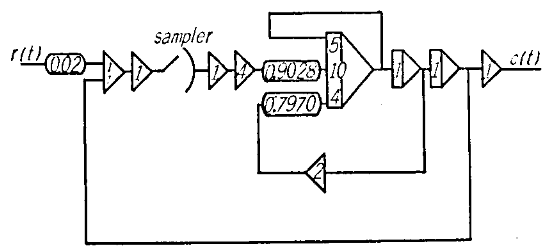

Fig. 15. Analogue simulation diagram.

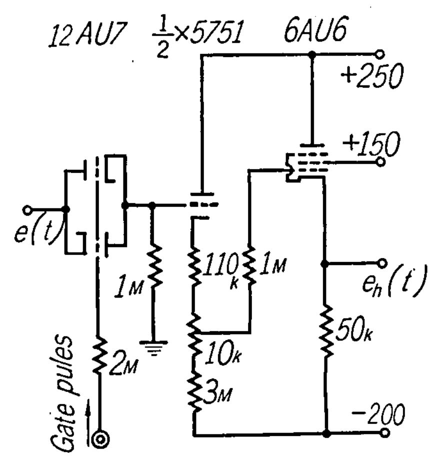

Fig. 16. Representation of a sampler with finite pulse width.

4. Conclusion

The response of a sampled-data feedback control system with finite pulse width can be predicted with good accuracy by the use of the theories of the Periodically Interrupted Electric Circuits described here.

Based on this new technique, the stability criterion of the sampled-data feedback control system with finite pulse width is easily derived and relatively is valuable and accuracy as was indicated in numerical results in the present work.

In an effort to examine the stability of the finite sampling control system, it is evident that the effects of the sampler with finite pulse width is a considerable important for the performance of the system, and that even if the controlled object is originally unstable, its system can be made stable by making use of a sampler with finite pulse width.

Acknowledgements

The authors with to thank Assistant Prof. S. Hoshino and Dr. S. Iwai of the Department of Electronics for their valuable advices and discussions in this work. Thanks are also due to Bachelor of Eng. S. Matsuo of Mitsubishi Electric Company at present and to staff members of the center of the Digital Computer (KDC-1), University of Kyoto, for their helps with our numerical computations.

References

1) G. Farmanfarma: Analysis of Linear Sampled-Data Systems with Finite Pulse Width; Open Loop; AIEE. Transactions, Vol. 75, pt. 1, pp. 808~819, Jan. (1957).
2) J. T. Tou: Digital and Sampled-Data Control System; McGraw-Hill Book Company, (1959).
3) G. Farmanfarma: General Analysis and Stability Study of Finite Pulsed Feedback Systems; AIEE. Transactions, Vol. 77, pt. 2, pp. 148~158, July (1958).
4) G. J. Murphy and H. B. Kennedy: Closed-Loop Analysis of Sampled-Data Systems with Appreciable Pulse Width; AIEE. Transactions, Vol. 77, pt. 2, pp. 659~665, Jan. (1959).
5) S. Hayashi and K. Mizukami: Analysis of Sampled-Data Feedback Control Systems with Finite Pulse Width; Convention Records at the General Meeting on Automatic Control in Japan, No. 124, pp. 41~42, Nov. (1962) and No. 130, pp. 59~60, Nov. (1963).
6) S. Hayashi and K. Mizukami: Analysis of Sampled-Data Feedback Control Systems with Finite Pulse Width II; Convention Records at the Annual Meeting of the Inst. of Elect. Eng. of Japan, No. 316, April (1963).
7) S. Hayashi: Periodically Interrupted Electric Circuits; Denki-Shoin (1961).